

**CENTRO DE INVESTIGACIÓN CIENTÍFICA Y DE EDUCACIÓN SUPERIOR
DE ENSENADA**



**PROGRAMA DE POSGRADO EN CIENCIAS
EN CIENCIAS DE LA TIERRA**

**STRUCTURAL EVOLUTION OF BASINS IN THE NORTHERN AND CENTRAL GULF
OF CALIFORNIA. IMPLICATIONS FOR RIFT KINEMATICS AND STRAIN
ACCOMMODATION**

**EVOLUCIÓN ESTRUCTURAL DE LAS CUENCAS DEL NORTE Y CENTRO DEL GOLFO
DE CALIFORNIA. IMPLICACIONES EN LA CINEMÁTICA DE APERTURA Y EN EL
ACOMODO DE LA DEFORMACIÓN**

TESIS

que para cubrir parcialmente los requisitos necesarios para obtener el grado de
DOCTOR EN CIENCIAS

Presenta:


MANUEL DE JESÚS ARAGÓN ARREOLA

Ensenada, Baja California, México, Agosto de 2006.

ABSTRACT of the thesis presented by **Manuel de Jesús Aragón Arreola** as a partial requirement to obtain the DOCTOR OF SCIENCE degree in EARTH SCIENCES. Ensenada, Baja California, Mexico. August 2006.

STRUCTURAL EVOLUTION OF BASINS IN THE NORTHERN AND CENTRAL GULF OF CALIFORNIA. IMPLICATIONS FOR RIFT KINEMATICS AND STRAIN ACCOMMODATION

Abstract approved by:



Jesús Arturo Martín Barajas

The Gulf of California rift forms the modern transtensional boundary between the Pacific and North America plates. Variations along its ~1,500 km-length go from the continental extension in the Salton Trough, to the north, to the accretion of new ocean floor, to the south. The northern Gulf contains the continent-ocean transition; obliquity here is 9-12° and the net displacement in the last ~6.3 Ma reaches ~255±10 km. The central Gulf, instead, contains the incipient spreading of new oceanic crust in the Guaymas basin. In this thesis the process and interpretation of multichannel seismic reflection data collected by PEMEX in the northern Gulf (~3800 km) and CORTES-P96 in the central Gulf (~200 km) allowed the structural mapping and tectono-sedimentary interpretation. Structure in this area is characterized by large strike-slip and transform faults oriented NW-SE, e.g., the inactive Amado, De Mar, Tiburón, San Pedro Nolasco and Yaqui faults to the east and the active Cerro Prieto, Canal de Ballenas, Guaymas and Carmen faults to the west. Several ~N-S oriented faults splay away and are probably the hard-link between the major faults; these linking structures include a top-to-the east detachment fault, the listric Wagner fault and several arrays of dense, low-throw shallow faults. The step over zones between the major faults are occupied by marine basin, e.g., the inactive Adair-Tepoca, Upper Tiburón and Yaqui basins to the east and the active Wagner-Consag, Upper Delfin, Lower Delfin and Guaymas basins to the west. The Adair-Tepoca and Upper Tiburón basins include three main seismo stratigraphic sequences that represent pre-rift, syn-rift and post-rift facies of sedimentation related to the evolution of the Amado, De Mar, and Tiburón faults. The faults and basins along the Gulf define two parallel rift margins; the eastern margin is inactive and forms an incipient drift margin; whereas the western margin accommodates the modern transtensional strain. The scarce age constraints indicate that onset of the eastern margin occurred in the latest Miocene and records the initial stage of focused rifting; however, marine condition may have existed since the latest middle Miocene time in the proto-Gulf stage. These stratigraphic relationships show that tectonic activity migrated from the eastern to the western margin during the late Pliocene. Strain migration in the northern Gulf lead to the formation of a basement high, which is cut by an inferred detachment fault and is crowned by a doubly-hinged anticline; this configuration suggests

that detachment faulting formed a roll-over anticline that marks the boundary between the inactive and active basins. I propose that the structure in the Gulf of California has resulted from the accommodation of highly partitioned oblique strain, in which the major faults mostly accommodated strike-slip motion, whereas the large magnitude extension in the northern Gulf has been accommodated by the subsidiary low-angle and high-angle normal faults.

Keywords: Gulf of California, oblique rifting, strain partitioning, seismic stratigraphy, continental rupture.

RESUMEN de la tesis de **Manuel de Jesús Aragón Arreola**, presentada como requisito parcial para la obtención del grado de DOCTOR EN CIENCIAS en CIENCIAS DE LA TIERRA. Ensenada, Baja California, México. Agosto 2006.

EVOLUCIÓN ESTRUCTURAL DE LAS CUENCAS DEL NORTE Y CENTRO DEL GOLFO DE CALIFORNIA. IMPLICACIONES EN LA CINEMÁTICA DE APERTURA Y EN EL ACOMODO DE LA DEFORMACIÓN

Resumen aprobado por:



Jesús Arturo Martín Barajas

El rift del Golfo de California forma el límite transtensivo entre las Placas Pacífica y Norteamericana. Las variaciones longitudinales en los ~1500 km del rift van de la extensión continental en la depresión de Salton, al norte, a la formación de piso oceánico en las cuencas del sur. Al parecer, la transición de apertura continental a oceánica ocurre en el norte del Golfo, donde la oblicuidad del rift es de 9-12°, y el desplazamiento acumulado desde hace ~6.3 Ma alcanza ~255±10 km; en cambio la parte central del Golfo presenta la dispersión incipiente de corteza oceánica en la Cuenca de Guaymas. En esta tesis, el procesamiento e interpretación de sísmica de reflexión multicanal colectada por PEMEX en el norte del Golfo (~3800 km) y por el proyecto CORTES-P96 en el centro del Golfo (~200 km), permitió la cartografía estructural y tectonosedimentaria. La estructura del centro-norte del Golfo se caracteriza por fallas laterales y transformes orientadas ~NW-SE, e.g. las fallas inactivas Amado, De Mar, Tiburón, San Pedro Nolasco y Yaqui al este y las fallas activas Cerro Prieto, Canal de Ballenas, Guaymas y Carmen, al oeste. De las fallas principales se desprenden fallas ~N-S que parecen formar la liga dura entre fallas mayores; las fallas secundarias incluyen el contacto inferido por fallas de *detachment* con buzamiento al este, la falla listrica Wagner y varios arreglos densos de fallas someras con poco desplazamiento. Los escalones entre fallas mayores están ocupados por cuencas marinas, como las inactivas Adair-Tepoca, Tiburón Superior y Yaqui al este y las activas Wagner-Consag, Delfín Superior, Delfín Inferior y Guaymas al oeste. Las cuencas Adair-Tepoca y Tiburón Superior contienen tres secuencias sismo-estratigráficas que representan facies sedimentarias de *pre-rift*, *sin-rift* y *post-rift* relacionadas a la evolución de las fallas Amado, De Mar y Tiburón. Las fallas y cuencas en el Golfo definen dos márgenes paralelos: el margen este es inactivo y forma un margen incipiente de deriva, mientras que el oeste acomoda la deformación transtensiva. Los datos de edades relativas son escasos, pero indican que el margen oriental inició en el Mioceno tardío y registra el estadio inicial de *rift* localizado; sin embargo las condiciones marinas parecen haber existido desde el estadio de proto-Golfo en el Mioceno medio-tardío; estos datos muestran que la migración de la deformación del margen este al oeste ocurrió en el Plioceno tardío. La migración de la deformación en el norte del Golfo definió un alto de basamento flanqueado por el

detachment inferido y coronado por un anticlinal de doble charnela; esta configuración sugiere que el corrimiento del *detachment* pudo dar lugar a la formación de un anticlinal de traslación. Este sistema estructural forma el límite entre las cuencas activas e inactivas. Propongo que la estructura del Golfo de California es resultado del acomodo de deformación altamente particionada, tal que las fallas mayores acomodan la mayoría del movimiento lateral, mientras que la gran cantidad de extensión en el norte del Golfo ha sido acomodada por fallas normales subsidiarias.

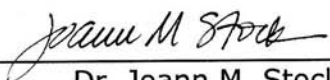
Palabras clave: Golfo de California, *rift* oblicuo, partición de la deformación, estratigrafía sísmica, ruptura continental.

TESIS DEFENDIDA POR
Manuel de Jesús Aragón Arreola

Y APROBADA POR EL SIGUIENTE COMITÉ



Dr. Jesús Arturo Martín Barajas
Director del Comité



Dr. Joann M. Stock
Miembro del Comité



Miembro del Comité



Dr. Juan García Abdeslem
Miembro del Comité



Dr. Luis Alberto Delgado Argote
Miembro del Comité



Dr. Antonio González Fernández
Miembro del Comité



Dr. Víctor Wong Ortega
*Coordinador del programa de
Ciencias de la Tierra*



Dr. Edgar G. Pavía López
Director de Estudios de Posgrado

25 de Agosto de 2006

A María
A Tinita

To the people of México, Venezuela, Honduras, Canada, USA and Argentina
To Mar, to the Pacific and to Ensenada de Todos los Santos
To whom had loved me, to whom I had loved
To my Valkyries and my Demons

A la gente de México, Venezuela, Honduras, Canadá, Estados Unidos y Argentina
A la Mar, al Pacífico y a la Ensenada de Todos los Santos
A quienes me han amado y a quienes he amado
A mis Valquirias y a mis Demonios

... 'Come, it's pleased so far,' thought Alice, and she went on. 'Would you tell me, please, which way I ought to go from here?'

'That depends a good deal on where you want to get to,' said the Cat.

'I don't much care where--' said Alice.

'Then it doesn't matter which way you go,' said the Cat.

'--so long as I get *somewhere*,' Alice added as an explanation.

'Oh, you're sure to do that,' said the Cat, 'if you only walk long enough.'

Alice felt that this could not be denied, so she tried another question. 'What sort of people live about here?'

'In *that* direction,' the Cat said, waving its right paw round, 'lives a Hatter: and in *that* direction,' waving the other paw, 'lives a March Hare. Visit either you like: they're both mad.'

'But I don't want to go among mad people,' Alice remarked.

'Oh, you can't help that,' said the Cat: 'we're all mad here. I'm mad. You're mad.'

'How do you know I'm mad?' said Alice.

'You must be,' said the Cat, 'or you wouldn't have come here.'

I love the Alice's Adventures in Wonderland of Lewis Carroll

Nel mezzo del cammin di nostra vita
mi ritrovai per una selva oscura,
ché la diritta via era smarrita.

Ahi quanto a dir qual era è cosa dura
esta selva selvaggia e aspra e forte
che nel pensier rinova la paura!

Canto I. Divina Comedia di Dante Alighieri

La suposición de que Remedios, la bella, poseía poderes de muerte, estaba entonces sustentada por cuatro hechos irrefutables. Aunque algunos hombres ligeros de palabra se complacían en decir que bien valía sacrificar la vida por una noche de amor con tan conturbadora mujer, la verdad fue que ninguno hizo esfuerzos por conseguirlo. Tal vez, no sólo para rendirla sino también para conjurar sus peligros, habría bastado con un sentimiento tan primitivo, y simple como el amor, pero eso fue lo único que no se le ocurrió a nadie.

de los Cien Años de Soledad, de Gabriel García Márquez

Cuando ellos dicen que soy productivo yo siento que estoy perdiendo el tiempo y cuando ellos dicen que estoy perdiendo el tiempo es cuando me siento productivo. Quién nos entiende.

ACKNOWLEDGEMENTS

I would like to acknowledge the help of several institutions. The *Consejo Nacional de Ciencia y Tecnología* granted scholarships for my M.Sc. and Ph.D. studies. Petróleos Mexicanos surveyed the data that I, by a joyful coincidence, had used for this work. The *Centro de Investigación Científica y de Educación Superior de Ensenada* (CICESE) allowed me to build up such a precious treasure of knowledge. The California Institute of Technology showed me how things shall be done. The University of Nuevo Mexico and Universidad de Guadalajara also helped me to widen my scientific vision. Geomaque Explorations Ltd. gave me the chance of pursuing just what really captured my interest.

I thank Arturo Martín for his helpful advice and extreme patience. Juan Contreras, with his peculiar and contagious enthusiasm helped with his always welcomed comments. Joann Stock and her thoughtful revisions and confidence, had opened to me the way to the leading edge in earth science.

My gratitude to the professors who showed me the reason to enjoy science: José Frez, Arturo Martín, Juan Contreras, Joann Stock, Alejandro Hinojosa, Alejandro Nava, Enrique Gómez, Phillip Walford, Juan Carlos Herguera, Rob Clayton, Mousumi Roy, Alonso Gallardo, Marco Pérez, Francisco Suárez, Francisco Núñez, Juan García, Luis Delgado. I thank all who reviewed and criticized my work, especially Paul Umhoefer and Gary Axen.

I appreciate the friendship and support of Lupita Martínez, Martha Barrera, Ivonne Best, Cecy González, Lupita Zamora, Citlalli Romero, José Mojarro, Luis Gradilla, Angel D. Hurtado, Sergio Arregui and Alfredo Ruiz. And also Edgar Pavía and Dolores Sarracino.

I thank all my friends in this weird quest of science: María Morandi, Concepción García, Vanessa Francisco, Adriana Arroyo, Dulce Vargas, Mónica Zegarra, Selene Solorza,

Sylvia Chacón, Rosa Carrillo, Samantha de la Gala, Paula García, Min Chen, Qinya Liu, Yaru, Raquel Negrete, Martha Armenta, Idalmis Fernández, Cristina Condori, Doris Piñeiro, Manuel Ng, José Mojarro, Alex Espinosa, Miguel Tenreiro, Julien Jouanno, Héctor García, Fernando Andrade, Ricardo Sepúlveda, Francisco Esparza, Zhen Luo. To all of us that joined in the brotherhood of the “Comuna del Bar del Sauzal”, Coco included. I thank all who have thrusted in me: Ernestina Arreola, María Morandi, Isabel Moctezuma, Martín Moctezuma, Olivia Castañeda, Armando Nicolau, Frida, Alma, Marshan. Also to my role models: Tanya Atwater, María F. Campa, Carlos Domingo, Pål Wessel, Maurice Ewing, Fernando Ortega, José Cabrujas. Also to the TED Science Project which became an unwilling obsession that had supported me in the last years of reflecting on science.

Chapter II was partially funded by Petróleos Mexicanos and CONACyT. I appreciate the helpful comments of Joann Stock, Juan Contreras and Becky Dorsey, and the thoughtful revision of Gary Axen, Paul Umhoefer and two anonymous reviewer. Chapter III. CICESE allowed the use of scientific facilities during the preparation of this work. Thanks to Petróleos Mexicanos for access to proprietary data and for permission to publish results. TED Science Project provided economic support. Chapter IV was partially funded by CONACyT. Universidad de los Andes supported M. Morandi in a sabbatical leave at CICESE. CORTES-P96 was made feasible by CICYT projects ANT94-0182-C02-01/02 and ANT94-0182-C02-00/02, and CICESE project 644107. A México-Spain project was funded by CICESE project 644104 and CONACyT project 28317T. This chapter was improved through discussions with Joann Stock, Juan Contreras, José Frez and Patricia Persaud. Paul Umhoefer and an anonymous reviewer are also greatly thanked.

SINOPSIS

Este trabajo ha sido escrito en idioma inglés para facilitar su difusión en la comunidad geocientífica; sin embargo, esta sección, se presenta en español para aclarar las generalidades de este trabajo a los lectores de habla hispana. Esta sinopsis es una traducción del Capítulo I de introducción, en donde se presenta el propósito de la tesis, se describe el problema fundamental, las generalidades sobre el proceso geológico que se aborda y la metodología de trabajo. Ruego a los lectores que si deciden leer esta sinopsis omitan la introducción y viceversa.

Propósito de este trabajo

Esta tesis aborda el problema de la evolución cinemática de la deformación en el *rift* oblicuo del Golfo de California. En este trabajo usé datos de sísmica de reflexión multicanal y, en menor cantidad, datos gravimétricos. Esta información muestra imágenes de la corteza superior del Golfo de California en las cuales interpreté y correlacioné las estructuras geológicas principales para producir cartografía geológica de aproximadamente 50,000 km² de la parte norte y centro del Golfo de California. Este trabajo explica el desarrollo de cuencas y fallas en esta región y discute la evolución tectónica de unos 600 km del límite entre las placas Norteamericana y Pacífico desde el Mioceno medio.

Dirijo este trabajo a los geocientíficos que trabajan el oeste de los Estados Unidos y el noroeste de México, además de aquellos investigadores que abordan problemas como dinámica de extensión, modelado analógico de la extensión y evolución tectónica de márgenes en separación. Además es probable que esta tesis atraiga la atención de la industria petrolera dado que el área de estudio es fuente potencial de hidrocarburos.

El problema: de la ruptura continental a la propagación de piso oceánico

El acomodo de la deformación durante la apertura continental involucra la evolución temporal de tres modos de extensión continental predichos por modelos numéricos, a saber: modo de complejo metamórfico, de *rift* amplio y de *rift* angosto (Buck, 1991). Los principales factores que controlan los cambios en el modo de extensión son la variación del espesor de corteza, la estructura térmica, la tasa de deformación y la reología de la litósfera (Buck, 1991; Ruppel, 1995; Hopper y Buck, 1996). Dada una corteza quebradiza gruesa la extensión provoca fallamiento normal distribuido en forma más o menos homogénea independientemente de la velocidad de extensión, en cambio con una corteza quebradiza delgada la extensión rápida produce *grabens* asimétricos con el eventual desarrollo de fallas lítricas, en tanto que la extensión lenta usualmente es acomodada por fallas lítricas (Lavie et al., 2000).

La región suroeste de los Estados Unidos y noroeste de México ha experimentado diferentes modos de extensión continental (Buck, 1991). Durante el Oligoceno temprano al Mioceno medio, la Provincia de Cuencas y Sierras registra extensión en los modos de complejo metamórfico y *rift* amplio (Stewart, 1998). Durante el Mioceno medio a tardío, la Provincia Extensional del Golfo experimentó extensión en el modo de *rift* amplio; desde el Mioceno tardío la deformación se localizó en una franja más estrecha alrededor del Golfo de California en el modo de *rift* angosto. Sin embargo, sólo la porción meridional de este *rift* ha llegado a formar piso oceánico nuevo (Stock y Hodges, 1989; Lonsdale, 1989). El estudio del Golfo de California es importante porque aporta información de un *rift* angosto en el que la ruptura continental ha pasado por diferentes modos de extensión continental hasta formar corteza oceánica nueva.

Los *rift* continentales son valles largos y angostos limitados por fallas en uno o en ambos lados (Scholz y Contreras, 1998). La evolución de estos valles promueve la formación de cuencas sedimentarias controladas por fallas, de tal forma que los medio *grabens* o los *grabens* asimétricos son elementos básicos de un *rift* continental (Rosendahl, 1987; Gawthorpe y Leeder, 2000; Contreras y Scholz, 2001).

La estratigrafía de las cuencas dentro de un *rift* continental desarrollado registra una etapa de subsidencia lenta llamada inicio de *rift*, a la cual sigue una etapa de incremento abrupto en la tasa de subsidencia, o clímax de *rift* (Prosser, 1993; Gawthorpe y Leeder, 2000). Estas etapas dependen del comportamiento de las fallas y presentan claras variaciones del registro estratigráfico, de tal forma que la arquitectura de las cuencas es función de los procesos tectónicos, además de los cambios climáticos y las variaciones eustáticas (Prosser, 1993; Cowie et al., 2000; Gawthorpe y Leeder, 2000; Gupta y Cowie, 2000).

Este trabajo aborda la evolución tectonoestratigráfica de las cuencas *rift* en el norte y centro del Golfo de California. El Capítulo II provee una descripción detallada de la estructura cartografiada en el norte del Golfo y propone que las cuencas abandonadas de la parte este del Golfo de California forman un margen de deriva incipiente. El Capítulo III describe las relaciones tectonoestratigráficas en las cuencas del norte del Golfo y propone un modelo esquemático de evolución de la deformación y subsidencia; aquí argumento que la estructura del *rift* angosto es resultado de la evolución de la deformación transtensiva. El Capítulo IV discute la evolución y el acomodo de la deformación en la parte central del Golfo. Finalmente, el Capítulo V expone las implicaciones tectónicas de este trabajo y esboza un modelo de evolución cinemática para el norte del Golfo.

Breve introducción a la geología del Rift del Golfo de California

El *rift* del Golfo de California alberga el límite transtensivo entre las placas Norteamericana y Pacífico y forma la porción oeste de la Provincia Extensional del Golfo (ver Fig. 1, Capítulo I). Se ha propuesto que, la formación de este *rift* es producto del acoplamiento mecánico del bloque continental de Baja California con la Placa Pacífico durante el Mioceno medio a tardío; este acoplamiento imprimió un movimiento hacia el noroeste a la Baja California, mismo que provocó el establecimiento de deformación oblicua orientada NW-SE (Stock y Hodges, 1989; Bohannon y Parsons, 1995).

La arquitectura axial del *rift* del Golfo de California consiste en un arreglo *en echelon* de fallas con paso derecho ligadas por cuencas *pull-apart* ((ver Fig. 1, Capítulo I; Lonsdale, 1989; Fenby y Gastil, 1991). La estructura del *rift* muestra variaciones notables en sentido longitudinal y transversal. Hacia el norte, el *rift* está compuesto por grandes fallas laterales ligadas por amplias zonas de deformación que contienen cuencas *pull-apart* en donde se apilan varios kilómetros de sedimentos; esta sección del *rift* está subyacida por corteza continental y transicional (Phillips, 1964; Henyey y Bischoff, 1973; Fuis y Kohler, 1984; Persaud et al., 2003; González-Fernández et al., 2005).

La parte central y sur del *rift* del Golfo de California está compuesta por fallas transformes ligadas por cuencas bien definidas que se desarrollan sobre corteza transicional y oceánica (Lonsdale, 1989; Fenby y Gastil, 1991). Estas cuencas contienen centenas de metros de sedimentos y en ellas se presenta abundante actividad magmática (Einsele et al., 1980; Curray et al., 1982a; Lonsdale, 1985; Lonsdale, 1989; Aragón-Arreola et al., 2005). Sin embargo, solamente la Cuenca de Alarcón, situada al sur, presenta desarrollo de piso oceánico nuevo (Lonsdale, 1989; Ness et al., 1991).

La estructura del Golfo de California también muestra cambios notables en sentido transversal a su dirección. El margen oriental se desarrolla en corteza continental más gruesa que el margen occidental (Phillips, 1964; Fuis y Kohler, 1984; Couch et al., 1991) y alberga cuencas y fallas abandonadas (Sumner, 1972; Lonsdale, 1989; Brown et al., 2004; Pacheco-Romero, 2004; Aragón-Arreola et al., 2005). Por otra parte, las cuencas activas en el margen central y oeste del *rift* registran actividad magmática probablemente asociada a la dispersión incipiente de piso oceánico (Curry et al., 1982a; Einsele et al., 1980; Lonsdale, 1989; Sawlan, 1991). Estos contrastes geológicos indican la asimetría en la evolución de la actividad tectónica relacionada al proceso de *rifting*.

Uno de los aspectos más controversiales en la historia del Golfo de California es la edad de las primeras incursiones marinas. La hipótesis más aceptada es que las condiciones marinas se establecieron alrededor de ~6.5-6.3 Ma (Oskin y Stock, 2003a); sin embargo, varios autores sugieren la presencia de sedimentos marinos desde el Mioceno medio (Delgado-Argote et al., 2000; Gastil et al., 1999; Helenes y Carreño, 1999; Helenes et al., 2005). Estas evidencias tienen que ser conciliadas para acotar los modelos cinemáticos y dinámicos sobre la apertura del Golfo de California. En esta tesis favorezco la última de estas interpretaciones dado que las muestras usadas por Helenes et al. (2005) provienen de una perforación realizada por Petróleos Mexicanos en la Cuenca Tiburón dentro del área de estudio.

Antecedentes sobre extensión oblicua

En un régimen de extensión no ortogonal, la oblicuidad α se define como el ángulo agudo formado entre el margen de las placas divergentes y el vector de movimiento relativo

(Teyssier et al., 1995). La oblicuidad puede variar dentro de un *rift*; por ejemplo en el Golfo de Adén α varía entre $\sim 51^\circ$ y $\sim 41^\circ$ (Dauteuil et al., 2001), mientras que en el Golfo de California, el rango de oblicuidad va desde los 10° hasta los 25° .

Los experimentos analógicos muestran que la evolución estructural de sistemas oblicuos incluye la nucleación, propagación e interacción de fallas que produce una serie de cuencas escalonadas a lo largo de una zona axial de deformación; si la extensión continúa las cuencas tienden a unirse para formar una zona de rift (Mart y Dauteuil, 2000). Estos experimentos también muestran que los cambios en el ángulo de oblicuidad producen variaciones en el estilo de deformación (Bonini et al., 1997; Dauteuil et al., 2001). Si la oblicuidad es alta ($\alpha \rightarrow 0$), la deformación se distribuye a lo largo de fallas laterales y normales de alto ángulo; las fallas laterales bordean el *rift* y se orientan subparalelas a la tendencia general del *rift*, mientras que las fallas normales se desarrollan oblicuas a la orientación general del *rift* y están limitadas por las fallas laterales. Si la oblicuidad es moderada o baja ($\alpha \rightarrow 90$), la deformación tiende a ser acomodada por fallas escalonadas de buzamiento moderado y desplazamiento compuesto cuya orientación es oblicua a la dirección del *rift* y al vector de movimiento entre placas (Withjack y Jamison, 1986; Keep y McClay, 1997; Bonini et al., 1997). La transición entre estos comportamientos se observa con $\alpha \approx 20-30^\circ$; además, es notorio que con oblicuidad alta la deformación es acomodada por partición (Teyssier et al., 1995; Withjack y Jamison, 1986).

El modelado analógico de dos episodios consecutivos de extensión ortogonal y oblicua muestra que la primera fase de extensión ejerce una clara influencia sobre los patrones de fallamiento producidos en la segunda fase. La extensión ortogonal seguida por extensión oblicua, produce arreglos complejos de fallas segmentadas que desarrollan rampas de

relevo; la mayoría de estas estructuras se orientan subparalelas a la dirección del *rift*. En estos experimentos se observa que si la oblicuidad $\alpha \geq 45^\circ$, las fallas maestras acomodan la mayor parte de la deformación, pero si $\alpha < 45^\circ$, la deformación está distribuida (Bonini et al., 1997; Keep y McClay, 1997). Cuando en los experimentos analógicos la extensión oblicua es seguida por extensión ortogonal, las fallas tienden a coalescer formando arreglos irregulares, pero continuos (Keep y McClay, 1997), además si la oblicuidad $\alpha \geq 45^\circ$, las fallas resultantes son principalmente de deslizamiento oblicuo y permanecen activas durante la segunda fase de extensión; si la oblicuidad $\alpha < 45^\circ$, se desarrollan varias fallas normales paralelas a la dirección del rift (Bonini et al., 1997). Estos modelos muestran que la distribución del fallamiento es asimétrica en cualquier secuencia de deformación (Bonini et al., 1997; Keep y McClay, 1997).

Los modelos analógicos y numéricos de apertura oblicua dan información valiosa sobre la evolución del Golfo de California. En este trabajo contrasto los resultados de ambos modelados con las observaciones geológicas para explicar algunos aspectos de este *rift*, como el estilo de deformación y sus variaciones espacio-temporales, la configuración de las cuencas y el retraso del inicio de la formación de piso oceánico *sensu stricto*.

Base de datos y metodología

La base de datos usada en los Capítulos II y III consiste de ~3600 km de líneas de sísmica de reflexión multicanal obtenida por Petróleos Mexicanos a principio de los años ochenta. Estos datos tienen una redundancia de 4800% y fueron adquiridos con un *streamer* de 2400 m de largo con 48 canales, un arreglo de cañones de aire de 21.98 l (1341 pulgadas cúbicas) y un intervalo de disparo de 25 m. La longitud de registro fue de 6.144 s con un

intervalo de muestreo de 2 ms. La calidad de los datos sísmicos es variable y es menor en la parte central y noroeste del Golfo, donde la razón señal/ruido es menor debido a ruido coherente y aleatorio, además de la alta dispersión; en esta región la estructura profunda no fue resuelta.

El procesamiento incluyó el manejo y acondicionamiento de los datos, el filtrado digital, correcciones por divergencia esférica e introducción de geometría, deconvolución predictiva, análisis de velocidad por semblanza, corrección por *normal move-out*, apilado y migración post-apilado en tiempo (Yilmaz, 1987; Sheriff y Geldart, 1995); la interpretación geológica se hizo a partir de datos migrados. La Figura 2 (ver Capítulo I) muestra un diagrama de flujo del procesamiento e incluye los parámetros de filtrado y correcciones. Para el procesamiento sísmico se emplearon los códigos de dominio público de *Seismic Unix* (<http://www.cwp.miles.edu/cwpcodes/>); para la interpretación geológica se utilizó el programa de dominio público SeisWide (<http://phys.ocean.dal.ca/~deping>). Los perfiles migrados, con y sin interpretación se presentan en el Apéndice 1, mientras que el Apéndice 2 presenta dos *script* tipo para el procesamiento de datos sísmicos usando los códigos de *Seismic Unix*. La cartografía estructural mostrada en los Capítulos II, III y IV fue diseñada para escala 1:500,000 y está basada en la interpretación y correlación de los elementos estructurales más prominentes.

Para el Capítulo IV se emplearon dos bases de datos. La primera incluye dos perfiles de sísmica de reflexión multicanal y los datos correspondientes de anomalía gravimétrica de aire libre. Estos datos fueron colectados en 1996 durante el proyecto *Crustal Offshore Research Transect by Extensive Seismic Profiling Project* CORTES-P96 a bordo del BO Hespérides, de bandera española (Dañobeitia et al., 1997). Los datos sísmicos fueron

procesados e interpretados en forma similar a la seguida con los datos de Petróleos Mexicanos. La anomalía gravimétrica de aire libre se empleó en forma cualitativa para acotar la interpretación. Los datos sísmicos fueron adquiridos con un *streamer* de 2400 m de largo con 96 canales, usando un arreglo de cañones de aire de 46.7 l (2850 pulgadas cúbicas), con un intervalo de disparo de 30 s a una velocidad de 5 nudos; este arreglo retorna una redundancia de 1600 %; el intervalo de muestreo fue de 2 ms y la longitud del registro fue de 15 s. La segunda base de datos usada en el Capítulo IV incluye cinco perfiles de sísmica de reflexión multicanal procesados e interpretados por [Albertin \(1989\)](#) para su tesis de maestría en la Universidad de Texas en Austin. Estos datos fueron colectados en 1978 por *Scripps Institution of Oceanography* durante la Expedición Guaymas.

A lo largo de este trabajo, las profundidades están reportadas en términos de segundos de tiempo doble de viaje. La profundidad y el espesor real de algunos rasgos geológicos han sido estimados con las velocidades de intervalo calculadas a partir de las velocidades de valor cuadrático medio (*rms*, *root mean square*, por sus siglas en Inglés) obtenidas en los análisis de velocidad por semblanza.

TABLE OF CONTENTS	Page
ABSTRACT	i
RESUMEN	ii
ACKNOWLEDGEMENTS	vi
SINOPSIS.....	viii
Propósito de este trabajo	viii
El problema: de la ruptura continental a la propagación de piso oceánico	ix
Breve introducción a la geología del Rift del Golfo de California	xi
Antecedentes sobre extensión oblicua.....	xii
Base de datos y metodología	xiv
I. INTRODUCTION	1
I.1. Scope of this work	1
I.2. Problem layout: from continental to mid-ocean rifting	1
I.3. Brief introduction on the geologic settings of the Gulf of California rift	3
I.4. Background of oblique extension	6
I.5. Data set and methodology	8
II. WESTWARD MIGRATION OF EXTENSION IN THE NORTHERN GULF OF CALIFORNIA.....	12
II.1. Abstract.....	12
II.2. Introduction	12
II.3. Geologic framework	14
II.4. Results: Structure of the northern Gulf of California	15
II.5. Discussion.....	21
II.6. Conclusions	25
III. TECTONOSEDIMENTARY EVOLUTION OF THE INACTIVE NEOGENE BASINS IN THE NORTHEASTERN GULF OF CALIFORNIA, MEXICO	26
III.1. Abstract	26
III.2. Introduction	27
III.3. Geologic setting of the northern Gulf of California.....	28
III.4. Results: seismostratigraphic record in the northeastern Gulf of California	32
III.4.1. The Upper Tiburón basin	33
III.4.2. The Adair-Tepoca basin	40
III.4.3. Seismostratigraphic correlation of the inactive basins	46
III.5. Discussion	47
III.5.1. Tectono-sedimentary evolution of the Upper Tiburón and Adair-Tepoca basins	48
III.5.2. Relevance of detachment faulting in oblique rifting.....	54
III.5.3. Constraints to the timing of early marine sedimentation in the northern Gulf.....	55
III.6. Conclusions	56
IV. STRUCTURE OF THE RIFT BASINS IN THE CENTRAL GULF OF CALIFORNIA: KINEMATIC IMPLICATIONS FOR OBLIQUE RIFTING	58
IV.1. Abstract	58
IV.2. Introduction	59

IV.3. Regional geological framework	63
IV.4. Observations and interpretation	67
IV.4.1. Structure of the Yaqui Basin	67
IV.4.2. Structure of the Guaymas Basin	74
IV.4.3. Seismic stratigraphy in the Yaqui Basin	74
IV.4.4. Seismic stratigraphy in the Guaymas Basin	77
IV.5. Discussion	78
IV.5.1. Basement structure	78
IV.5.2. Geometry of fault arrays	78
IV.5.3. Strain accommodation in the central Gulf	82
IV.5.4. Sedimentary basins	83
IV.5.5. Magmatism	87
IV.5.6. Kinematic implications	88
IV.6. Conclusions	90
V. DISCUSSION	93
V.1. The Gulf of California and the Basin and Range Province	94
V.2. Structural geometry, strain partitioning and the accommodation of large amount of extension in the northern Gulf	95
V.3. Role of sedimentation in the accommodation of extension and the delay of spreading of new oceanic floor	100
V.4. Asymmetry of rifting of western North America	102
VI. CONCLUSIONS	107
VII. CITED REFERENCES	109
APPENDIX 1. MIGRATED AND INTERPRETED MULTICHANNEL SEISMIC REFLECTION PROFILES OF THE NORTHERN GULF OF CALIFORNIA	118
APPENDIX 2. TYPE SCRIPTS FOR PROCESSING OF MULTICHANNEL SEISMIC REFLECTION DATA USING THE PUBLIC DOMAIN CODES OF SEISMIC UNIX	119

LIST OF FIGURES

Figure	Page
1	5
2	10
3	13
4	17-18

1 Tectonic map of the Gulf of California rift region (after Lonsdale, 1989; Fenby and Gastil, 1991); the digital elevation model is plotted as background. The Gulf of California rift hosts the modern transtensional boundary of the North America and Pacific plates that is formed by right-stepping faults linked by pull-apart basins (highlighted). The inset map shows the regional plate boundary framework and the main tectonic provinces around the Gulf, including the Sierra Madre Occidental (SMO), the Basin and Range Province (B&R), the Trans Mexican Volcanic Belt (TMV) and the Peninsular Ranges of Baja California (BC). The shaded area represents the Gulf Extensional Province. The relative motion of the Pacific Plate with respect to the North America Plate is also shown. Other abbreviations: F, fault; B, basin; MAT, Middle America Trench.

2 Flow diagram for processing and interpretation of multichannel seismic data.

3 a). Regional tectonic framework of western North America and northwestern México (after [Stock and Hodges, 1989](#); [Lonsdale, 1989](#); [Fenby and Gastil, 1991](#)). The arrow shows the relative motion of the Pacific-North America plates. b). Layout of processed seismic lines. c). Structural map of the northern Gulf of California. The eastern margin contains inactive basins and faults, while the western margin includes active basins of the modern rift. The pattern of active depocenters and shallow fault arrays are from [Persaud et al. \(2003\)](#). Faults outside data coverage are from [Fenby and Gastil \(1991\)](#). PA, Pacific Plate; GC, Gulf of California; GEP, Gulf Extensional Province; B&R, Basin and Range Province; SMO, Sierra Madre Occidental; CP, Colorado Plateau; ITI, Isla Tiburón; IAG, Isla Ángel de la Guarda.

4 Main geological features in the northern Gulf of California as imaged in the seismic reflection profiles. a). Subsidence in the Wagner basin is controlled by the Wagner fault. Eastward, the Adair graben forms the northern end of the Adair-Tepoca basin. Note that sequence boundary B-C is correlated across both basin systems. b). Sequence B in the Adair-Tepoca basin was syntectonic to the Amado fault; while sequence C drapes the structural relief and represents post-tectonic deposition. c). The Upper Delfin and Adair-Tepoca basins are bounded by a wide anticline; note the same stratal relation between the active and inactive basins mentioned above. d). The Upper Tiburón basin is bounded by the De Mar and Tiburón faults. Sequence A represent the older deposits in the northern Gulf and pre-dates the onset of narrow rifting. Sequence B

was syntectonic to the growth of the basin-bounding faults; sequence C represents post-tectonic sedimentation.

- 5 The eastern Gulf of California contains abandoned rift basins, while active rifting occurs in the western Gulf (Lonsdale, 1989; Fenby and Gastil, 1991; Persaud et al., 2003; Aragón-Arreola et al., 2005; this study). The eastern Gulf constitutes an abandoned rift margin (see inset map). Same abbreviations as in Figure 3. 24

- 6 a). Geologic map of the northern Gulf of California after the interpretation and correlation of multichannel seismic reflection profiles (from Aragón-Arreola and Martín-Barajas, 2007). The eastern margin hosts the inactive Upper Tiburón and Adair-Tepoca basin, controlled by growth of large transtensional faults, whereas the western margin hosts the modern Lower Delfín, Upper Delfín, Consag and Wagner basins, localized within a large stepover zone of the Canal de Ballenas transform fault and the Cerro Prieto fault. PEMEX drilled an exploratory hole of ~4800 m in the Upper Tiburón basin (W). The highlighted profiles are shown in further figures. b). Regional tectonic framework of northwestern México (after Lonsdale, 1989). The Gulf of California, within the Gulf Extensional Province (GEP), hosts a highly oblique rift that forms the modern transtensional boundary between the Pacific (PA) and North America (NA) plates. c). Interpreted seismic reflection data, highlighting the profiles presented in this paper. Other abbreviations: Baja California (BC); Basin and Range province (B&R); Sierra Madre Occidental (SMO); Isla Tiburón (ITI); Isla Ángel de la Guarda (IAG); reference line (RL). 29

- 7 Migrated and interpreted seismic profile across the central section of the Upper Tiburón basin. The sedimentary column is formed by three main seismic sequences that represent pre-rift (sequence A), syn-rift (sequence B) and post-rift facies (sequence C). Note that sediments of the syn-tectonic sequence B accrete toward the west (sb: sequence boundary). 34

- 8 Migrated and interpreted seismic profile across the northern half of the Upper Tiburón basin. Note the three main seismic sequences interpreted as pre-rift (sequence A), syn-rift (sequence B) and post-rift facies (sequence C). Here the syn-tectonic sequence B accretes toward the east. To the west, sequence A and B are folded and truncated at the basement; we infer the presence of a top-to-the east detachment fault (sb: sequence boundary). 35

- 9 Migrated and interpreted seismic profile across the northern end of the Upper Tiburón basin and the southern end of the Adair-Tepoca basin. Reflectors display parallel patterns over this region. To the west, sequence A and B are folded and truncated at the basement; thus we infer a top-to-the east detachment fault. Sequence C drapes the relief, and extends and

- thickens downward into the Lower Delfin basin (sb: sequence boundary). 36
- 10 Summary of interpreted seismic profiles across the Upper Tiburón basin; location of boxes is shown in Figure 6. The interpreted pre-rift sequence A onlap and blanket the basement and is displaced by the basin bounding faults. The syn-rift sequence B form growth strata that accrete on the basin bounding faults; note the change of sedimentary accretion direction across the basin (highlighted by the large arrows in boxes A to G), to the south sediments accrete westward (boxes A-D), whilst to the north sediments accrete eastward (boxes E-G). The post-rift sequence C drapes the relief, extending and thickening downward into the Lower Delfin basin (boxes G-H). At the northwest, sequence A and B are folded and truncated at the basement; thus we infer the presence of a top-to-the east detachment fault (boxes F-H). Figures 7, 8 and 9 only show part of the summarized interpretations in the boxes D, G and H; use reference line (RL) for correspondence. (DMF: De Mar fault; DHA, doubly hinged anticline). 38
- 11 Migrated and interpreted seismic profile across the northern half of the Adair-Tepoca basin. Sequence I is interpreted to represent syn-rift facies, whereas in this profile sequence B and sequence C drape and smooth the relief. Sequence I and B are folded and build the doubly-hinged anticline that forms the western boundary of the Adair-Tepoca basin (sb: sequence boundary). 41
- 12 Migrated and interpreted seismic profile across the northern Adair-Tepoca basin. Sequence I fill by onlap the Adair Graben and is likely associated to the growth of the Amado fault, whereas sequence B and sequence C drape and smooth the relief. Sequence I and B are folded and build the northern end of the doubly-hinged anticline that bounds the Adair-Tepoca basin (sb: sequence boundary). 42
- 13 Summary of interpreted seismic profiles across the Adair-Tepoca basin; location of boxes is shown in Figure 6. Sediments in the northern sequence I formed growth strata associated to growth of the Amado fault (L to O); far south, sequence I may have fill a broad depression (H to K). The south-deepening shape of the Adair graben suggests that this trough canalized sediments into the Adair-Tepoca basin. The lowermost strata of sequence B form divergent patterns likely syntectonic to the Amado fault (L), whereas the upper strata drape the relief and form a broad hammock-shaped sequence that reflect deposition in a preexisting basin (H to K). The upper sequence C is post-tectonic to the Amado fault and peneplained the bathymetric relief. Toward the west, sequence I and B are folded and extend beyond the doubly-hinged anticline that bounds the Adair-Tepoca basin. Figures 9, 11 and 12 only show part of the summarized interpretations in boxes H, M and N; use reference line (RL)

- for correspondence. (DHA, doubly hinged anticline; AG, Adair graben; CPF, Cerro Prieto fault). 44
- 14 Schematic model of evolution for the northern segment of the Upper Tiburón basin in the northern Gulf of California (DMF: De Mar fault; DHA: doubly-hinged anticline/roll over anticline?; iDF: inferred detachment fault). 49
- 15 Main tectonic features of the central Gulf of California (after [Fenby and Gastil, 1991](#)) showing analyzed and compiled profiles from [Albertin \(1989\)](#); the bathymetric data is plotted as background. The shaded area over the Guaymas Basin shows the interpreted extent of transitional crust ([Albertin, 1989](#)). The five sites drilled by the Deep Sea Drilling Project Leg 64 are also shown ([Curry et al., 1982a, 1982b](#)). Note that the Ballenas Transform Fault is oriented 6-7° more northerly than the Guaymas Transform Fault. The N-S oriented Bahía de los Ángeles (BAG) and Bahía de las Ánimas (BAnG) grabens in Baja California and the Empalme Graben in Sonora were formed during mid-Miocene time ([Delgado-Argote et al., 2000](#); [Mora-Álvarez and McDowell, 2000](#); [Roldán-Quintana, et al., 2004](#)), while the half-graben Loreto (LoB), Concepción (CoB) and Santa Rosalía (SrB) basins, in the Baja California coastal plain, evolved during late Miocene-early Pliocene time ([Dorsey and Umhoefer, 2000](#); [Ledesma-Vásquez and Johnson, 2001](#)). The dashed box indicates area detailed in [Figure 22](#). The inset sketches the main tectonic features around the Gulf of California, including the Gulf Extensional Province, the Gulf of California rift; and the area with new oceanic floor. The Gulf of California rift forms the transtensional boundary of the North America (NA) and Pacific (PA) plates. Other abbreviations: TF, transform fault; PI, Pedro Nolasco Island; TI, Tortuga Island; MAT, Mid America Trench. 61
- 16 Free air gravity anomaly of the central Gulf of California ([CONMAR, 1987](#)), showing the simplified main tectonic features (after [Fenby and Gastil, 1991](#)). The shaded area over the Guaymas Basin represents the interpreted extent of transitional crust ([Albertin, 1989](#)). The Guaymas Transform Fault splits the central Gulf of California in two domains. The northeastern domain extends over the Yaqui Basin and contains the Pedro Nolasco Gravity High (PNGH) and an adjacent gravity low, lying parallel to the Ballenas and Tiburón transform faults. The southwestern domain coincides with the Guaymas Basin and contains the Tortuga Gravity High (TGH), oriented parallel to the Guaymas Transform Fault. The dashed box indicates the area detailed in [Figure 22](#). Other abbreviation: TF, transform fault; SMGH, San Miguel Gravity High; NGL, North Guaymas Low. 66
- 17 Profile P307 across the Yaqui and northern Guaymas basins in the

- central Gulf of California showing the free-air gravity anomaly profile (upper), the migrated section (center), and the interpreted structural and seismostratigraphic features (lower). Location of sequence labels indicates the locus of sequence maximum thickness. Site 479 of the Deep Sea Drilling Project is projected to the profile. 69
- 18 Profile P309 across the northern Yaqui Basins offshore Sonoran in the central Gulf of California showing the free-air gravity anomaly profile (upper), the migrated section (center), and the interpreted structural and seismostratigraphic features (lower). 70
- 19 Detail of Profile P307 (migrated section) across the eastern margin of the Yaqui Basins highlighting interpreted structural and seismostratigraphic features. Location of sequence labels indicates the locus of the maximum sequence thickness. Site 479 of the Deep Sea Drilling Project is projected to the profile. 71
- 20 Detail of Profile P307 (migrated section) across the northern Guaymas Basins. Note the westward migration of the maximum sequence thickness (indicated by location of sequence labels). The highlighted high-amplitude reflectors are interpreted as a zone of sills intruding a shallow stratigraphic interval within Sequence II. 72
- 21 Seismostratigraphic interpretation of analyzed and compiled multichannel seismic reflection profiles. Profiles A1 through A4 were taken from Albertin (1989). The dashed lines show the structural correlation; line weight and dash length indicate the relative importance of each fault. This correlation was used to compile the structural map of Figure D8. Sites 479, 480 and 481 of the Deep Sea Drilling Project are projected into the corresponding profiles. Note that Profile P309 is oblique to the main structural fabric, while profile A4 lies nearly parallel to the main fault orientation. 73
- 22 Structural map of the central Gulf of California compiled after the interpretation of multichannel seismic reflection profiles shown in Figure D7. The free-air gravity anomaly is presented as background (after CONMAR, 1987). Shaded area over the Guaymas Basin indicates the interpreted extent of transitional crust (Albertin, 1989); the sites drilled by the Deep Sea Drilling Project are also shown (Curry et al., 1982a, 1982b). The mapped faults are drafted with solid-bold lines, while the shaded zone tie to each fault represents the relative throw and dip direction. The tectonic features off the profile coverage were taken from Fenby and Gastil (1991). The central Gulf can be separated in two tectono-sedimentary domains. In the eastern domain, the East and West Pedro Nolasco faults, that probably form the southernmost segment of the Tiburón Fault System, co-evolved with the large-throw Yaqui Fault, which controlled the half-graben Yaqui Basin. In the western domain the

active Guaymas Transform Fault controls evolution of the Guaymas Basin, in an early stage this basin evolved as a half-graben, but now hosts the Guaymas Spreading Center. The shift from continental to oceanic crust in the Guaymas Basin must be localized south of profile A2 and north of profile A3. Abbreviations: TF, transform fault; PN, Pedro Nolasco Island; TO, Tortuga Island; TGH, Tortuga Gravity High; TVR, Tortuga Volcanic Ridge. 80

- 23 Main structural elements in the northern Gulf of California plotted in an equal angle stereographic projection. The rift obliquity in the northern Gulf varies between 9° and 12° , as can be estimated by the acute angle formed by the rift orientation and the predicted motion vectors of Baja California with respect to fixed North America. Assuming a simple shear model of deformation (upper right sketch), the major faults have accommodated most of the strike-slip motion of the North America-Pacific plate boundary, while the secondary structures mainly accrue the extensional deformation. 96

- 24 Composite schematic profile from the Pacific Ocean to the Sierra Madre Occidental across the Adair-Tepoca and Wagner-Consag basins segment of the northern Gulf of California showing the main tectonic features involved in the rupture of continental lithosphere of western North America. The lower part of the figure illustrates the temporal evolution of the major tectonic events. Triangles represent volcanic activity. See text for further explanations. References: *1: [Stock and Hodges \(1989\)](#); [Bohannon and Parsons \(1995\)](#); *2: [Gastil et al. \(1975\)](#); [Núñez-Cornú et al. \(1996\)](#); 3*: [Lee et al. \(1996\)](#); [Martín-Barajas \(2000\)](#); [Axen and Fletcher \(1998\)](#); *4: [Persaud et al. \(2003\)](#); [Aragón-Arreola et al. \(2003\)](#); [Martín-Barajas et al. \(2002\)](#); *5: [Fuis and Kohler \(1984\)](#); [Couch et al. \(1991\)](#); [Núñez-Cornú et al. \(1996\)](#); [González-Fernández et al., \(2005\)](#); *6: [Aragón-Arreola et al. \(2005\)](#); [Aragón-Arreola and Martín-Barajas \(2007\)](#); *7: [Aragón-Arreola et al. \(2003\)](#); [Oskin et al. \(2001\)](#); [Oskin and Stock \(2003b\)](#); *8: [Phillips \(1964\)](#); [Henyey and Bischoff \(1973\)](#); [Couch et al. \(1991\)](#); *9: [Couch et al. \(1991\)](#); [Gans \(1997\)](#); [Mora-Álvarez and McDowell \(2000\)](#); *10: [Couch et al. \(1991\)](#); [Wernicke et al. \(1988\)](#); [Stewart \(1998\)](#); *11: [McDowell and Clabaugh \(1979\)](#). 104

LIST OF TABLES

Table		Page
1	Maximum sequence thickness measured in seconds of two-way travel time, estimated interval velocities and computed maximum sequence thickness in meters of each interpreted seismostratigraphic sequence in the Yaqui and Guaymas basins, of the central Gulf of California. The interval velocities were estimated by semblance velocity analysis.	75

I. INTRODUCTION

I.1. Scope of this work

This work addresses the problem of the kinematic evolution of strain in the highly oblique Gulf of California rift. In this work I used seismic reflection and gravity data to image the upper crustal structure of the Gulf of California; using these images I interpreted and correlated the major geological features to produce a sub-surface geologic map of ~50,000 km² of the northern and central Gulf of California. This work explains the development of basins and faults within this area, and discusses the tectonic evolution since middle Miocene time of ~600 km of the Pacific and North America plate boundary.

I address this work to the geoscientists working in the western United States and northwestern México, as well as researchers in dynamics of extension, analog modeling of extension, and tectonic evolution of rifted margins. In addition, it is likely that this work could be of interest to the oil industry since the studied area is a source of hydrocarbon resources.

I.2. Problem layout: from continental to mid-ocean rifting

Accommodation of deformation during continental rifting involves the temporal evolution of modes of continental extension predicted by numerical models, known as the core complex, the wide rift and the narrow rift modes of extension (Buck, 1991). The main factors controlling the change in extensional mode include the variation in crustal thickness, thermal structure, strain rate and lithospheric rheology (Buck, 1991; Ruppel, 1995; Hopper and Buck, 1996). Given a thick and brittle crust, the extensional deformation leads to the definition of multiple and distributed normal faults regardless of the strain rate.

In contrast, given a thin and brittle crust, the fast rate of cohesion reduction leads to the formation of asymmetric grabens and eventually to the development of large offset listric faults, while with very low rates of cohesion reduction, the strain tends to be accommodated by listric faulting ([Lavie et al., 2000](#)).

The southwestern United States and northwestern México have experienced the three modes of extension ([Buck, 1991](#)) mentioned above. During early Oligocene to mid Miocene time, the Basin and Range Province extended in the core complex and wide rift modes ([Stewart, 1998](#)). Later, in mid-to-late Miocene time, the Gulf Extensional Province extended in the wide rift mode. Finally, since the late Miocene, the strain localized into the Gulf of California in the narrow rift mode; nevertheless, only the southernmost portion of this rift has led to the formation of new oceanic floor ([Stock and Hodges, 1989](#); [Lonsdale, 1989](#)). The study of the Gulf of California is important because it provides information of a narrow rift in which the continental rupture has passed throughout different modes of continental extension until breaking new oceanic crust.

Continental rifts are long and narrow valleys bounded by faults on one or both sides ([Scholz and Contreras, 1998](#)). The rift evolution yields the formation of fault-controlled sedimentary basins, such that either half grabens or asymmetric grabens become the basic element of continental rifts ([Rosendahl, 1987](#); [Gawthorpe and Leeder, 2000](#); [Contreras and Scholz, 2001](#)).

The basin stratigraphy in a developed continental rift records an early stage of slow subsidence or rift initiation followed by an abrupt increase of subsidence rate or rift climax ([Prosser, 1993](#); [Gawthorpe and Leeder, 2000](#)). These stages depend on variations in the fault behavior and display conspicuous variations of stratigraphic record; thus, the basin

architecture is function of the tectonic processes linked to the climatic and eustatic sea-level changes (Prosser, 1993; Cowie et al., 2000; Gawthorpe and Leeder, 2000; Gupta and Cowie, 2000).

This work addresses the tectono-sedimentary evolution of rift basins in the northern and central Gulf of California. Chapter II provides a detailed description of the mapped structure of the northern Gulf and proposes that the abandoned basins in the eastern Gulf of California rift form an incipient drifting margin. Chapter III describes the tectonosedimentary relations and proposes an sketch model of evolution for the basins of the northern Gulf; here I argue that the structural geometry fully resulted from transtensional strain. Chapter IV discusses evolution of strain accommodation in the central Gulf of California. Finally, Chapter V synthesizes the tectonic implications of this work and outlines a model of kinematic evolution of the northern Gulf of California rift.

1.3. Brief introduction on the geologic settings of the Gulf of California rift

The Gulf of California rift hosts the transtensional boundary of the North America and Pacific plates and forms the western portion of the Gulf Extensional Province (Fig. 1). It appears that the evolution of this rift is related to the mechanical coupling of the continental block of Baja California with the Pacific Plate during mid-to-late Miocene time; this coupling imported a northwestward motion on the Baja California block that resulted in the onset of NW-SE oriented oblique deformation (Stock and Hodges, 1989; Bohannon and Parsons, 1995).

The axial architecture of the Gulf of California rift consists of an en echelon array of right-stepping faults linked by pull-apart basins (Lonsdale, 1989; Fenby and Gastil, 1991). The

rift structure shows conspicuous along-and across-strike variations. Northward the modern rift consists of some large strike-slip faults linked by broad deformation zones that contain pull-apart basins with kilometers of sediments; this rift section is underlain by continental and transitional crust (Phillips, 1964; Henyey and Bischoff, 1973; Fuis and Kohler, 1984; Persaud et al., 2003; González-Fernández et al., 2005).

The central and southern Gulf of California rift is built by oceanic-like transform faults linked by well-defined basins floored by transitional and oceanic crust (Lonsdale, 1989; Fenby and Gastil, 1991). These basins contain hundreds of meters of sediments and record conspicuous magmatic activity (Einsele et al., 1980; Curray et al., 1982a; Lonsdale, 1985; Lonsdale, 1989; Aragón-Arreola et al., 2005). However, only the southernmost Alarcón Basin hosts an appreciable width of true oceanic floor (Lonsdale, 1989; Ness et al., 1991).

Figure 1. Tectonic map of the Gulf of California rift region (after Lonsdale, 1989; Fenby and Gastil, 1991); the digital elevation model is plotted as background. The Gulf of California rift hosts the modern transtensional boundary of the North America and Pacific plates that is formed by right-stepping faults linked by pull-apart basins. The inset map shows the regional plate boundary framework and the main tectonic provinces around the Gulf, including the Sierra Madre Occidental (SMO), the Basin and Range Province (B&R), the Trans Mexican Volcanic Belt (TMV) and the Peninsular Ranges of Baja California (BC). The shaded area represents the Gulf Extensional Province. The relative motion of the Pacific Plate with respect to the North America Plate is also shown. Other abbreviations: F, fault; B, basin; MAT, Middle America Trench

Figura 1. Mapa tectónico de la región del rift del Golfo de California (tomado de Lonsdale, 1989; Fenby y Gastil, 1991), usando como información de fondo el modelo digital de elevaciones. El rift del Golfo de California aloja la frontera transtensiva de las placas Norteamérica y Pacífica; que está formada por fallas de salto derecho ligadas por cuencas tipo *pull-apart*. El recuadro muestra el marco regional de límites de placas y las principales provincias tectónicas alrededor del Golfo, incluyendo la Sierra Madre Occidental (SMO), la provincia de Sierras y Cuencas (B&R), el Eje Volcánico Transmexicano (TMV) y las Sierras Peninsulares de Baja California (BC). El área sombreada representa la Provincia Extensional del Golfo. Se muestra también el movimiento relativo de la Placa Pacífico con respecto a la Placa Norteamericana. Otras abreviaturas: F, falla; B, Cuenca; MAT, Trinchera Mesoamericana.

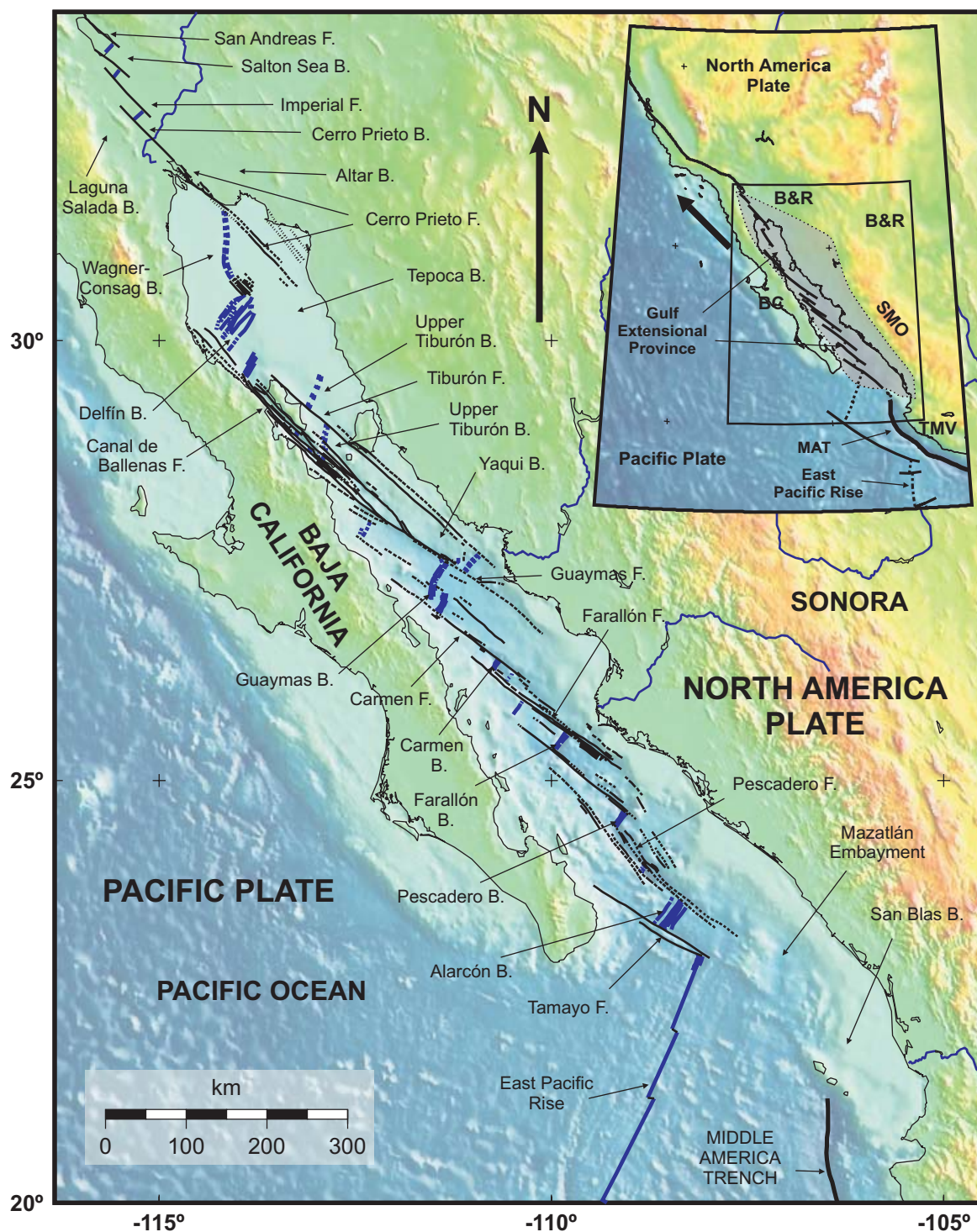


Figure 1

The structure of the Gulf of California rift also shows noticeable changes across strike. The eastern margin sits on thicker continental crust than the western margin (Phillips, 1964; Fuis and Kohler, 1984; Couch et al., 1991) and hosts abandoned basins and faults (Sumner, 1972; Lonsdale, 1989; Brown et al., 2004; Pacheco-Romero, 2004; Aragón-Arreola et al., 2005). Besides, the basins in the central and western rift record magmatic activity likely associated with incipient oceanic spreading (Curry et al., 1982a; Einsele et al., 1980; Lonsdale, 1989; Sawlan, 1991). These geological contrasts indicate the asymmetric evolution of the tectonic activity related to the rifting process.

One of the more controversial issues in the geological history of the Gulf of California is the timing of early marine sedimentation. One recent hypothesis is that the marine conditions were not established in the northern Gulf until ~6.5-6.3 Ma (Oskin and Stock, 2003a); however several authors suggest the presence of marine sediments since mid Miocene time (Delgado-Argote et al., 2000; Gastil et al., 1999; Helenes and Carreño, 1999; Helenes et al., 2005). These controversial interpretations have to be reconciled to constrain the rifting of the Gulf of California. In this thesis I follow the later interpretation since the samples used by Helenes et al. (2005) were collected in a well drilled by Petróleos Mexicanos in the Tiburón Basin; this is, within the studied area.

1.4. Background of oblique extension

In non-orthogonal extension, obliquity α is defined as the acute angle formed between the diverging plate margins and the plate motion vector (Teyssier et al., 1995). Obliquity may vary within a rift, *e.g.* in the Gulf of Aden α varies from ~51° to ~41° (Dauteuil et al., 2001), while in the Gulf of California obliquity ranges between 10 and 25°.

Analog experiments show that the structural evolution of oblique rift systems includes the nucleation, propagation and fault interaction that produces a set of en echelon basins along an axial zone of deformation; with continued extension the basins tend to coalesce and merge into a single single rift (Mart and Dauteuil, 2000). These experiments also show that variations in obliquity result in changes of deformation style (Bonini et al., 1997; Dauteuil et al., 2001). With high obliquity ($\alpha \rightarrow 0$) the deformation is partitioned into strike-slip and high angle normal faults; the strike-slip faults usually bound the rift zone and are oriented sub-parallel to the rift trend, while the normal faults form at high angles to the rift direction and are bounded by the strike-slip faults. At moderate or low obliquity ($\alpha \rightarrow 90$), the deformation is accommodated by moderately dipping compose-slip faults oriented oblique to the rift trend and plate motion vector and disposed in a staggered array (Withjack and Jamison, 1986; Keep and McClay, 1997; Bonini et al., 1997). The transition between these end-member behaviors is observed at $\alpha \approx 20-30^\circ$ it is notable that at high obliquity most of the strain is partitioned (Teyssier et al., 1995; Withjack and Jamison, 1986).

The analog modeling of two consecutive episodes of orthogonal and oblique extension shows that the first phase of extension clearly influences the fault patterns produced by the second phase. Orthogonal rifting followed by oblique extension produces marked segmentation of fault systems, development of relay ramps and complex interacting fault arrays, in which most structures are oriented near to the rift direction. If $\alpha \geq 45^\circ$, the master faults of the first stage continue to take up most of the displacement during the oblique stage, whereas if $\alpha < 45^\circ$, deformation is distributed (Keep and McClay, 1997; Bonini et al., 1997). In oblique rifting followed by orthogonal extension, faults coalesce and form continuous, but irregular arrays (Keep and McClay, 1997). If $\alpha \geq 45^\circ$ the

resulting faults are mainly oblique-slip structures that remain active during the orthogonal phase; when $\alpha < 45^\circ$, several rift-parallel normal faults are developed (Bonini et al., 1997). These models also show that fault distribution is always asymmetric regardless the sequence of deformation (Bonini et al., 1997; Keep and McClay, 1997).

The analog and numerical models of oblique rifting provide valuable hints about the evolution of the Gulf of California. Throughout this work I contrast the results of both types of modeling with the geological observations in order to understand key issues of this rift system, including strain accommodation style and its spatio-temporal variations, the basinal configuration and the delay of oceanic-style spreading.

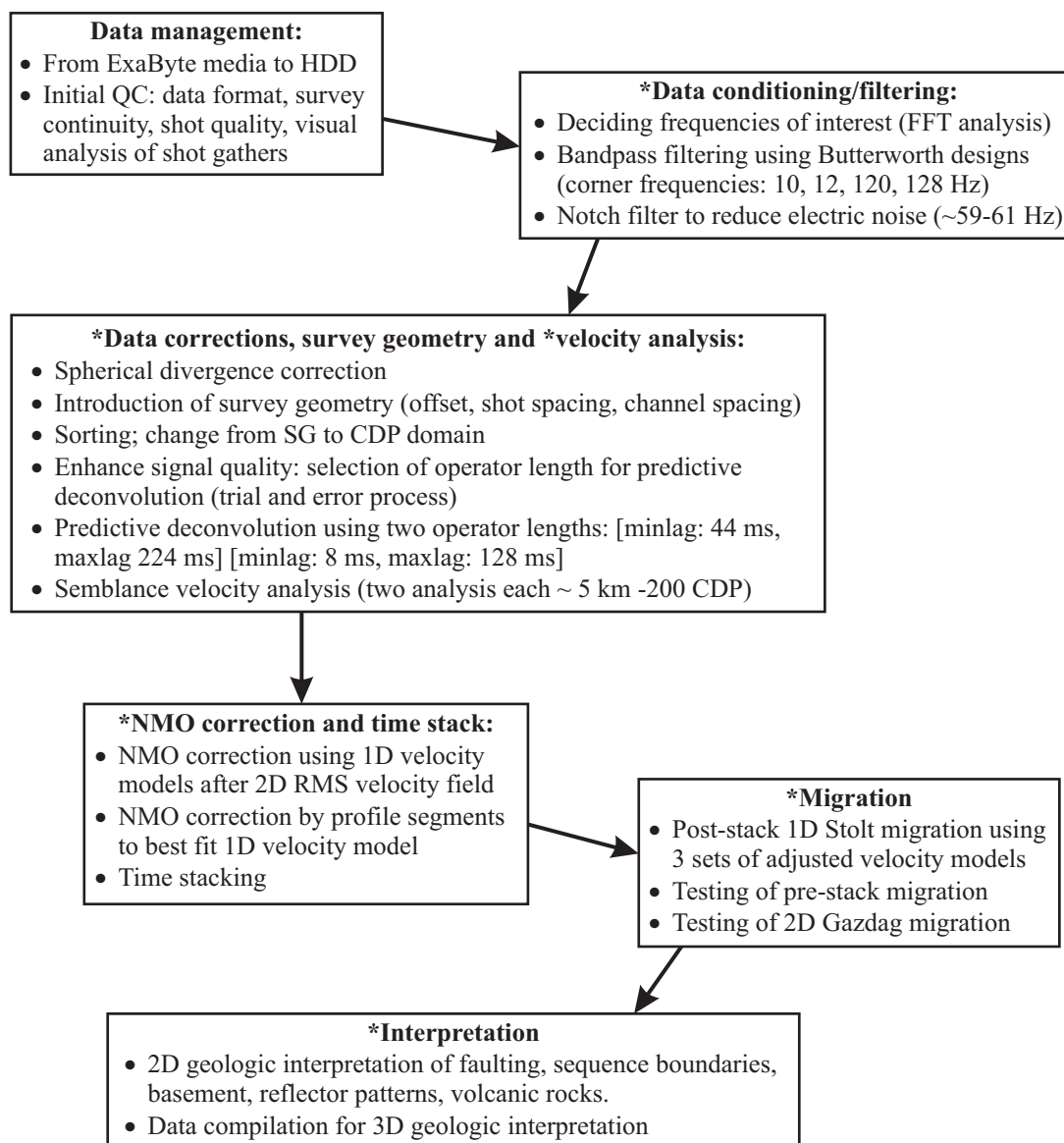
1.5. Data set and methodology

The data base used in Chapters II and III consists of ~3600 km of lines of multichannel seismic reflection data surveyed by Petróleos Mexicanos in the early 1980's. These data have a 48-fold and were acquired with a 48-channel, 2400 m-long streamer, a 21.98 l (1341 cu. in.) air gun array, and a shot interval of 25 m. Record length was 6.144 s with a sampling rate of 2 ms. The quality of seismic data varies within the surveyed area and is lower beneath the central and northeastern Gulf, where the signal-to-noise ratio is low due to coherent and random noise and high scattering; in this area the deep structure was not resolved.

Processing included data management, digital filtering, data corrections including spherical spreading correction, introduction of field survey geometry, predictive deconvolution, semblance velocity analysis, normal move-out correction, stacking and post-stack time migration (see Yilmaz, 1987; Sheriff and Geldart, 1995); the geological interpretation was

performed on migrated seismic data. **Figure 2** shows a flow diagram of steps followed for the processing and interpretation of multichannel seismic data; this diagram also includes the filtering correction parameters. The seismic processing was performed using the public domain codes of Seismic Unix (<http://www.cwp.miles.edu/cwpcodes/>), while the public domain SeisWide program (<http://phys.ocean.dal.ca/~deping>) was used for geologic interpretation. The migrated profiles with and without interpretation are presented in **Appendix 1**; whereas **Appendix 2** presents two type scripts for the processing of seismic reflection data using Seismic Unix. The structural mapping shown in the Chapters II, III and IV was designed for 1:500,000 scale and is based on the interpretation and correlation of prominent structural elements.

Two data sets were used in Chapter IV. The first includes two multichannel seismic reflection profiles and the corresponding free-air gravity data. These data were surveyed in 1996 during the Crustal Offshore Research Transect by Extensive Seismic Profiling Project CORTES-P96 on board the Spanish RVIB Hespérides ([Dañobeitia et al., 1997](#)). The seismic data were processed and interpreted following a sequence similar to that previously described for the Petróleos Mexicanos data and the free-air gravity anomaly was used in a qualitative way to constrain the interpretation. The seismic data were acquired with a 96-channel, 2400 m-long streamer, using a 2850 cu. in. (46.7 l) air gun array as the wave source; with a 30 s shot interval and 5 knots cruise speed, this layout returned a 16 fold record. The sampling interval was 2 ms and the record length 15 s. The second data set used in Chapter IV includes five multichannel seismic reflection profiles processed and interpreted by [Albertin \(1989\)](#) for his M.Sc. thesis. These data were collected in 1978 by the Scripps Institution of Oceanography during the Guaymas



Abbreviations:

HDD: Hard disk drive
 QC: Quality control
 FFT: Fast Fourier transform
 SG: Shot gather
 CDP: Common depth point
 NMO: Normal move out
 RMS: Root mean square
 nD: Degree of freedom in models
 *: Trial and error approach

Figure 2. Flow diagram followed to process and to interpret multichannel seismic data.

Figura 2. Diagrama de flujo seguido en el procesado e interpretación de datos sísmicos

Expedition.

Depths in this work are given in terms of seconds of two-way travel time. The depths and thickness of geological features were estimated with the interval velocities calculated after the root mean square velocities obtained from the semblance velocity analysis.

II. WESTWARD MIGRATION OF EXTENSION IN THE NORTHERN GULF OF CALIFORNIA

Aragón-Arreola, M., and Martín-Barajas, A., 2007. Westward migration of extension in the northern Gulf of California, México. *Geology*, 35(6).

II.1. Abstract

Interpretation of industry seismic lines indicates that the eastern margin of the northern Gulf of California contains the inactive Adair-Tepoca and Upper Tiburón basins. The western margin is active and includes the Wagner, Consag, Upper Delfín and Lower Delfín basins. These basin systems are separated by a wide basement high across which the upper strata in the inactive basins correspond to the middle and lower strata in the active basins, recording the westward migration of strain and subsidence during late Pliocene time. Our results illustrate the formation of an abandoned rift margin along the eastern Gulf of California.

II.2. Introduction

The Gulf of California is a well-developed transtensional plate margin linked to the rupture of Baja California from southwestern North America ([Fig. 3](#)). In middle Miocene time, extensional deformation affected the Gulf Extensional Province ([Stock and Hodges, 1989](#); [Gans, 1997](#); [Axen and Fletcher, 1998](#)), but sometime during the middle to late Miocene, the strain localized into the highly oblique Gulf of California rift, which is now dominated by large transform faults linked by pull-apart basins ([Lonsdale, 1989](#); [Stock and Hodges, 1989](#); [Oskin et al., 2001](#)). However, little is known about how strain evolved during the history of focused rifting. Based on processing and interpretation of seismic profiles we

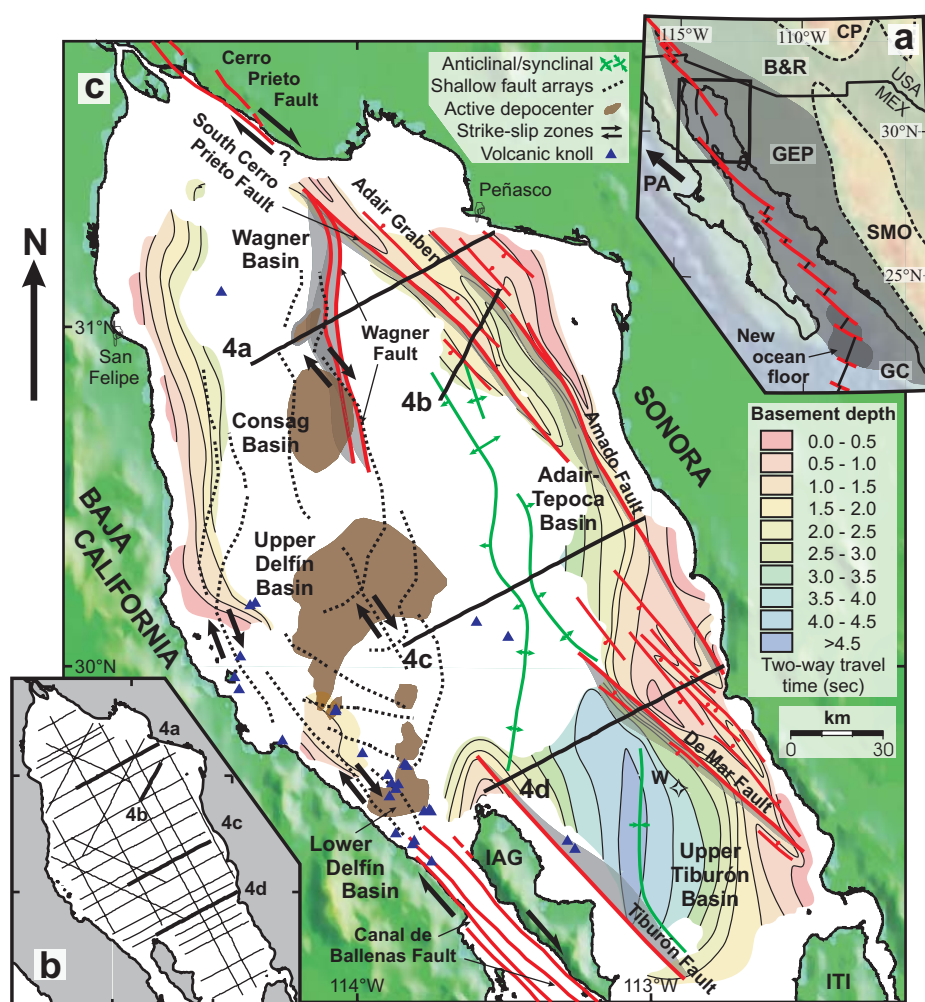


Figure 3. a). Regional tectonic framework of western North America and northwestern México (after Stock and Hodges, 1989; Lonsdale, 1989; Fenby and Gastil, 1991). The arrow shows the relative motion of the Pacific-North America plates. b). Layout of processed seismic lines. c). Structural map of the northern Gulf of California. The eastern margin contains inactive basins and faults, while the western margin includes active basins of the modern rift. The pattern of active depocenters and shallow fault arrays are from Persaud et al. (2003). Faults outside data coverage are from Fenby and Gastil (1991). PA, Pacific Plate; GC, Gulf of California; GEP, Gulf Extensional Province; B&R, Basin and Range Province; SMO, Sierra Madre Occidental; CP, Colorado Plateau; ITI, Isla Tiburón; IAG, Isla Ángel de la Guarda.

Figura 3. a). Relaciones tectónicas regionales en el oeste de Norteamérica y noroeste de México (tomado de Stock y Hodges, 1989; Lonsdale, 1989; Fenby y Gastil, 1991). La flecha representa el movimiento relativo de las placa Pacífica y Placa Norteamérica. b). Localización de las líneas sísmicas procesadas. c). Mapa estructural del Norte del Golfo de California. El margen este alberga fallas y cuencas inactivas, mientras que el margen oeste contiene las cuencas activas del rift moderno. Los depocentros activos y arreglos de fallas fueron tomados de Persaud et al. (2003). Las fallas fuera la cobertura de la base de datos provienen de Fenby y Gastil (1991). PA, Placa Pacífica; GC, Golfo de California; GEP, Provincia Extensional del Golfo; B&R, Provincia de Cuencas y Sierras; SMO, Sierra Madre Occidental; CP, Meseta del Colorado; ITI, Isla Tiburón; IAG, Isla Ángel de la Guarda.

compile a structural map of the northern Gulf of California (the northern Gulf), documenting structures related with the initial stage of focused rifting. We show that the crustal strain and subsidence migrated westward to form the modern rift configuration. Finally, we propose that the eastern Gulf forms an abandoned rift margin.

II.3. Geologic framework

Evolution of the Gulf of California is related with transfer of the Baja California from the North America to the Pacific plate. This process started ~12 Ma ago and imposed a northwestward motion on Baja California that triggered the localization of most of the Pacific-North America plate motion into the Gulf Extensional Province ([Stock and Hodges, 1989](#)). The timing of onset of focused extension is controversial; it has been suggested that oblique extension was preceded by a period of nearly orthogonal extension known as the proto-Gulf stage, which was accompanied by the first marine incursions (12-6 Ma; [Stock and Hodges, 1989](#); [Henry and Aranda-Gomez, 2000](#); [Umhoefer et al., 2002](#)). Around the northern Gulf, the early marine sedimentation occurred during latest Middle Miocene time ([Delgado-Argote et al., 2000](#); [Gastil et al., 1999](#); [Helenes and Carreño, 1999](#); [McDougall et al., 1999](#); [Helenes et al., 2005](#)), but it is unclear if deposition was related with oblique or orthogonal extension. Nevertheless, the marine environment became established by 6.5-6.3 Ma, synchronous with the full localization of oblique strain into the Gulf ([Oskin et al., 2001](#); [Oskin and Stock, 2003](#)).

Previous works documented that the eastern margin of the Gulf contains several inactive basins, including the Upper Tiburón, Lower Tiburón and Yaqui basins; it is interpreted that these basins were formed as incipient spreading centers ([Phillips, 1964](#); [Fenby and Gastil,](#)

1991; Lonsdale, 1989) abandoned ~3 Ma ago (Stock, 2000). However, these studies lacked the data to resolve the structural pattern of the inactive basins, such that the data base used here may help to clarify these conclusions.

The crustal structure displays contrasts across the northern Gulf. Toward the east, the crust is continental and thicker than in the west, where it is likely formed by a mix of continental, igneous and sedimentary rocks (Phillips, 1964; Persaud et al., 2003; González-Fernández et al., 2005). Moreover, the shoulders of the northern Gulf differ in the amount and age of extension and volcanism; in central Sonora, the extension produced basin and range type deformation and the exhumation of metamorphic core complexes during late Oligocene-middle Miocene time, coeval with arc-related volcanism (Nourse et al., 1994; Gans, 1997; Martín-Barajas, 2000). In contrast, extension in Baja California was accrued in high-to-moderate angle normal faults, and some detachment faults, and started in late-middle Miocene time after cessation of arc-volcanism (Axen, 1995; Lee et al., 1996). Moreover, discrete post-subduction volcanism has occurred along the coastal plain of Baja California (Sawlan, 1991; Martín-Barajas, 2000). Thus, extensional strain is older and of larger magnitude in the eastern than in the western margin of the northern Gulf.

II.4. Results: Structure of the northern Gulf of California

The main structural fabric of the northern Gulf consists of NW-SE striking faults of moderate dip (Fig. 3) with >1 s of throw (>1 km). The larger faults offshore Sonora include the west-dipping Amado fault, and the conjugate De Mar and Tiburón faults (Fig. 4; see also Annex 1); these faults do not cut the uppermost strata, and are now inactive. The major faults display an en echelon array with intervening basins that mimics the active

structural fabric of the Gulf (Fenby and Gastil, 1991; Lonsdale, 1989), which suggests that they had accommodated significant dextral shear. Our data show that the active Cerro Prieto fault extends into the northern Gulf; however, its southernmost segment is inactive and draped by undeformed strata (Figs. 4a, 4b). The data also reveal that numerous minor faults develop in the shallow section of the major structures.

Several NW-striking secondary faults were identified near the coast of Sonora. These structures display <1 s of throw and define horsts and grabens of moderate relief that are draped by sediments. One of these faults paired with the Amado fault, bounds the ~10 km-wide Adair graben, which extends >50 km (Figs. 3, 4a, 4b). In the north-central Gulf, the Wagner fault zone branches out from the Cerro Prieto fault and dips to the west at

Figure 4 (following two pages). Main geological features in the northern Gulf of California as imaged in the seismic reflection profiles. a). Subsidence in the Wagner basin is controlled by the Wagner fault. Eastward, the Adair graben forms the northern end of the Adair-Tepoca basin. Note that sequence boundary B-C is correlated across both basin systems. b). Sequence B in the Adair-Tepoca basin was syntectonic to the Amado fault; while sequence C drapes the structural relief and represents post-tectonic deposition. c). The Upper Delfin and Adair-Tepoca basins are bounded by a wide anticline; note the same stratal relation between the active and inactive basins mentioned above. d). The Upper Tiburón basin is bounded by the De Mar and Tiburón faults. Sequence A represent the older deposits in the northern Gulf and pre-dates the onset of narrow rifting. Sequence B was syntectonic to the growth of the basin-bounding faults; sequence C represents post-tectonic sedimentation.

Figura 4 (siguientes dos páginas). Principales rasgos geológicos en el Norte del Golfo de California mostrados en los perfiles de sísmica de reflexión. a). La subsidencia en la Cuenca Wagner es controlada por la Falla Wagner. Hacia el este, el Graben de Adair forma la sección norte de la Cuenca Adair-Tepoca. Note que el límite de secuencia B-C se correlaciona a través de ambos sistemas de cuencas. b). La Secuencia B en la Cuenca Adair-Tepoca fue sintectónica con la Falla Amado, mientras que la Secuencia C cubre el relieve estructural y representa depósitos post tectónicos. c). Las cuencas Delfin Superior y Adair-Tepoca están separadas por un anticlinal; note las mismas relaciones entre los estratos de las cuencas activas e inactivas mencionadas anteriormente. d). La Cuenca Tiburón está limitada por las fallas De Mar y Tiburón. La Secuencia A representa los depósitos más antiguos en el norte del Golfo que preceden el establecimiento del rift estrecho. La Secuencia B fue sintectónica con el crecimiento de las fallas que limitan las cuencas; la Secuencia C representa sedimentación post tectónica.

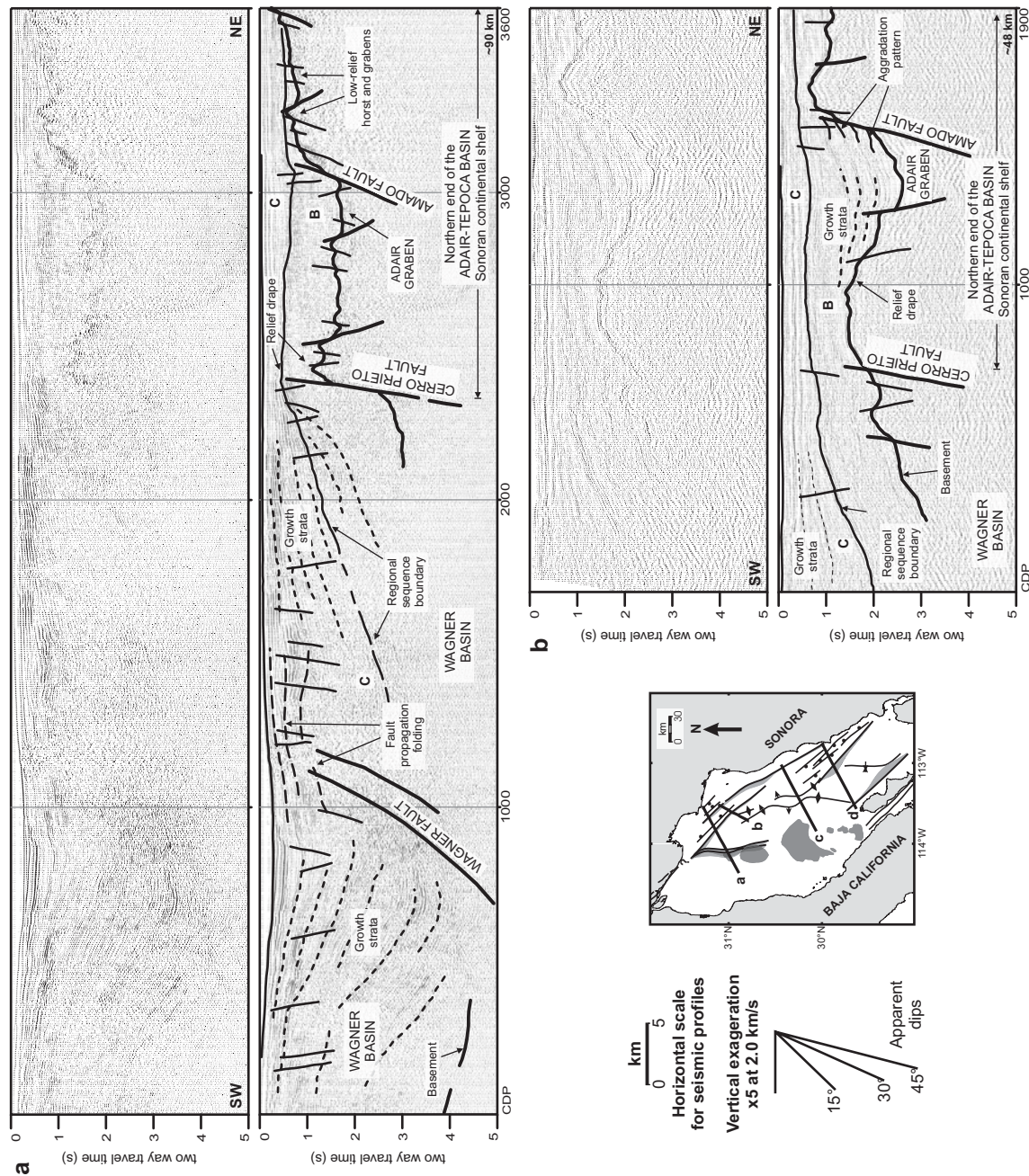


Figure 4

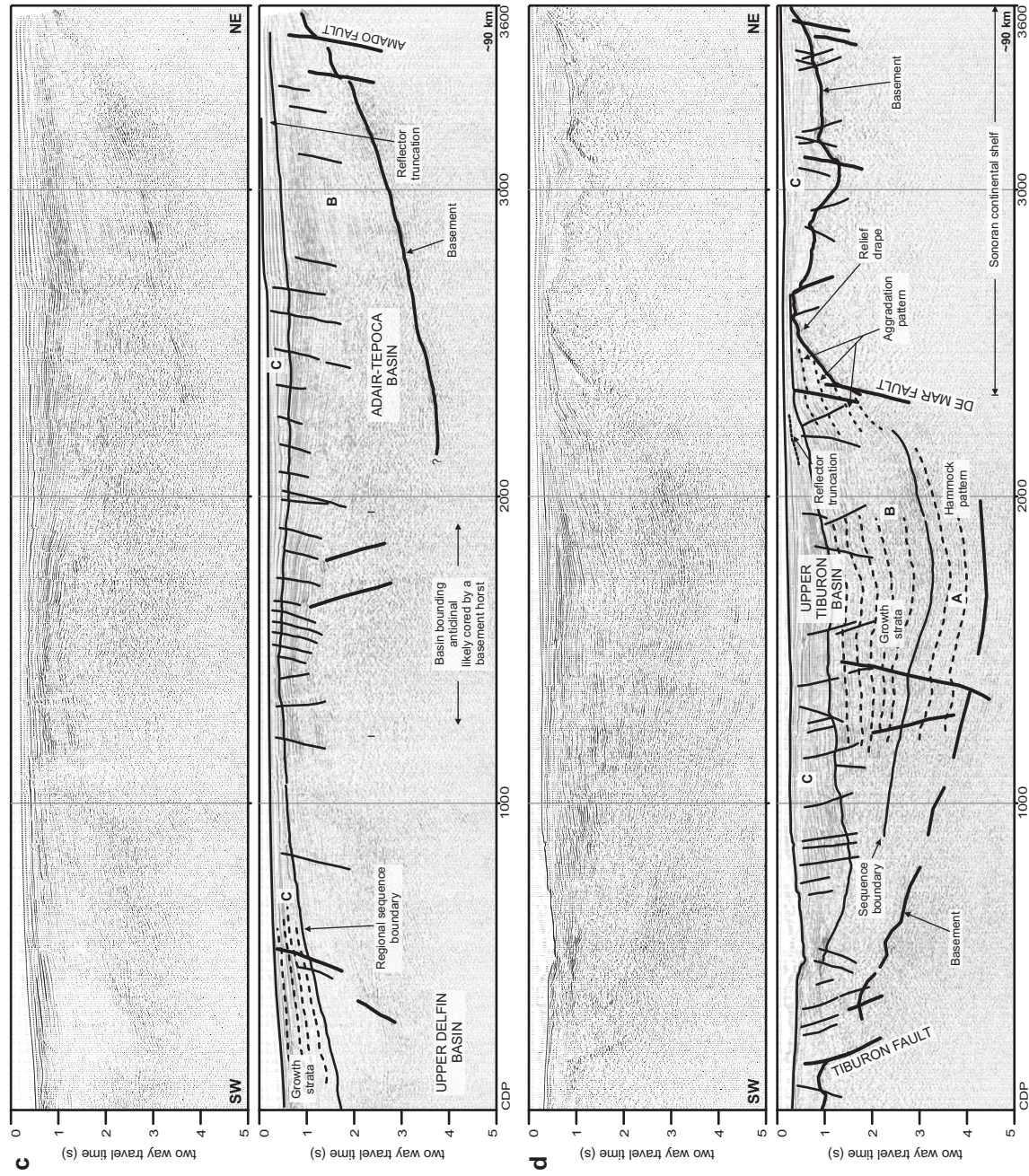


Figure 4 (continuation).

moderate angle that tends to shallow with depth, suggesting listric fault geometry. The strata overlying the Wagner fault define fault-propagation folds and are cut by multiple ~N-S striking subsidiary faults that lie along the axis of the Wagner and Consag basins (Figs. 3, 4a). Further south, in the Upper Delfin and Lower Delfin basins, the shallow sediments are cut by dense fault arrays that crown and splay away from the northern strands of the Canal de Ballenas fault (Persaud et al., 2003; this study).

The data clearly image the acoustic basement in the northeastern Gulf (Fig. 3). Here the basement is depicted as a sharp reflector that outlines the rhombochasmic Adair-Tepoca and Upper Tiburón basins. The Adair-Tepoca basin has a stratal thickness up to ~3.8 s (~4.8 km) and is bounded by the Amado fault and several minor faults to the east, a structural high to the west (see below), and terminates northward into the Adair graben (Figs. 3, 4a, 4b). This basin contains two seismic sequences; the lower is formed by growth strata and aggradation patterns that accrete eastward against the basin bounding faults, suggesting the syntectonic evolution of faulting and sedimentation (B; Figs. 4a, 4b). The upper sequence is formed by nearly parallel strata that onlap to the east and drape the basement relief (C; Figs. 4a, 4b).

The Upper Tiburón basin has a stratal thickness of up to ~4.8 s (~6.0 km) and is bounded by the De Mar fault to the east and the Tiburón fault to the west (Figs. 3, 4d). This basin contains three seismic sequences; the lower is formed by a hammock reflector pattern cut by the basin-bounding faults (A; Fig. 4d). The middle sequence is built by growth strata that accrete on the basin bounding faults, revealing the syntectonic sedimentation (B; Fig. 4d). The upper sequence is formed by nearly parallel strata that onlap and drape the shallow (<1.5 s) and faulted basement offshore Sonora; toward the top this sequence

includes local unconformities, but they do not separate changes in the stratal pattern (C; Figs. 4a, 4b).

The lateral continuity of seismic reflectors across the northeastern Gulf reveals the correlation of sequences B and C of the Adair-Tepoca and Upper Tiburón basins. The sequence C forms condensed sections that drape the Amado, De Mar and Tiburón faults and fills the basement relief offshore Sonora. The data also show that reflectors of sequence C are locally truncated at the sea bottom, but do not record active faulting (Fig. 4c), indicating that this region is now structurally inactive.

The basement in the central-west margin of the northern Gulf is poorly defined, but suggests a broad rhombochasmic depression limited by the Cerro Prieto and Canal de Ballenas faults. This depression contains the Wagner, Consag, Upper and Lower Delfín basins (Fig. 3) that form a set of shallow sags oriented N-NE (Persaud et al., 2003). Here the stratal thickness is poorly estimated, but exceeds 4.0 s (~4-5? Km; Figs. 4a, 4c). The reflectors can be traced across contiguous sags and display multiple truncations, suggesting that the active basins tend to coalesce. Our data also show growth strata within the Wagner and Consag basins that form aggradation patterns against the Wagner fault (Fig. 4a), indicating syntectonic sedimentation.

The boundary between the active and inactive basins consists of a broad anticline. This flat-topped, ~20 km-wide, doubly-hinged structure trends NNW-SSE and extends ~120 km from the Tiburón to the Cerro Prieto fault (Figs. 3, 4b, 4c); the data suggest that this anticline is cored by a basement high. This anticline is built by condensed sequences cut by numerous small-throw faults. A conspicuous feature is that the B-C sequence boundary in the inactive basins can be traced across the entire anticline and deepens to the west into the

active basins (Figs. 4a, 4c). These seismic relationships indicate that once subsidence and sedimentation shifted from the eastern to the western basins.

II.5. Discussion

We interpret that the lower sequence in the Upper Tiburón basin (A; Fig. 4d) was deposited in a sag-shaped depression with no obvious association to any major fault. In contrast sequence B in the Adair-Tepoca and Upper Tiburón basins comprises growth strata associated with the Amado, De Mar and Tiburón faults, which are parallel to the main structural fabric of the Gulf of California rift (Figs. 1, 3). The syntectonic evolution of sequence B reveals that the major faults accrued more than 1 km of throw, and possibly large strike-slip motion, based on the en echelon pattern (Fig. 3). The recognition of linked seismic sequences in the Adair-Tepoca and Upper Tiburón basins associated with growth faults suggests that sequence B records the onset of focused extension in the northern Gulf, while sequence A represents pre-rift deposition probably linked to the proto Gulf Stage (Stock and Hodges, 1989; Henry and Aranda-Gomez, 2000).

Our results indicate that sequence C records the abandonment of the eastern basins. This sequence drapes and is post-tectonic to the major faults; additionally, the unconformities and stratal truncation within this sequence (Figs. 4b, 4d) suggest erosional stages probably tied to the cease of tectonic activity. Moreover, the correlation of the B-C sequence boundary from the Adair-Tepoca and Upper Tiburón basins into the Wagner, Consag, and Upper Delfín basins (Figs. 4a, 4b, 4c) supports that strain and associated subsidence waned in the eastern basins as they relocated to the west. This sequence boundary was traced down to ~3.0 s into the Wagner and Consag basins (Figs. 4a, 4b); thus, most of the

stratigraphic section in the active basins postdates the shift of deformation.

Here we infer pre-rift and syn-rift deposition, and the migration of strain and subsidence, but we lack time constraints for these events. The reconstruction of conjugate margins in the Upper Delfin basin segment suggests that rifting began ~6-7 Ma ([Oskin et al., 2001](#); [Oskin and Stock, 2003](#)). However, microfossil data from a ~4800 m well drilled by PEMEX in the Upper Tiburón basin (W; [Fig. 3](#)) show that the upper ~3500 m post-date the late-middle Miocene; the lower section that mostly correlates with sequence A lacks of biostratigraphic control due to poor faunal preservation ([Helenes et al., 2005](#)). Thus, the pre-rift sequence A pre-dates or be at least of late-middle Miocene age, which suggests that it was deposited during the proto-Gulf stage ([Stock and Hodges, 1989](#); [Henry and Aranda-Gomez, 2000](#)). The upper 800 m in well W that correlate with sequence C, were deposited in Pliocene-Pleistocene time ([Helenes et al., 2005](#)), suggesting that migration of strain occurred in that time. Thus, our interpretation agrees with reconstructions in which ~3.3-2.0 Ma, the Upper Tiburón basin and Tiburón fault became inactive as the Lower Delfin basin and Canal de Ballenas fault initiated ([Nagy and Stock, 2000](#); [Stock, 2000](#)).

The shift of subsidence in narrow basins has been explained by the lateral contrast of heat flow caused by attenuation of continental crust during rifting ([Sandiford et al., 2003](#)). Additionally, large sediment piles likely play a roll in the lithospheric weakening, since sediments thermally insulate the lower crust ([Lavie and Steckler, 1997](#)). This insulation favors the lateral heat transfer that may trigger the migration of deformation in the vicinity of rift basins ([Sandiford et al., 2003](#)). The northern Gulf meets both conditions: it contains kilometeric sedimentary columns and its western shoulder records volcanic activity since the early Miocene ([Sawlan, 1991](#); [Martín-Barajas, 2000](#)). Moreover, the onshore

volcanism and the numerous volcanic knolls in the active basins (Fig. 3), also suggest a sustained heat source near Baja California.

The Wagner, Consag, Upper and Lower Delfin basins lay in a large stepover of the Canal de Ballenas and Cerro Prieto faults; here, subsidence is diffusely controlled by shallow fault arrays that branch out from the major faults (Lonsdale, 1989; Nagy and Stock, 2000; Stock, 2000; Persaud et al., 2003). However, our data reveal that the likely listric Wagner fault roots the shallow deformation and yields the formation of thick growth strata; thus, this fault is likely the main control of subsidence in the Wagner and Consag basins (Figs. 3, 4a). We argue that vertical propagation of the Wagner fault results in the distributed faulting that controls the modern depocenter of these basins. Furthermore, subsidence of the Upper Delfin and Lower Delfin basins is related with horse-tail structures splaying away the Canal de Ballenas fault (Fig. 3; Persaud et al., 2003). We speculate that these shallow faults may also be linked to the propagation of deep structures, similar to the Wagner fault.

The pattern of inactive basins is a conspicuous feature along the eastern Gulf of California rift (Fig. 5). North of the Adair-Tepoca and Upper Tiburón basin system, the Altar and East Mesa basins contain deltaic successions that onlap late Miocene marine deposits, these basins are above the base level and are now inactive (Pacheco-Romero et al., 2006). In the central Gulf, the Yaqui basin is an inactive half-graben abandoned during late Pliocene time (Aragón-Arreola et al., 2005). Farther south, the eastern margin contains the inactive San Blas, Tamayo, Nayarit, and Tres Mariás troughs (Brown et al., 2006; Sutherland et al., 2006). We propose that the inactive basins along the eastern Gulf of California constitute an abandoned rift margin that is forming an incipient drift margin.

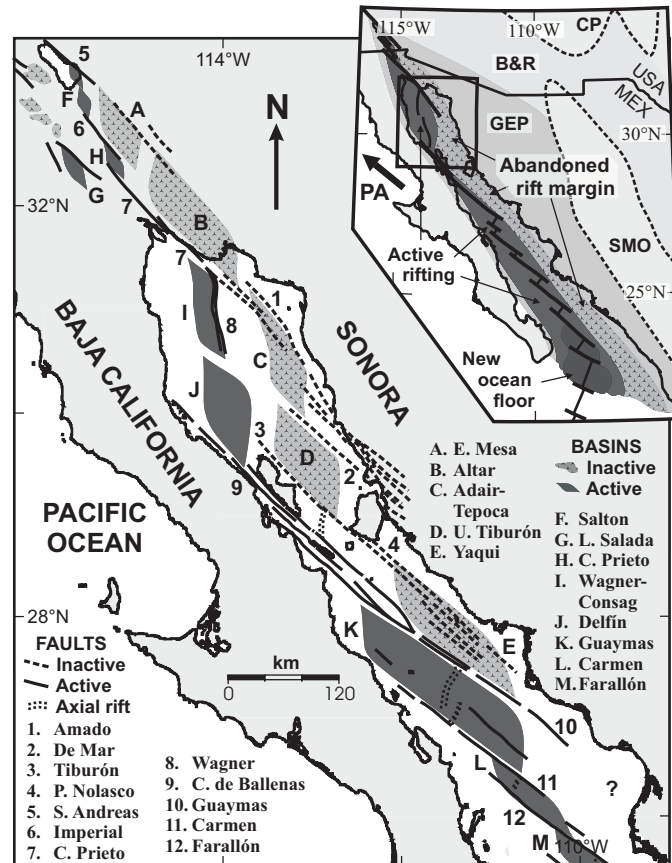


Figure 5. The eastern Gulf of California contains abandoned rift basins, while active rifting occurs in the western Gulf (Lonsdale, 1989; Fenby and Gastil, 1991; Persaud et al., 2003; Aragón-Arreola et al., 2005; this study). The eastern Gulf constitutes an abandoned rift margin (see inset map). Same abbreviations as in Figure 3.

Figura 5. El este del Golfo de California alberga sistemas de cuencas y fallas abandonados, mientras que el *rift* activo ocurre en la parte oeste del Golfo (Lonsdale, 1989; Fenby and Gastil, 1991; Persaud et al., 2003; Aragón-Arreola et al., 2005; este trabajo). El este del Golfo constituye un margen abandonado (ver el mapa insertado). Mismas abreviaturas que en la Figura 3.

II.6. Conclusions

Our results indicate that focused extension in the northern Gulf of California occurred through a process of localization and re-localization of strain that resulted in two diachronous basin systems controlled by large dextral-oblique faults. The inactive margin includes the Adair-Tepoca and Upper Tiburón basins, controlled by the Amado, de Mar and Tiburón faults. During middle to late Pliocene time, the strain localized to the west, giving rise to the Wagner, Consag, Upper and Lower Delfín basins, which are controlled by the Wagner fault and the fault arrays that branch away the Cerro Prieto and Canal de Ballenas faults. The pattern of inactive fault-basin systems in the east is present along the entire length of the Gulf and forms an abandoned rift margin, while active rifting is located in the western Gulf.

III. TECTONOSEDIMENTARY EVOLUTION OF THE INACTIVE NEOGENE BASINS IN THE NORTHEASTERN GULF OF CALIFORNIA, MEXICO

III.1. Abstract

The eastern margin of the Gulf of California contains the structures and sedimentation related to the early oblique deformation of the Gulf of California rift, whereas the western margin accommodates the modern transtensional strain. The process of ~3800 km of multichannel seismic reflection data collected by PEMEX in the early 1980's allowed the interpretation of the tectono-sedimentary environment of the inactive basins in the northeastern Gulf. Our results indicate that the Upper Tiburón and Adair-Tepoca basins include pre-rift, syn-rift and post-rift facies related to the evolution of large transtensional faults. The early marine sediments were accumulated in a broad depression and form the lower sequence in the Upper Tiburón basin; deposition of this sequence probably initiated in the latest Middle Miocene and represent pre-rift facies with respect to the latest Miocene localization of oblique strain along the Tiburón, De Mar, and Amado faults. The growth of these faults resulted in the syn-tectonic and synchronous evolution of the Adair-Tepoca and Upper Tiburon basins. The syn-rift facies in the Adair-Tepoca basin include southward progradating sediments canalized thorough the Adair graben, these strata may be related to the early flow of the Colorado River into the Gulf; whereas the syn-rift facies in the Tiburón basin were deposited in a growing pull-apart system defined in the stepover of the Tiburón and De Mar faults. During the late Pliocene the transtensional deformation wane in the northeastern Gulf and migrated toward the west, resulting in the deposition of post-rift facies that drape and peneplane the pre-existing relief. We infer that the wide basement

high that separates the active and inactive basins in the northern Gulf is displaced by a top-to-the east detachment fault; such that the doubly-hinged anticline that crowns the basement high may represent a large roll-over anticline. Our work implies that a) the northern Gulf contains marine strata deposited during the proto-Gulf stage, prior to the generalized marine incursion of the latest Miocene; b) the localization of oblique strain into the Gulf of California may have been a gradual instead of a sudden process; and c) oblique extension may have been accommodated in the northeastern Gulf by large strike-slip faults and coeval detachment faults.

III.2. Introduction

Evolution of the Gulf of California is related to the post Middle Miocene reconfiguration of the Pacific-North America plate boundary from a convergent margin to the modern transtensional rift system (Fig. 6; Lonsdale, 1989; Stock and Hodges, 1989; Stock and Lee, 1994; Bohannon and Parsons, 1995). The early stage of this rift is related to the focusing of oblique extension that resulted in the formation of a new structural fabric and the definition of extensional basins (Stock and Lee, 1994; Bohannon and Parsons, 1995; Stock and Hodges, 1989; Stock, 2000).

The analog and numerical models of rifting indicate that the architecture of sedimentary successions within rift basins is function of the space-temporal evolution of deformation; therefore, the interpretation of the seismostratigraphic record can be used as a proxy to understand the tectonic history of rift basins (Contreras, et al., 1997; Gupta et al., 1998; Cowie et al., 2000; Gawthorpe and Leeder, 2000; Contreras and Scholz, 2001). A large seismic reflection data base collected by Petróleos Mexicanos (PEMEX) in the northern

Gulf of California (the northern Gulf) gives us the opportunity to study the tectonosedimentary evolution of the inactive Upper Tiburón and Adair-Tepoca basins, formed during the early stage of oblique rifting. We propose that the older sedimentation responded to distributed deformation, while subsequent deposition was controlled by the growth of major transtensional faults and defined a system of synchronously subsiding basins in the stepover zone of such faults.

III.3. Geologic setting of the northern Gulf of California

The post Middle Miocene reconfiguration of the Pacific-North America plate boundary has yielded the formation of the highly-oblique Gulf of California rift. During the early phase

Figure 6. a). Geologic map of the northern Gulf of California after the interpretation and correlation of multichannel seismic reflection profiles (from Aragón-Arreola and Martín-Barajas, 2007). The eastern margin hosts the inactive Upper Tiburón and Adair-Tepoca basin, controlled by growth of large transtensional faults, whereas the western margin hosts the modern Lower Delfín, Upper Delfín, Consag and Wagner basins, localized within a large stepover zone of the Canal de Ballenas transform fault and the Cerro Prieto fault. PEMEX drilled an exploratory hole of ~4800 m in the Upper Tiburón basin (W). The highlighted profiles are shown in further figures. **b).** Regional tectonic framework of northwestern México (after Lonsdale, 1989). The Gulf of California, within the Gulf Extensional Province (GEP), hosts a highly oblique rift that forms the modern transtensional boundary between the Pacific (PA) and North America (NA) plates. **c).** Interpreted seismic reflection data, highlighting the profiles presented in this paper. Other abbreviations: Baja California (BC); Basin and Range province (B&R); Sierra Madre Occidental (SMO); Isla Tiburón (ITI); Isla Ángel de la Guarda (IAG); reference line (RL).

Figura 6. a). Mapa geológico del norte del Golfo de California a partir de la interpretación y correlación de perfiles de sísmica de reflexión multicanal (tomado de Aragón-Arreola y Martín-Barajas, 2007). El margen este contiene las cuencas inactivas Adair-Tepoca y Tiburón Superior, controladas por el crecimiento de grandes fallas transtensivas. El margen oeste contiene las cuencas activas Delfín Inferior, Delfín Superior, Consag y Wagner, localizadas entre la Falla Transforme Canal de Ballenas y la Falla Cerro Prieto. En la Cuenca Tiburón Superior PEMEX perforó un pozo exploratorio de ~4800 m (W). Los perfiles resaltados se muestran en las figuras siguientes. **b).** Marco tectónico regional del noroeste de México (tomado de Lonsdale, 1989). El Golfo de California, dentro de la Provincia Extensional del Golfo (GEP), contiene un *rift* altamente oblicuo que forma el límite transtensivo entre las placas Pacífica (PA) y Norteamericana (NA). **c).** Líneas de sísmica de reflexión interpretadas, resaltando los perfiles mostrados. Otras abreviaciones: Baja California (BC); Provincia de Sierras y Cuencas (B&R); Sierra Madre Occidental (SMO); Isla Tiburón (ITI); Isla Ángel de la Guarda (IAG); línea de referencia (RL).

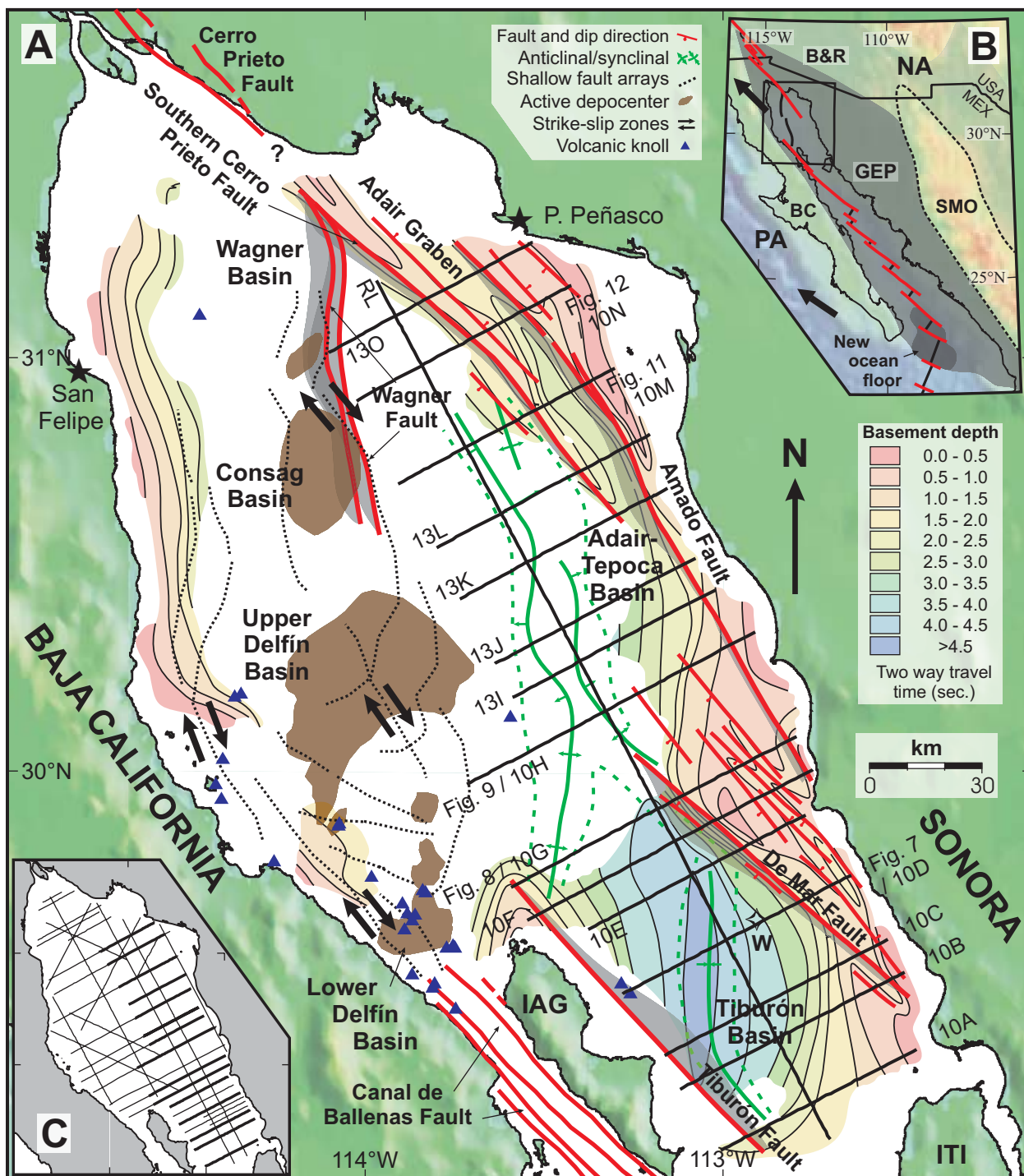


Figure 6. Aragón-Arreola

of this reconfiguration, the transtensional strain may have been partitioned, such that the orthogonal extension was accommodated inland forming graben basins within the Gulf Extensional Province, while the strike-slip motion was accrued offshore western Baja California; this period is known as the proto-Gulf stage ([Karig and Jensky, 1972](#); [Spencer and Normark, 1979](#); [Stock and Hodges, 1989](#); [Henry and Aranda-Gómez, 2000](#)). However, some authors suggest that the Gulf Extensional Province has accommodated significant oblique strain since the Middle Miocene ([Bohannon and Parsons, 1995](#); [Gans, 1997](#); [Fletcher and Munguía, 2000](#)). During the Late Miocene, most of the transtensional strain focused in the western edge of the Gulf Extensional Province and formed a narrow rift zone in the Gulf of California region ([Lonsdale, 1989](#); [Stock and Hodges, 1989](#)).

The Gulf of California rift is composed by two parallel margins built by en echelon arrays of NW-SE oriented faults linked by sedimentary basins; the eastern margin is tectonically inactive and forms an incipient drift margin ([Fig. 6](#)); whereas the western margin accommodates the modern transtensional extension ([Lonsdale, 1989](#); [Fenby y Gastil, 1991](#); [Aragón-Arreola and Martín-Barajas, 2007](#)). In the northern Gulf, the inactive eastern margin contains the Tiburón, De Mar and Amado faults that controlled the evolution of the Upper Tiburón and Adair-Tepoca basins, which occupy two rhombochasmic basement depressions and hold sedimentary columns of ~6.0 and 4.8 km, respectively ([Aragón-Arreola and Martín-Barajas, 2007](#)). The active margin contains the Canal de Ballenas transform fault to the south and the Cerro Prieto fault to the north ([Fig. 6](#)); these major structures define and bound a broad stepover zone with shallow and diffuse deformation that contains the Lower Delfín, Upper Delfín, Consag and Wagner basins, the last two basin hold >4.0 km of sediments ([Nagy and Stock, 2000](#); [Persaud et al., 2003](#); [Aragón-](#)

[Arreola and Martín-Barajas, 2007](#)). The stepover zone is underneath by a poorly-defined basement depression ([Aragón-Arreola and Martín-Barajas, 2007](#)). Additionally, the western rift margin records Plio-Pleistocene volcanism of andesitic and rhyolic composition ([Martín-Barajas et al., 2002](#)).

The variations in the shallow crustal structure across the northern Gulf correspond to changes in the deep crustal structure. Beneath the inactive eastern margin, the crust is continental and ranges in thickness from ~18-20 km ([Phillips, 1964](#); [González-Fernández et al., 2005](#)), whereas beneath the active western margin, the crust is likely thinner and its composition is not well known, although it is probably transitional and is composed by a thick sedimentary lid that covers thinned continental crust; this region is cut by numerous igneous intrusions ([Couch et al., 1991](#); [Persaud et al., 2003](#); [González-Fernández et al., 2005](#)).

The early marine incursions in the Gulf of California region apparently occurred during Middle Miocene time in the proto Gulf stage and are related to the crustal thinning caused by extensional deformation ([Henry and Aranda-Gómez, 2000](#)). Around the northern Gulf, the early marine deposits have been documented in Bahía de los Ángeles, Isla Tiburón, and central Sonora ([Ponce, 1971](#); [Gastil et al., 1999](#); [Delgado-Argote et al., 2000](#)). Recently, the micropaleontological studies of nanoplankton and palynomorphs in well samples obtained by PEMEX in the Upper Tiburón basin (W; [Fig. 6](#)) document latest Middle Miocene sediments within the northern Gulf ([Helenes et al., 2005](#)). The Middle Miocene deposits are likely associated with discrete marine incursions that might have come throughout a seaway located in central Baja California ([Helenes and Carreño, 1999](#)). Nevertheless, the stage of early marine sedimentation is still poorly constrained.

The establishment of generalized marine conditions in the Gulf of California occurred between ~6.5-6.3 Ma and correlates with the localization of most of the oblique strain and the onset of focused rifting in this region (Stock, 2000; Oskin et al., 2001; Oskin and Stock, 2003a and 2003b). The marine basins related to a generalized marine incursion around the northern Gulf are located in its eastern margin and include the Yaqui, Upper Tiburón, Adair-Tepoca, Altar, and East Mesa basins; these basins were controlled by systems of large growth faults and their deposition probably elapsed the Late Miocene-Middle Pliocene time (Nagy and Stock, 2000; Stock, 2000; Aragón-Arreola et al., 2005; Pacheco-Romero et al., 2006; Aragón-Arreola and Martín-Barajas, 2007). The onset of marine conditions related to focused rifting also resulted in the formation of fault-controlled basins in the eastern coastal plain of Baja California and southern California, including the Santa Rosalía, and Loreto basins (Dorsey and Umhoefer, 2000; Ochoa-Landín et al., 2000), and the Imperial and Vallecitos-Fish Creek basins (Winker and Kidwell, 1996; Dorsey et al., 2007); these basins developed synchronously the larger basins of the eastern Gulf.

III.4. Results: seismostratigraphic record in the northeastern Gulf of California

The eastern inactive margin of the northern Gulf of California contains the sigmoidal-shaped Upper Tiburón and Adair-Tepoca basins that cover ~11,000 km² and lie beneath a smooth and shallow bathymetry (Figs. 6). These basins are bounded by the major Tiburón, De Mar, and Amado faults and define a system of staggered fault-bounded basins. Here we describe the seismic patterns of the main sequences in order to interpret the tectono-sedimentary history of these basins. The results are based on the analysis of seismic

profiles included in [Appendix 1](#).

III.4.1. The Upper Tiburón basin

The Upper Tiburón basin displays a well defined sigmoidal shape limited to the northeast and southwest by the De Mar and Tiburón faults, respectively. The southeastern boundary consists of a basement ramp that extends into the Gulf from Isla Tiburón. The northwestern limit of this basin is formed by a doubly-hinged anticline that extends toward the northwest from the northern end of Tiburón fault and Isla Ángel de la Guarda ([Figs. 6; Aragón-Arreola and Martín-Barajas, 2007](#)). The maximum thickness of the sedimentary column reaches ~4.8 s (~6.0 km) and is formed by three main seismic sequences.

The lower sequence ([sequence A in Figs. 7, 8, 9, 10](#)), has a maximum thickness of ~1.5 s, and is formed by parallel reflectors displaying a broad hammock pattern. The thickness of this sequence is nearly constant across a great portion of the basin, but pinches out toward the south ([Fig. 10A](#)) and thins toward north ([Fig. 10H](#)). The data do not clearly image the eastern and western termination of sequence A, but the constant thickness in this sequence leads to interpret that it is displaced by the De Mar and Tiburón faults. The lower reflectors apparently onlap the acoustic basement ([Figs. 7, 9, ~CDP 2000-2700](#)); however, toward the northwest, the reflectors are folded and truncated at the basement, and define the core of a doubly-hinged anticline ([Figs. 8, ~CDP 200-500; 9, ~CDP 200-600; Fig. 10](#)). These reflector relations suggest that sequence A filled a broad depression; while the sharp truncation and folding suggests that this sequence was displaced by a low-angle, east-dipping detachment fault ([Figs. 10F; 10G; 10H](#)); however the trace of such fault is not imaged in our data. The upper reflectors of sequence A are truncated at sequence boundary AB, indicating an erosional unconformity ([Figs. 7, ~CDP 1000-1300; 8, ~CDP 1500](#)).

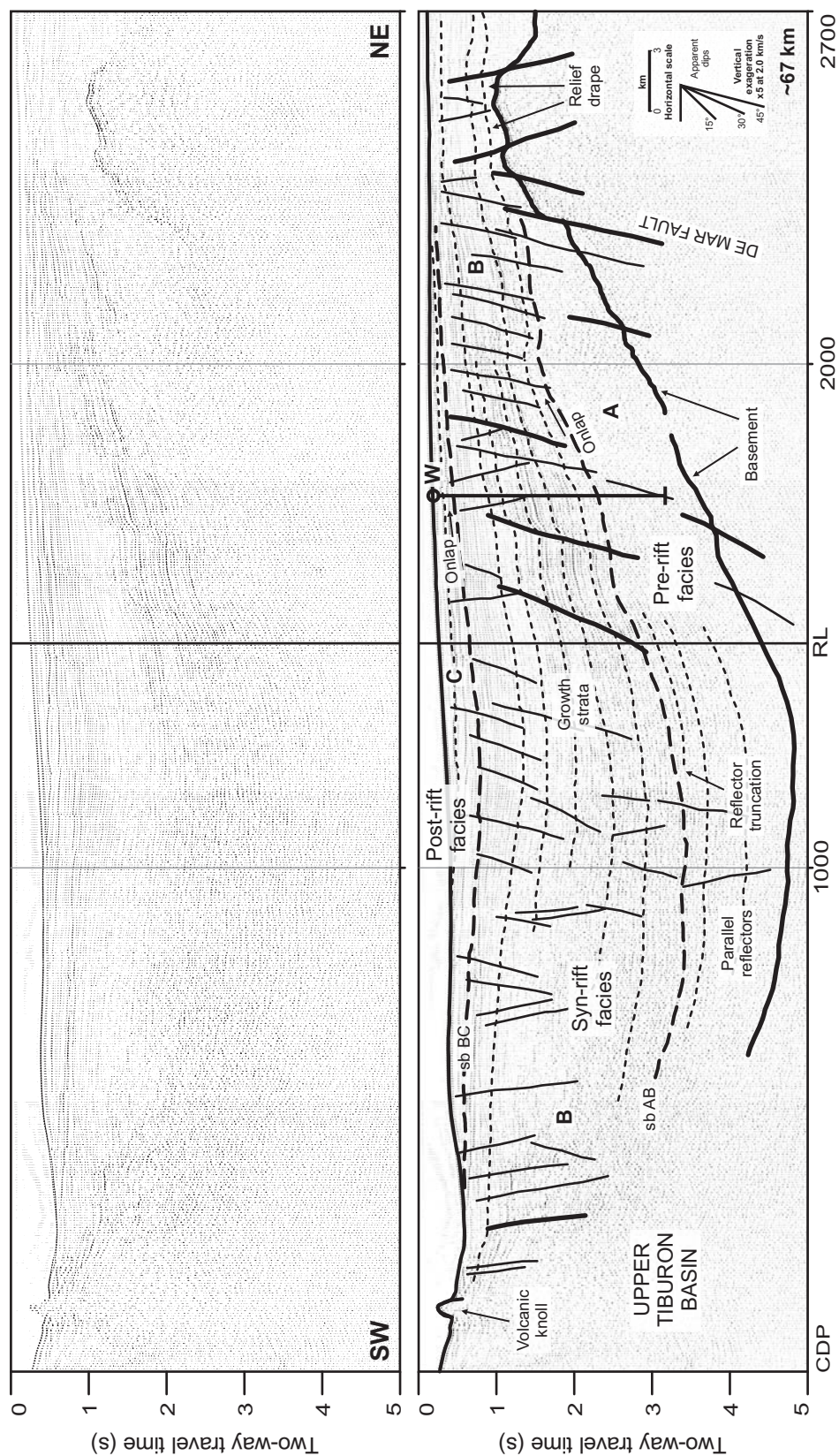


Figure 7. Migrated and interpreted seismic profile across the central section of the Upper Tiburón basin. The sedimentary column is formed by three main seismic sequences that represent pre-rift (sequence A), syn-rift (sequence B) and post-rift facies (sequence C). Note that sediments of the syn-tectonic sequence B accrete toward the west (sb: sequence boundary).

Figura 7. Perfil sísmico migrado e interpretado a través de la sección central de la Cuenca Tiburón Superior. La columna sedimentaria está compuesta por tres secuencias sísmicas que representan facies prerift (secuencia A), sinrift (secuencia B) y postrift (secuencia C). Note que la acreción sedimentaria es hacia el oeste en la secuencia sintectónica B (sb: límite de secuencia).

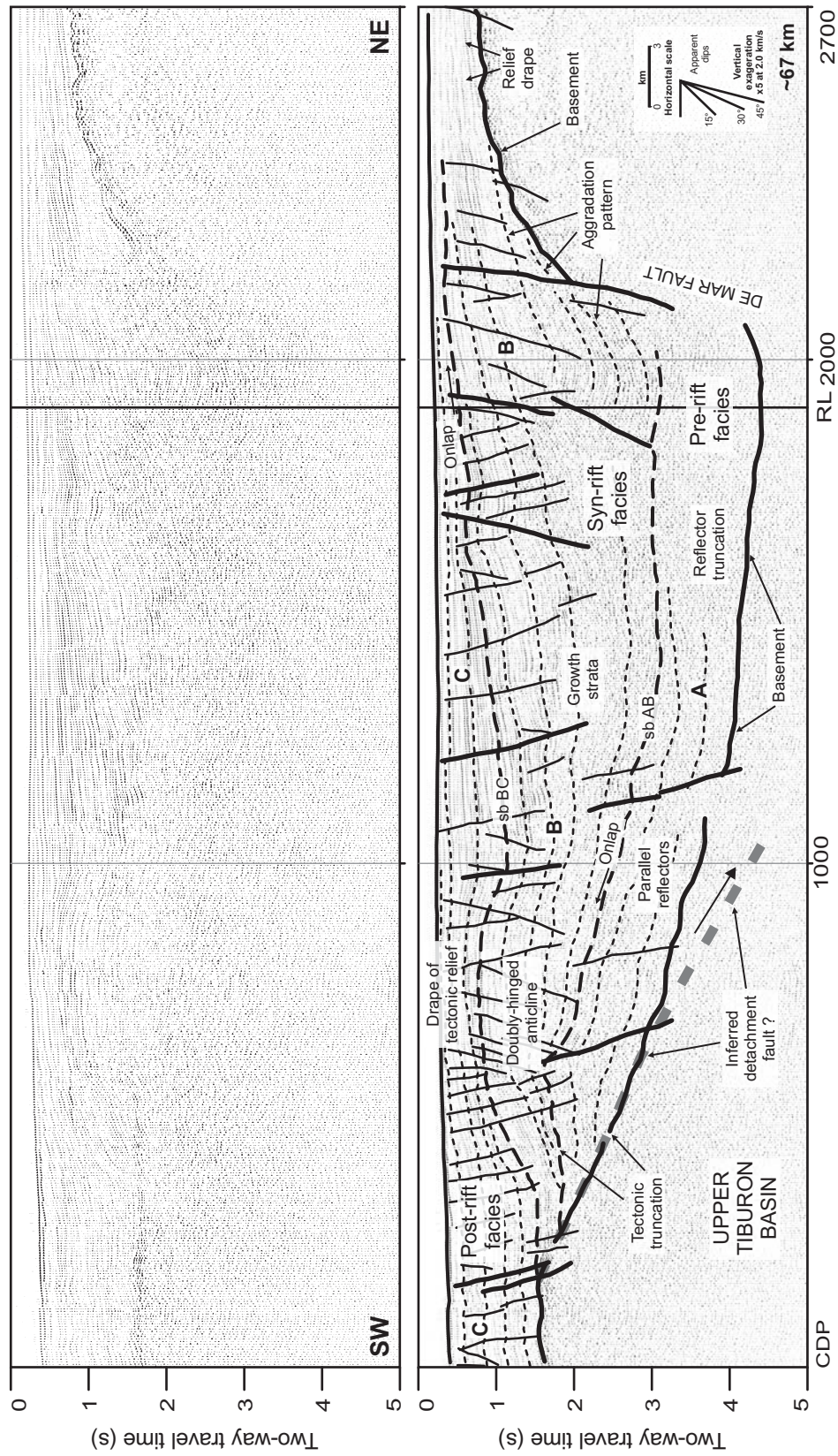


Figure 8. Migrated and interpreted seismic profile across the northern half of the Upper Tiburón basin. Note the three main seismic sequences interpreted as pre-rift (sequence A), syn-rift (sequence B) and post-rift facies (sequence C). Here the syn-tectonic sequence B accretes toward the east. To the west, sequence A and B are folded and truncated at the basement; we infer the presence of a top-to-the east detachment fault (sb: sequence boundary).

Figura 8. Perfil sísmico migrado e interpretado a través de la sección central de la Cuenca Tiburón Superior. Note las tres secuencias sísmicas que representan facies *prerift* (secuencia A), *sinrift* (secuencia B) y *postrift* (secuencia C). Aquí la acreción de la secuencia B es al este. Al oeste las secuencias A y B están plegadas y truncadas por el basamento; inferimos la una falla *detachment* con buzamiento al este (sb: límite de secuencia).

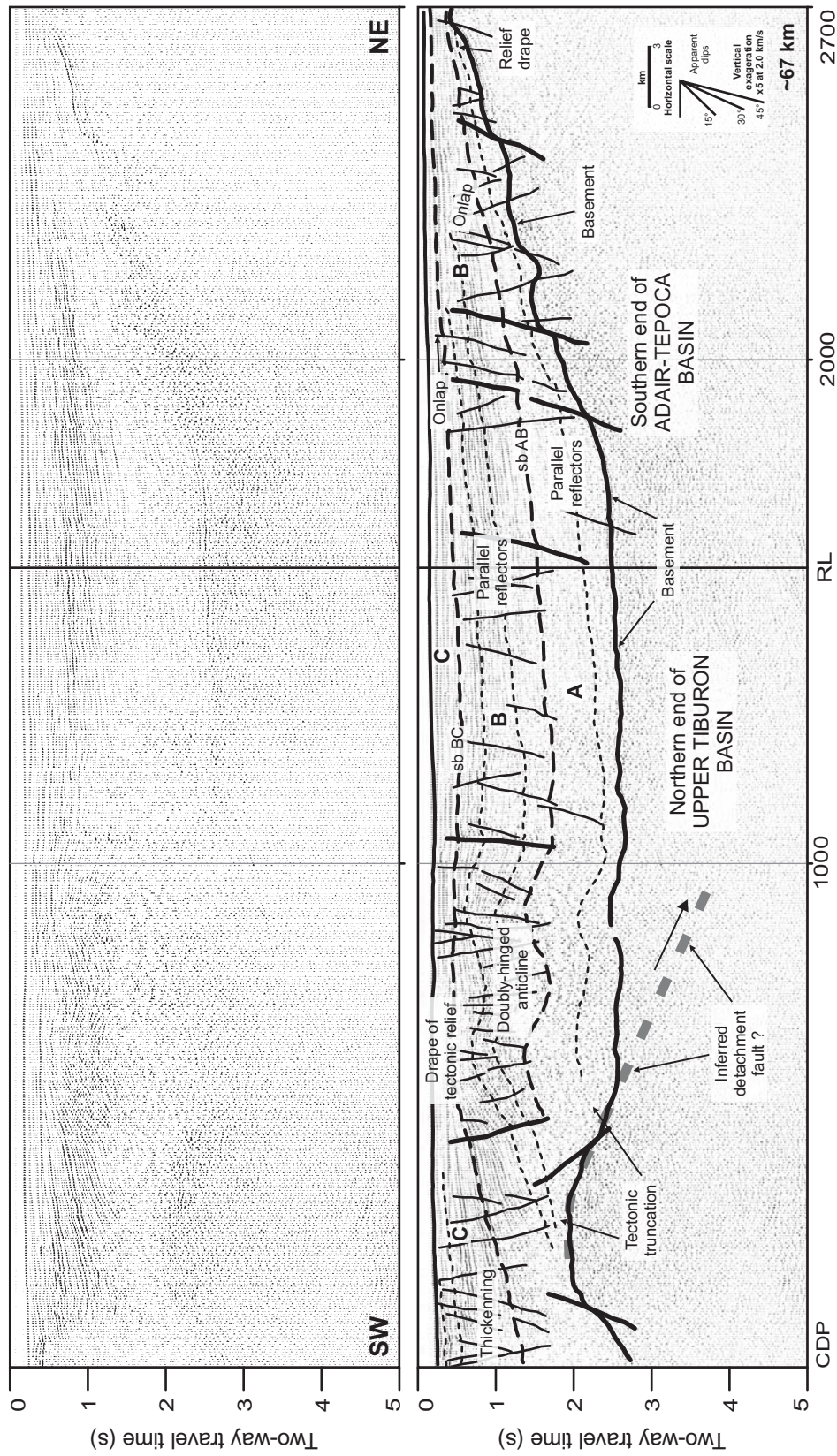


Figure 9. Migrated and interpreted seismic profile across the northern end of the Upper Tiburón basin and the southern end of the Adair-Tepoca basin. Reflectors display parallel patterns over this region. To the west, sequence A and B are folded and truncated at the basement; thus we infer a top-to-the east detachment fault. Sequence C drapes the relief, and extends and thickens downward into the Lower Delfín basin (sb: sequence boundary).

Figura 9. Perfil sísmico migrado e interpretado a través del norte de Cuenca Tiburón Superior y el sur de la Cuenca de la Cuenca Adair-Tepoca. Aquí los reflectores muestran patrones paralelos. Al oeste las secuencias A y B están plegadas y truncadas por el basamento; así que inferimos una falla de *detachment* buzante al este. La secuencia C cubre el relieve y se extiende y engrosa hacia la Cuenca Delfín Inferior (sb: límite de secuencia)..

The middle sequence (sequence B in Figs. 7, 8, 9, 10) has a maximum thickness of ~3.4 s, and is built by divergent reflectors (Figs. 7, ~CDP 1000-2000; 8, ~CDP 600-1700) that accrete into the maximum throw of the basin-bounding faults (e.g. Fig. 8, ~CDP 2000-2200). Toward the southern and northern tips of the Upper Tiburón basin, the reflectors shift to a parallel configuration (Figs. 9). We interpret the fanning and accretion of reflectors as growth strata accreting on growing faults. It is remarkable that the fanning direction and therefore, the sedimentary accretion direction, change along the Upper Tiburón basin, since the southern reflectors accrete to the west on the Tiburón fault (Figs. 10A; 10B; 10C; 10D), whereas to the north reflectors accrete to the east on the De Mar fault (Figs. 10E; 10F; 10G). The lower strata of sequence B onlap the underlying sequence A and outline the erosional sequence boundary AB (Figs. 7, ~CDP 1800-2100; 8, ~CDP

Figure 10. Summary of interpreted seismic profiles across the Upper Tiburón basin; location of boxes is shown in **Figure 6**. The interpreted pre-rift sequence A onlap and blanket the basement and is displaced by the basin bounding faults. The syn-rift sequence B form growth strata that accrete on the basin bounding faults; note the change of sedimentary accretion direction across the basin (highlighted by large arrows in boxes A to G), to the south sediments accrete westward (A-D), whilst to the north sediments accrete eastward (E-G). The post-rift sequence C drapes the relief, extending and thickening downward into the Lower Delfín basin (G-H). At the northwest, sequence A and B are folded and truncated at the basement; thus we infer the presence of a top-to-the east detachment fault (F-H). **Figures 7, 8 and 9** only show part of the summarized interpretations in boxes D, G and H; use reference line (RL) for correspondence. (DMF: De Mar fault; DHA, doubly hinged anticline).

Figura 10. Resumen de perfiles sísmicos interpretados a través de la Cuenca Tiburón Superior; la ubicación de los cuadros se muestra en la **Figura 6**. La secuencia A, *prerift*, cubre el basamento y es desplazada por las fallas que limitan la cuenca. La secuencia B, *synrift*, forma estratos de crecimiento que acrecionan en las fallas que limitan la cuenca; note el cambio en la dirección de acreción sedimentaria a través de la cuenca (resaltados por las flechas más grandes en los cuadros A a G), al sur los sedimentos acrecionan al oeste (A-D), mientras que al norte acrecionan al este (E-G). La secuencia C, *postrift* cubre el relieve y se extiende y engrosa hacia la Cuenca Delfín Inferior (G-H). Hacia el noroeste, las secuencias A y B están plegadas y truncadas por el basamento; así que inferimos una falla de *detachment* buzante al este (F-H). Las **Figuras 7, 8 y 9** muestran parte de las líneas cuya interpretación se resume en los cuadros D, G y H; use la línea de referencia (RL) para encontrar correspondencia. (DMF: Falla De Mar; DHA: anticlinal de doble charnela).

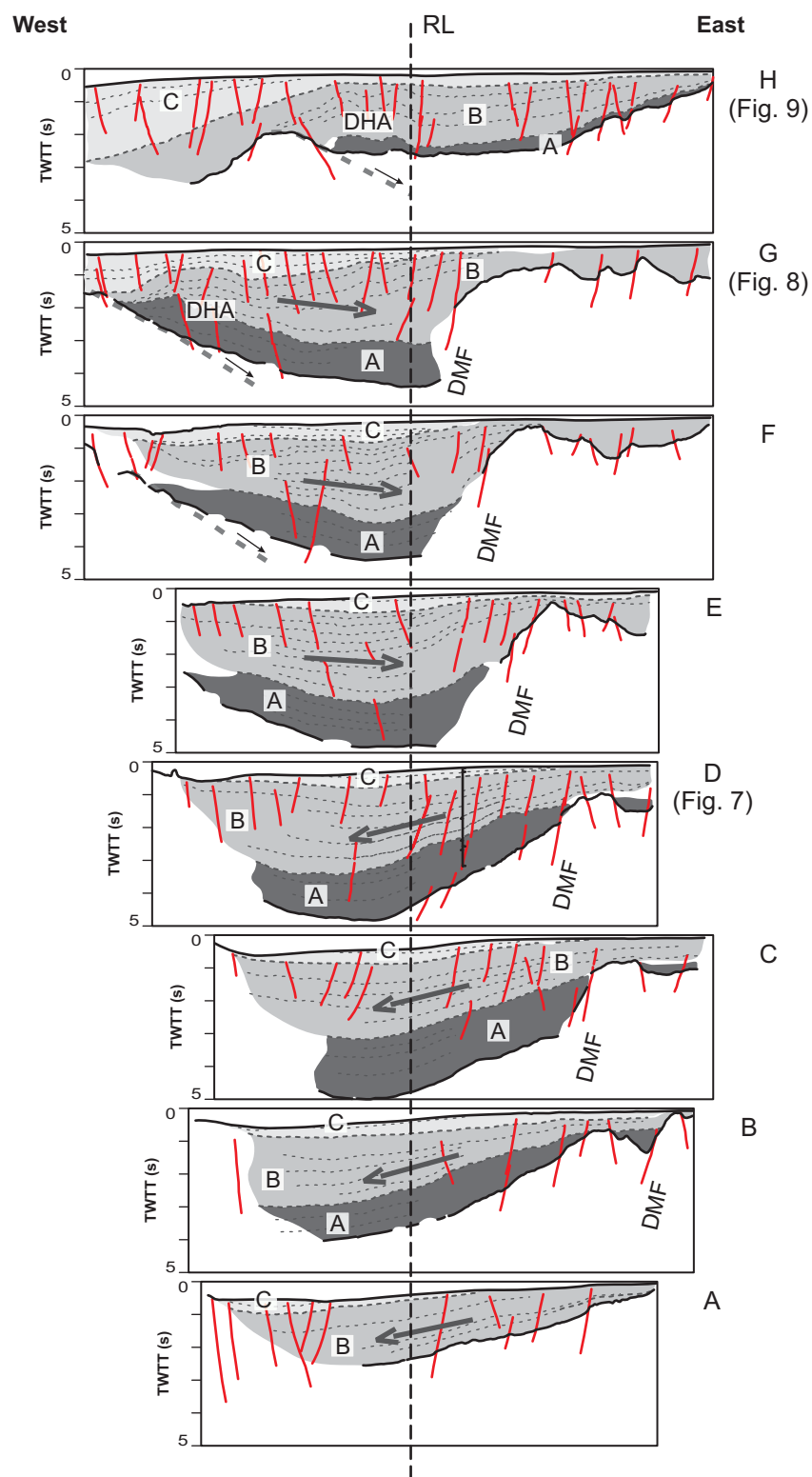


Figure 10.

600-1000); whereas the upper sequence reflectors lie parallel to the sequence boundary BC, which forms a gentle bowl-shape surface (Figs 10). Toward the east, the sequence reflectors form condensed sections that drape the De Mar fault and the basement offshore Sonora (Figs. 6; 7, ~CDP 2400-2700; 8, ~CDP 2100-2700). Toward the northwest sequence B is folded across the doubly-hinged anticline. Additionally, the reflectors are truncated at the basement and at sequence boundary AB (Figs. 8, ~CDP 200-600; 9, ~CDP 200-400). The reflector patterns interpreted in sequence B suggest that deposition was syntectonic to the growth of the conjugated Tiburón and De Mar faults, while folding and truncation of reflectors suggest the presence of a top-to-the east detachment fault (Figs. 10F; 10G; 10H).

The upper sequence (sequence C in Figs. 7, 8, 9, 10), with a maximum thickness of ~0.7 s, is formed by nearly parallel reflectors that outline a broad hammock pattern. The reflectors onlap sequence boundary BC (Figs. 7, ~CDP 1700-2000; 8, ~CDP 1600-2000; 9, ~CDP 1500-1900) and fill the bowl-shaped depression formed on top of sequence B. This sequence drapes and smoothes the bathymetric relief offshore Sonora and covers the doubly-hinged anticline in the northwestern Upper Tiburón basin; moreover, sequence C extends beyond the doubly-hinged anticline and significantly thickens to form the middle and upper strata of the active Lower and Upper Delfín basin; the sequence boundary BC also deepens into adjacent active basin (Figs. 8, ~CDP 1-500; 9, ~CDP 1-600; Fig. 10; see Chapter II). Sequence C includes several local unconformities, but they do not separate changes in the stratal pattern (Figs. 7, ~CDP 1000-2000); besides, these unconformities were not traced across the entire basin. The uppermost reflectors in the central portion of sequence C lie nearly parallel to the sea bottom; but near the edges reflectors are also

truncated at the sea bottom (Figs. 7, ~CDP 500-700; 7, ~CDP 2100-2300; 8, ~CDP 900-1100; 8, ~CDP 2000-2200; 9, ~CDP 1000-1200). These reflector patterns suggest that deposition of sequence C is post-tectonic to the growth of the Tiburón and De Mar faults and peneplained the bathymetric relief; in addition, the nearly-flat relief and the truncation of reflectors at the sea bottom indicate that this region is no longer subsiding.

Two volcanic knolls were identified above the trace of the Tiburón fault, in the central-west portion of the Upper Tiburón basin (Fig. 7, ~CDP 100); these knolls are composed of andesitic rocks (Martín-Barajas et al., 2002). These volcanoes should be very recent in age since their morphology is well preserved.

III.4.2. The Adair-Tepoca basin

The Adair-Tepoca basin displays a partially defined sigmoidal shape limited by the northern strands of the De Mar fault to the south and by the Adair graben to the north. The eastern limit is formed by the Amado fault and a west-dipping basement ramp that extend from offshore Sonora. Toward the west the boundary of this basin is the eastern flank of the doubly-hinged anticline that extends from the northern tip of the Tiburón fault to the southern end of the Cerro Prieto fault (Figs. 6; Aragón-Arreola and Martín-Barajas, 2007). The combined thickness of the sedimentary column reaches up to ~3.8 s (~4.8 km) and is formed by three seismostratigraphic sequences.

The lower sequence (sequence I in Figs. 11, 12, 13), with a maximum thickness of ~2.4 s (Fig. 11, ~CDP 1500), forms a southward deepening set of reflectors that extends over the northern and central portions of the Adair-Tepoca basin (Fig. 6; 13J to 13O). The strata in the southern half of sequence I outline a hammock-shaped configuration formed by nearly-parallel reflectors that onlap the acoustic basement offshore Sonora (Figs. 6, 13J, 13K,

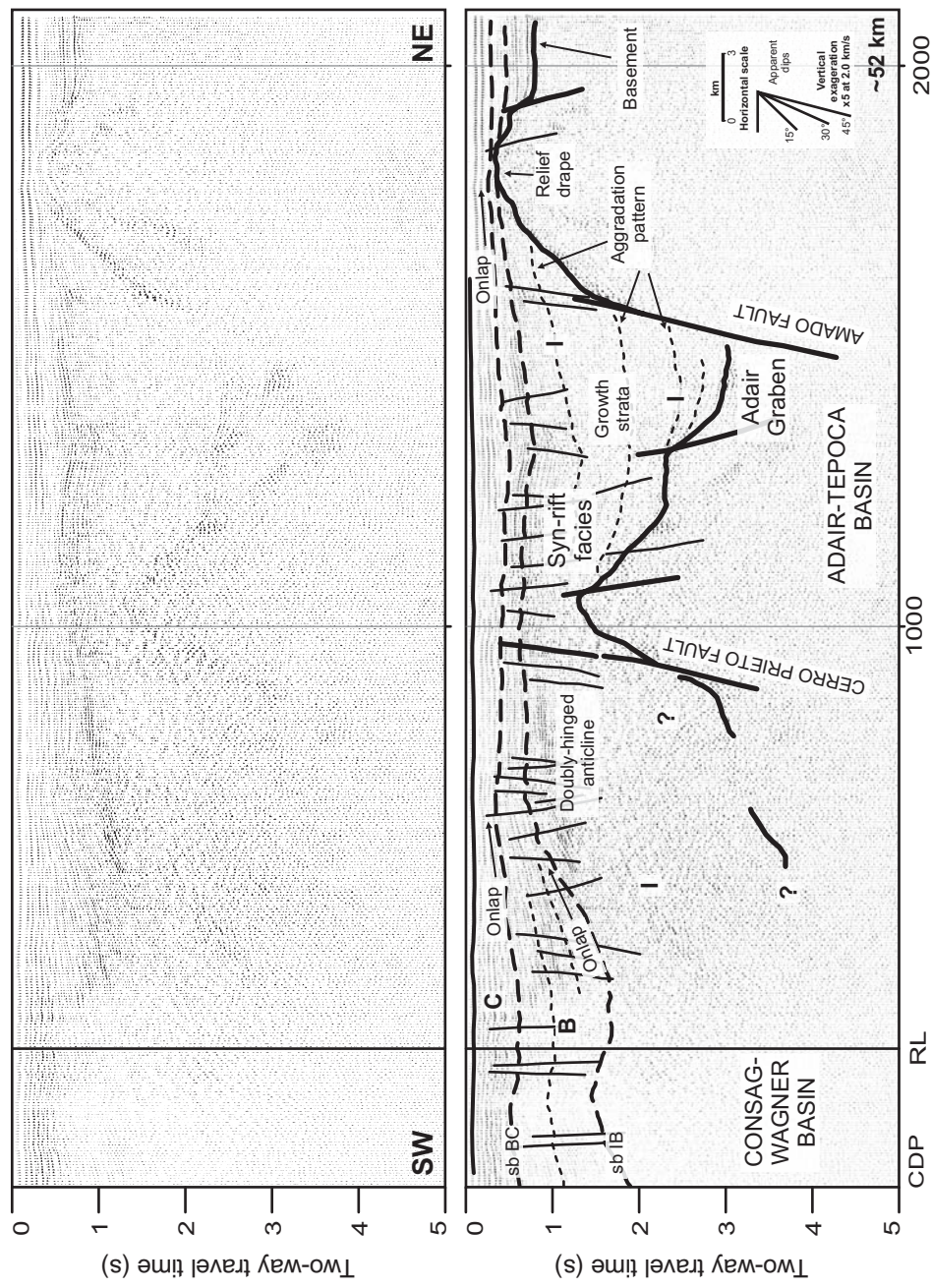


Figure 11. Migrated and interpreted seismic profile across the northern half of the Adair-Tepoca basin. Sequence I is interpreted to represent syn-rift facies, whereas in this profile sequence B and sequence C drape and smooth the relief. Sequence I and B are folded and build the doubly-hinged anticline that forms the western boundary of the Adair-Tepoca basin (sb: sequence boundary).

Figura 11. Perfil sísmico migrado e interpretado a través de la mitad norte de la Cuenca Adair-Tepoca. Se interpreta que la secuencia I representa facies *synrift*, mientras que en este perfil las secuencias B y C cubren y suavizan el relieve. Las secuencias I y B están plegadas y forman parte del anticlinal de doble charnela que constituye el límite oeste de la cuenca Adair-Tepoca. (sb: límite de secuencia).

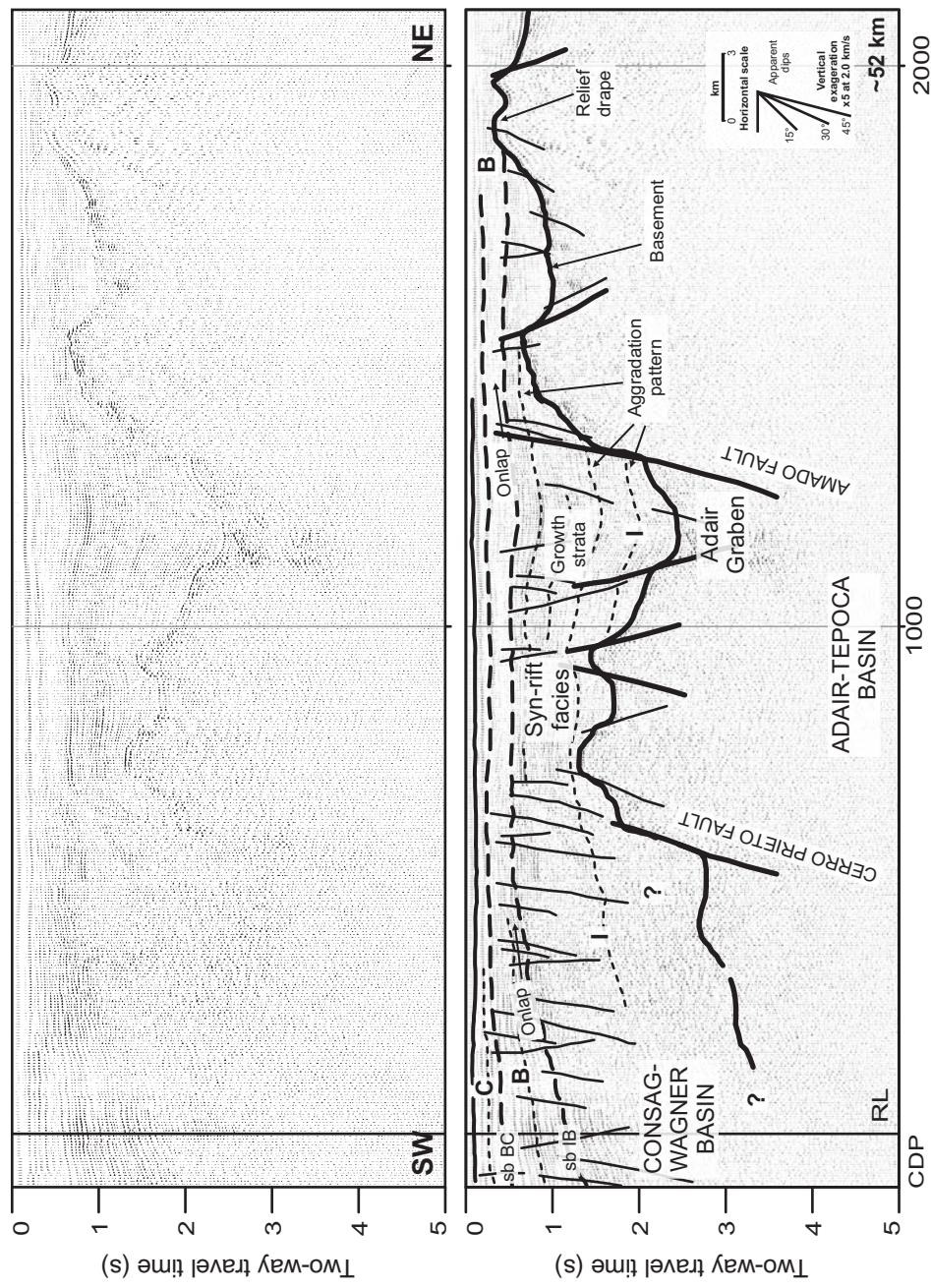


Figure 12. Migrated and interpreted seismic profile across the northern Adair-Tepoca basin. Sequence I fill by onlap the Adair Graben and is likely associated to the growth of the Amado fault, whereas sequence B and sequence C drape and smooth the relief. Sequence I and B are folded and build the northern end of the doubly-hinged anticline that bounds the Adair-Tepoca basin (sb: sequence boundary).

Figura 12. Perfil sísmico migrado e interpretado a través del norte de la Cuenca Adair-Tepoca. La secuencia I rellena por *onlap* el Graben Adair y está probablemente ligada al crecimiento de la Falla Amado, en tanto que las secuencias B y C cubren y suavizan el relieve. Las secuencias I y B están plegadas y forman la parte más al norte del anticlinal de doble charnela que limita la cuenca Adair-Tepoca. (sb: límite de secuencia).

also Chapter II, Fig. 4c). Toward the north, the strata fill by onlap the asymmetric Adair graben, which deepen to the south. Here sequence I is built by divergent reflectors that accrete against the Amado fault; the divergent and accretion patterns are interpreted as growth strata (Figs. 11, ~CDP 1000-2600; 12, ~CDP 800-1400; 13L-13O). Toward the west, the strata of sequence I are folded across the doubly-hinged anticline that bound the western margin of the Adair-Tepoca basin; sequence I extends beyond the doubly-hinged anticline and forms the lower strata of the adjacent Upper Delfín basin (Figs. 13I to 13K), and Consag-Wagner basins, where reflectors seem to be organized in a parallel configuration (Figs. 11, ~CDP 1-600; 12, ~CDP 1-1400; 13L to 13O). The uppermost reflectors in sequence I lie parallel to the sequence boundary IB, which is a subtly defined

Figure 13. Summary of interpreted seismic profiles across the Adair-Tepoca basin; location of boxes is shown in Figure 6. Sediments in the northern sequence I formed growth strata associated to growth of the Amado fault (L to O); far south, sequence I may have filled a broad depression (H to K). The south-deepening shape of the Adair graben suggests that this trough canalized sediments into the Adair-Tepoca basin. The lowermost strata of sequence B form divergent patterns likely syntectonic to the Amado fault (L), whereas the upper strata drape the relief and form a broad hammock-shaped sequence that reflect deposition in a preexisting basin (H to K). The upper sequence C is post-tectonic to the Amado fault and peneplained the bathymetric relief. Toward the west, sequence I and B are folded and extend beyond the doubly-hinged anticline that bounds the Adair-Tepoca basin. Figures 9, 11 and 12 only show part of the summarized interpretations in boxes H, M and N; use reference line (RL) for correspondence. (DHA, doubly hinged anticline; AG, Adair graben; CPF, Cerro Prieto fault).

Figura 13. Resumen de perfiles sísmicos interpretados a través de la Cuenca Adair-Tepoca; la ubicación de los cuadros se muestra en la Figura 6. Los sedimentos en la parte norte de la secuencia I forman estratos de crecimiento asociados con desarrollo de la Falla Amado (L a O); hacia el sur, la secuencia I parece haber rellenado una amplia depresión (H a K). La profundización hacia el sur del graben de Adair sugiere que esta fosa canalizó sedimentos hacia la Cuenca Adair-Tepoca. Los estratos más inferiores de la secuencia B forman patrones divergentes probablemente sin-tectónicos a la Falla Amado (L), mientras que los estratos superiores cubren el relieve y forman una secuencia hamacada amplia (H a K). La secuencia superior C es post-tectónica a la Falla Amado y cubre y suaviza el relieve. Hacia el oeste, la secuencia I y la secuencia B están plegadas y se extienden más allá del anticlinal de doble charnela que limita la Cuenca Adair-Tepoca. Las Figuras 9, 11 y 12 muestran parte de las líneas cuya interpretación se resume en los cuadros H, M y N; use la línea de referencia (RL) para encontrar correspondencia. (DHA: anticlinal de doble charnela; AG, graben de Adair; CPF, Falla Cerro Prieto).

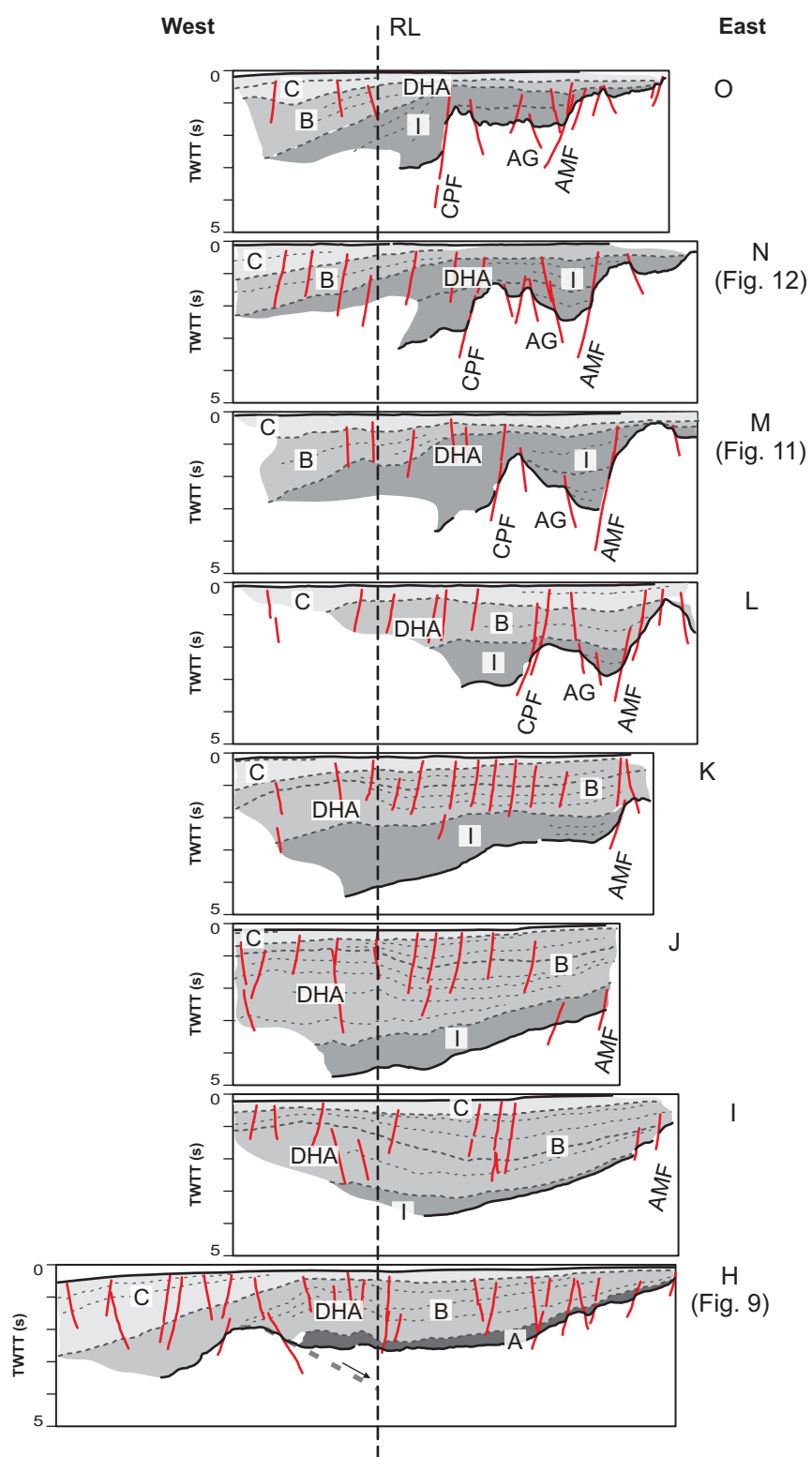


Figure 13.

boundary that steadily gains depth to the south within the Adair-Tepoca basin. Based on these seismo stratigraphic relationships we suggest that sedimentation in the northern half of sequence I formed growth strata controlled by growth of the Amado fault, whereas far south, the sequence may have filled a broad depression. The southward-deepening of seismic reflectors in the Adair graben suggests that this structure canalized sediments into the Adair-Tepoca basin; such canalization of sediments may result in the southward progradation of sedimentation, however the available data do not allow testing of this hypothesis.

The middle sequence (sequence B; Figs. 9, 11, 12, 13) also thickens southward and forms a package that reaches a maximum thickness of ~2.8 s (Fig. 13I). The reflector patterns display a variety of patterns within this sequence; toward the north, the reflectors are organized in a nearly-parallel array and outline a tabular-shaped sequence (Figs. 11, ~CDP 700-1600; Figs. 12, ~CDP 700-1400; 13M-13O). However, near the southern edge of the Adair graben the reflectors built divergent patterns that accrete and aggrade against the Amado fault (Fig. 13L). Far south, the reflectors show again a nearly-parallel configuration that outlines a broad hammock-shaped sequence (Figs. 9, ~CDP 800-2000; 13H-13I). The lower reflectors gently onlap sequence boundary IB, whereas the upper reflectors lie nearly parallel to the sequence boundary BC. The western reflectors of sequence B are folded across the upper levels of the doubly-hinged anticline; additionally, the southernmost reflectors are truncated at the basement and at the sequence boundary AB (Figs. 8, ~CDP 200-600; 9, ~CDP 200-400). These reflector patterns suggest that deposition of the lower strata of sequence B was syntectonic to the Amado fault, the relief-draping of the uppermost strata suggests that this section is either post-tectonic to the Amado fault or that

sediment supply largely exceeds subsidence. The southward deepening morphology of sequence B reflects the shape of a preexisting basin and suggest that this sequence could also be partially related to the inferred canalization of sediments throughout the Adair graben.

The upper sequence in the Adair-Tepoca basin (sequence C; Figs. 9, 11, 12, 13), is formed by nearly parallel reflectors that pinch out toward the east. The reflectors onlap the sequence boundary BC (Figs. 9, ~CDP 1500-1900; 11, ~CDP 300-600; 12, ~CDP 200-500) and drape the smooth topography on top of sequence B. Sequence C also drapes the doubly-hinged anticline and extends into the active Lower Delfín basin, where sequence C significantly thickens; sequence boundary BC also deepens to the west into adjacent active Wagner-Consag basin (Figs. 9, ~CDP 1-1000; 11, ~CDP 1-700; 12, ~CDP 1-500; 10K-100). The uppermost reflectors of sequence C lie nearly parallel to the sea bottom; and are truncated at the sea bottom near the edges of this sequence (Fig. 12, ~CDP 400-500). These reflector patterns suggest that sequence C is fully post-tectonic to the Amado fault and peneplained the bathymetric relief; as in the Upper Tiburón basin, the nearly-flat relief and the truncation of reflectors at the sea bottom indicate that this region is no longer subsiding.

III.4.3. Seismostratigraphic correlation of the inactive basins

The boundary between the Upper Tiburón and Adair-Tepoca basins is the deformation zone associated to the northern tip of the De Mar fault (Fig. 6). In this region the De Mar fault loses expression and appears to be gradually replaced by an array of small-heave, antithetic faults; this fault array defines a ~5 km-wide anticline (Figs. 8, ~CDP 1800-2200; see also Fig. 4, ~CDP 2100-2400 in Chapter II). This anticline strikes ~NW-SE and was

mapped by ~30 km from the northern strands of the De Mar fault to the eastern shoulder of the large doubly-hinged anticline that separates the active and inactive basins of the northern Gulf (Figs. 6; 9, ~CDP 600-1000).

The correlation across these two adjacent basins reveals that reflectors of sequence B and sequence C of the Upper Tiburón and Adair-Tepoca basin are laterally continuous and can be traced across the anticline formed in the northwestern projection of the De Mar fault. By contrast, sequence A is constrained to the lower section of the Upper Tiburón basin; this sequence thins toward the north and is folded and apparently truncated by an inferred detachment fault that juxtapose the strata and the acoustic basement (Figs. 8; 9; 10F; 10G; 10H), which suggest the tectonic termination of the northern side of sequence A. Sequence I is also constrained to the lower section of the Adair-Tepoca basin; this sequence onlap the basement as it deepens to the south, but sequence I terminates near the southern edge of this basin, between profiles I and H (Figs. 6; 13); however the low-quality of the deep seismic data beneath the northwestern projection of the De Mar fault does not properly image the southern termination of this sequence.

The correlation of sequence B and sequence C of the Upper Tiburón and Adair-Tepoca basins indicates the coeval deposition of a large portion of the stratigraphic succession in these two currently inactive basins.

III.5. Discussion

The structure in the inactive basins along the northeastern Gulf of California is mainly controlled by three large strike-slip faults; the Tiburón, De Mar and Amado faults which bound the sigmoidal Upper Tiburón and Adair-Tepoca basins (Figs. 3; 6; Aragón-Arreola

and Martín-Barajas, 2007). This structural style is similar to the pattern in the modern rift basins of the northwestern Gulf, where the stepover zone between the Canal de Ballenas and Cerro Prieto faults contains the Lower Delfín, Upper Delfín, and Consag-Wagner basins (Persaud et al., 2003). Thus, the whole structural fabric in the northern Gulf is related to the post-late Miocene oblique rifting of the Gulf of California (Lonsdale, 1989; Stock and Hodges, 1989; Aragón-Arreola and Martín-Barajas, 2007). Here we discuss the evolution of the stratigraphy in response to the structural evolution of the main fault pattern in the inactive margin of this transtensional system. Here, the main faults likely exerted a first order control on sedimentation, as expected due to the syn-tectonically evolution of basins and faults (Prosser, 1993; Cowie et al., 2000; Dawers and Underhill, 2000; Gawthorpe and Leeder, 2000; Gupta and Cowie, 2000).

III.5.1. Tectono-sedimentary evolution of the Upper Tiburón and

Adair-Tepoca basins

The correlation across the eastern margin of the northern Gulf reveals the synchronous evolution of a large portion of the stratigraphic record in the Upper Tiburón and Adair-Tepoca basins. These inactive basins are located in two adjacent segments of the Gulf of California rift: the Upper Tiburón-Upper Delfín and the Adair-Tepoca-Wagner-Consag segment.

The sigmoidal-shaped Upper Tiburón basin contains three main sequences that record its tectono-sedimentary history. The sequence A in the lower section of this basin display a broad hammock shape that appears to be deposited in a broad depression (Fig. 14); here the nearly-constant thickness of the sequence and the reflector parallelism suggest that subsidence was diffusely controlled. Sequence A is displaced by the De Mar and Tiburón

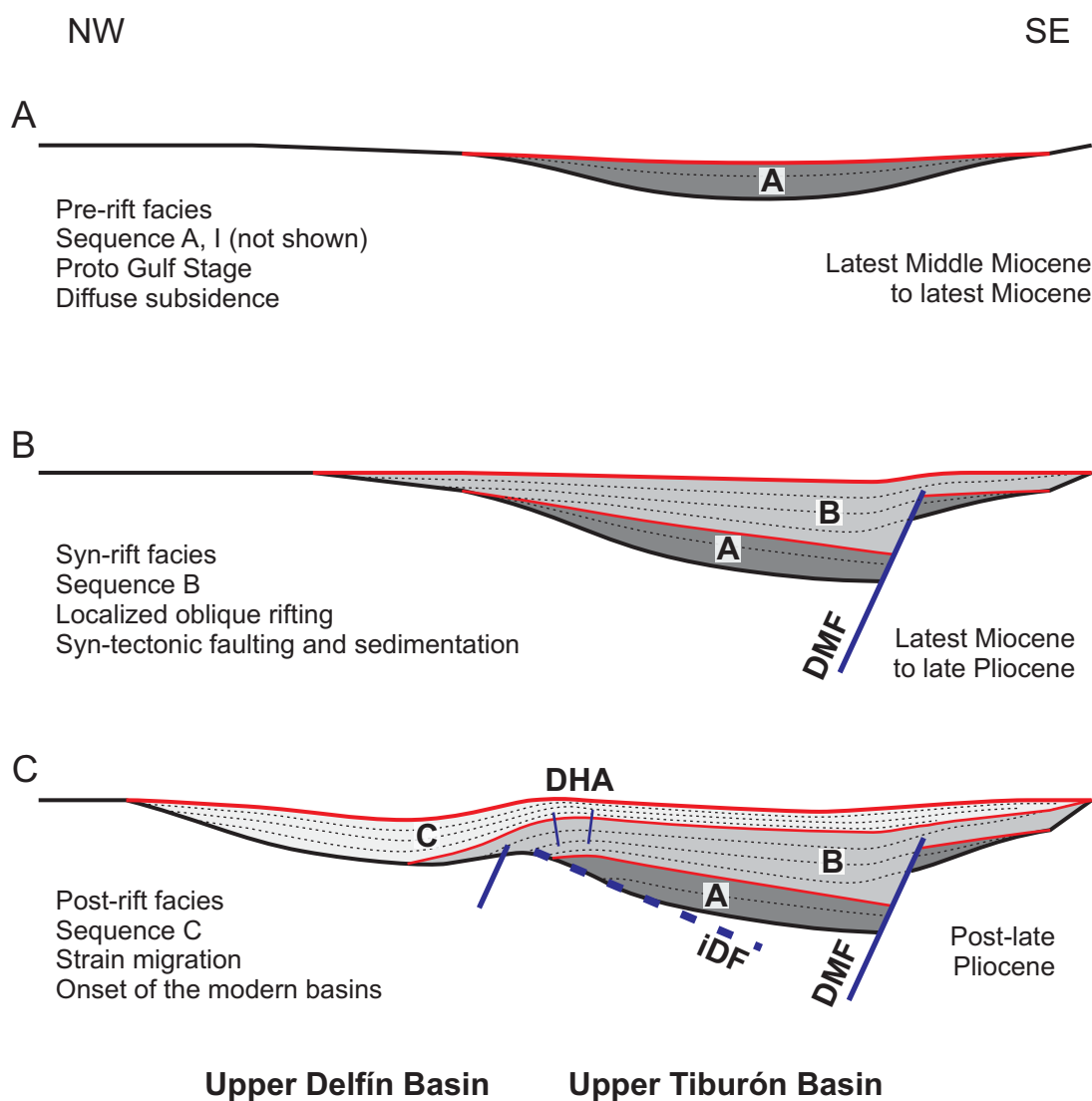


Figure 14. Schematic model of evolution for the northern segment of the Upper Tiburón basin in the northern Gulf of California (DMF: De Mar fault; DHA: doubly-hinged anticline/roll over anticline?; iDF: inferred detachment fault).

Figura 14. Perfil esquemático de evolución para el segmento norte de la Cuenca Tiburón Superior en el norte del Golfo de California (DMF: Falla De Mar; DHA: anticlinal de doble charnela; iDF: falla *detachment* inferida).

faults indicating that deposition occurred prior to the propagation of these faults.

A great portion of sequence A was intersected at the lower interval of a ~4800 m well W drilled by PEMEX (Figs. 6; 7). Unpublished results of the microfossil associations identified in samples of the lower ~1000 m section of this well indicate a latest Middle Miocene age and shallow marine environments (Martín-Barajas et al., 2005; Helenes, pers. comm.). If these results are correct, sequence A was likely deposited sometime during the latest-Middle Miocene in a broad and shallow marine basin (Figs. 14A; 14B). Regardless the age of these strata, sequence A represents pre-rift facies with respect to the growth of the Tiburón and Amado faults (cf. Prosser, 1993).

The deposition of sequence I in the Adair-Tepoca basin and sequence B in both the Upper Tiburón and Adair-Tepoca basins was controlled by the accommodation space generated by growth of the Tiburón, De Mar and Amado and the interactions while their evolution.

The lower sequence I, constrained to the Adair-Tepoca, was previously included within sequence B (Chapter II); however these strata can also be treated as a separate sequence attending to the variety of reflector patterns in this stratigraphic interval and the subtle, but regional sequence boundary IB (Figs. 11; 12). The seismic interpretation indicates that sediments of sequence I entered into the Adair-Tepoca basin via the through-going faults that built the Adair graben; here the sediments formed growth strata against the Amado fault. The deposits of sequence I deepened and went further away the southern termination of the Adair graben, filling an ample depression that gave rise to the hammock-shaped reflectors in the southern half of this sequence. These lateral variations suggests that sequence I represents syn-rift facies (cf. Prosser, 1993) formed by a southward prograding submarine fan; in such system the sediments would enter into the northern

Gulf through the inlet generated at the northern tip of the Amado fault (cf. [Gupta et al., 1998](#); [Cowie et al., 2000](#); [Gawthorpe and Leeder, 2000](#)). However, it should be noted that this hypothesis is based on profiles oriented perpendicular to the interpreted progradating direction; unfortunately we lack data that image the longitudinal axis of the Adair graben. Our suggestion of a submarine fan in the Adair-Tepoca basin implies the entrance of a massive source of sediments through the Adair graben, and the control of sedimentation by the Amado fault. This fault is linked to the localization of oblique deformation into the Gulf, which occurred between ~6.5-6.3 Ma, according to the reconstruction of conjugate margins across the Upper Tiburón-Upper Delfín basin segment ([Oskin et al., 2001](#); [Oskin and Stock, 2003a](#)). In the other hand, the localized oblique strain promoted the capture of the Colorado River, which began to flow into the Salton Trough, by ~5.3 Ma, during the latest Miocene ([Winker and Kidwell, 1996](#); [Dorsey et al., 2006](#); [Dorsey et al., 2007](#)). The analog and numerical models of extensional fault-controlled basins predict that the main drainages flow into the basins throughout the tips or relay ramps of the basin-bounding faults ([Gupta et al., 1998](#); [Cowie et al., 2000](#); [Dawers and Underhill, 2000](#); [Gawthorpe and Leeder, 2000](#)). The concurrence of strain localization, syntectonic sedimentation, the capture of the Colorado River during the latest Miocene, and the events predicted by models of extensional basins suggest that the Colorado River became the main source of sediments for the syn-rift facies of the northern Gulf of California. However, we lack time constraints of sequence I to support such hypothesis.

The sequence B can be traced across the Upper Tiburón and Adair-Tepoca basins, and form laterally continuous strata across these basins of adjacent rift segments.

Sequence B in the Upper Tiburón basin displays well-defined growth strata controlled by

the dip-slip motion of the Tiburón and De Mar faults. The conjugated Tiburón and De Mar faults display up to ~2.0 s of vertical throw (~2.0 km at 2,000 m/s P-wave velocity), and are inferred to accommodate a large amount of strike-slip motion (Nagy and Stock, 2000; Stock, 2000; Aragón-Arreola and Martín-Barajas, 2007). Thus the space generated within this couple of faults responds to wrench-type deformation that generated a pull-apart basin. We observe an along-the-basin shift in the polarity of sedimentary accretion where strata of the southern half of sequence B accrete westward against the Tiburón fault, whereas their northern counterpart accretes eastward against the De Mar fault (Fig. 10); this polarity shift support that sequence B was deposited in an evolving pull-apart basin. However, our data is oriented nearly perpendicular and parallel to the main basin-bounding faults, i.e. Tiburón and De Mar faults, and prevents the proper mapping of the shallow and small-heave faults (e.g. Figs. 7, ~CDP 700-2000; 8, ~CDP 1000-2000) that likely form the subsidiary and oblique fault arrays expected in pull-apart deformation.

Sequence B was fully sampled by well W (Figs. 6; 7); here the unpublished results of the microfossil associations indicate that sedimentation occurred between Late Miocene to Pliocene time in shallow marine environments (Martín-Barajas et al., 2005). Therefore, we propose that sequence B also represents syn-rift facies (cf. Prosser, 1993) in the northeastern Gulf (Fig. 14B).

The correlative sequence B in the Adair-Tepoca basin displays a somehow similar behavior than the underlying sequence I. The lower section also displays the canalization of sediments interpreted as a southward prograding submarine fan; however, the upper section of this sequence drapes the relief of the Amado fault, indicating either the post-tectonic deposition or that sediment supply from the Colorado River largely exceeds

accommodation space generated by the Amado fault; we favor the second explanation since no major sequence boundaries were identified within sequence B.

Sequence C can also be traced across the Upper Tiburón and Adair-Tepoca basins. Deposition of sequence C occurred after the waning and death of the large Tiburón, De Mar and Amado faults (Fig. 14C). The reflector patterns indicate that this sequence smoothed the preexisting relief and covers most faults related to tectonic activity, moreover, some areas show truncation at the sea bottom and indicate structural inversion. Results of microfossil associations identified in well W (~400-600 m, the uppermost sampled interval) indicate a latest Pliocene age for sequence C, also in shallow marine conditions (Martín-Barajas et al., 2005). Therefore we interpret that sequence C represent post-rift facies.

We identified two volcanic knolls of inferred young age over the trace of the Tiburón basin. Although magmatism is beyond the scope of this work, we suggests that these volcanoes could be related to a leak of magmatic material throughout the weak zone formed by the Tiburón fault; the source area for these melts could be the Lower Delfín basin that concentrate most of the magmatic activity in the northern Gulf (Persaud et al., 2003).

In summary, sequence A in the Upper Tiburón basin records sedimentation within a broad depression prior to the propagation of faults related to the Gulf of California rift (Fig. 14A). The onset of the Tiburón, De Mar and Amado faults gave rise to the formation of syn-rift facies; sequence I in the Adair-Tepoca basin is probably related to a submarine fan linked to the early entrance of the Colorado River, whereas sequence B was deposited in an evolving pull-apart basin in the stepover of the Tiburón and De Mar faults (Fig. 14B) while

progradation of submarine fan continued in the Adair-Tepoca basin. Finally, sequence C marks the stall of tectonic activity in the major basin-bounding faults that resulted in the development of post-rift facies and the smoothing of tectonic relief along the eastern rift margin in the northern Gulf (Fig. 14C).

III.5.2. Relevance of detachment faulting in oblique rifting

We have shown that the basement high that separates the active and inactive basins of the northern Gulf is probably cut by an east-dipping detachment fault. However, the trace of such fault is not imaged in our data; the observations that support this interpretation include the folding and truncation of sequence A and sequence B in the Upper Tiburón basin (Figs. 8; 9; 10F; 10G; 10H); besides, the doubly-hinged anticline that crowns the basement high and the inferred trace of the detachment fault can also be interpreted as a roll-over anticline (Fig. 14C). Therefore, we are confident on our interpretation of a top-to-the east detachment fault.

The reconstruction of conjugate margins across the Upper Tiburón-Upper Delfín basin segment indicates $\sim 255 \pm 10$ km of extension along an orientation of N50°W (Oskin et al., 2001; Oskin and Stock, 2003a). An attractive idea is that low-angle faults may accommodate this extension. The presence of low-angle faulting that accrues few tens of kilometers of extension has been documented in the onshore region of northeastern Baja California and in the Salton Trough (Axen and Fletcher, 1998; Axen et al., 1999; Pacheco-Romero et al., 2006; Dorsey et al., 2007). By contrast, in the marine region there are few studies that document low-angle faults; the few reports of such structures include the documentation of the likely listric Wagner fault that controls evolution of the Wagner-Consag basin (Hurtado, 2002; Aragón-Arreola and Martín-Barajas, 2007). Additionally,

the lateral variability of crustal thickness across the Upper Tiburón-Upper Delfín basin segment has been explained by a metamorphic core complex caused by detachment faulting ([González-Fernández et al., 2005](#)). Here we infer a top-to-the east detachment fault across of the northern edge of the Upper Tiburón basin that would cause the formation of a up to 20 km wide roll-over anticline and the definition of the basement high that separate the active and inactive basins due to the uplift of the lower plate. This detachment fault becomes a prime-order candidate to accommodate a considerable amount of extension in the northern Gulf; but, the estimation of slip is beyond the scope of this work.

III.5.3. Constraints to the timing of early marine sedimentation in the northern Gulf

The timing of early marine incursions and consequent sedimentation in-and-around the northern Gulf of California is still under debate. On one side, chronostratigraphic data suggest that the early marine incursions occurred during the onset of nearly-orthogonal extension in the Gulf during Middle Miocene time ([Karig and Jensky, 1972](#); [Gastil et al., 1975](#); [Stock and Hodges, 1989](#); [Gastil et al., 1999](#)); it is also suggested that these incursions might come in discrete pulses throughout a seaway located in central Baja California ([Helenes and Carreño, 1999](#)). Such latest Middle Miocene marine incursions have been documented in Bahía de los Ángeles, Isla Tiburón and central Sonora ([Ponce, 1971](#); [Gastil et al., 1999](#); [Delgado-Argote et al., 2000](#)). On the other side, based on the detailed reconstruction of conjugate margins across the Upper Tiburón-Upper Delfín basin segment, [Oskin and Stock \(2003b\)](#) indicate that the generalized marine flooding is related to the localization of oblique extension between ~6.5-6.3 Ma; this reconstruction argues

that the volcanic field of Isla Tiburón, offshore Sonora, and the Puertecitos Volcanic Province, onshore Baja California (Fig. 6) were adjacent by ~6.4 Ma, and later rifted apart by oblique deformation (Oskin et al., 2001; Oskin and Stock, 2003a). Consequently, this reconstruction implies that sediments in the Upper Tiburón and Upper Delfín basins should be younger than ~6.5-6.3 Ma. However, the microfossil data from well W seem to contradict this conclusion and support that the pre-rift marine facies of sequence A in the Upper Tiburón basin likely commenced in the latest Middle Miocene (Figs. 7; 8; Helenes et al., 2005). Therefore, at least one marine incursion that resulted in sedimentation of more than 1000 m occurred during the proto-Gulf stage (Karig and Jensky, 1972; Stock and Hodges, 1989), prior to the generalized marine flooding documented ca. 6.3 Ma (Oskin et al., 2001; Oskin and Stock, 2003a, 2003b; Dorsey et al., 2007). This suggests that the localization of strain into the Gulf of California region may have been a gradual instead of a sudden process, which has been already proposed by Gans (1997) and Fletcher and Munguía (2000). The mutually conflicting interpretations of when the marine sedimentation initiated within the northern Gulf still have to be reconciled to constrain the history of oblique rifting in the Gulf of California.

III.6. Conclusions

The Upper Tiburón and Adair-Tepoca basins formed a system of synchronously subsiding basins that include pre-rift, syn-rift and post-rift facies related to the evolution of the Tiburón, De Mar and Amado faults. The pre-rift facies are recorded in the lower sequence A of the Upper Tiburón basin and were deposited during the proto-Gulf stage, probably in the latest Middle Miocene. This sequence is formed by marine sediments accumulated in a

broad depression controlled by diffuse subsidence. Accumulation of the syn-rift facies started in the latest Miocene, when the oblique strain localized in the Gulf of California. The syn-rift facies include sequence I in the Adair-Tepoca basin and sequence B, correlated in both basins. In the Adair-Tepoca basin sequence I is formed by a southward deepening strata formed by an inferred submarine fan probably associated to the early entrance of the Colorado River into the Gulf, whereas sequence B records the exceed of accommodation space by sediment supply. Sequence B in the Upper Tiburón basin is formed by strata deposited in a pull-apart basin formed in the stepover of the Tiburón and De Mar faults. Sequence C is also correlated across both basins and drapes the tectonic relief; this sequence was accumulated as oblique strain wane in the northeastern Gulf and migrated to the west during the latest Pliocene. We infer a top-to-the east detachment fault that probably caused the formation of the basement high that separates the active and inactive basins in the northern Gulf; this inferred detachment fault is a prime candidate to accommodate significant amount of extension related to the opening of the northern Gulf of California.

IV. STRUCTURE OF THE RIFT BASINS IN THE CENTRAL GULF OF CALIFORNIA: KINEMATIC IMPLICATIONS FOR OBLIQUE RIFTING

Aragón-Arreola, M., Morandi, M., Martín-Barajas, A., Delgado-Argote, L., and González-Fernández, A., 2005. Structure of the rift basins in the central Gulf of California: kinematic implications for oblique rifting. *Tectonophysics*, 409(1-4): 19-38, doi:10.1016/j.tecto.2005.08.002.

IV.1. Abstract

We use structural and seismostratigraphic interpretation of multichannel seismic reflection data to understand the structure and kinematic history of the central Gulf of California. Our analysis reveals that oblique strain in the central Gulf formed two tectono-sedimentary domains during distinct deformation stages. The northeastern domain, offshore Sonora, is bounded by the East and West Pedro Nolasco faults which may constitute the southernmost segments of the Tiburón Fault System. Within this domain, the dip-slip Yaqui Fault controlled deposition of ~3.9 km of sediments in the half-graben Yaqui Basin. The southwestern domain, offshore Baja California, is bounded by the Guaymas Transform Fault, which controlled the accumulation of ~1.45 km of sediments within a half-graben that formed the early Guaymas Basin. The tectono-sedimentary activity offshore Sonora likely ranges from late Miocene-Pliocene to late Pliocene time, while activity in the Guaymas Basin commenced in late Pliocene time. Extinction of the main faults offshore Sonora was nearly coeval with the initiation of the Guaymas Transform Fault. Our results suggest that oblique strain has been accommodated by strain partitioning since the onset of rifting in the central Gulf. The Guaymas Basin is now a nascent spreading center, but previously it evolved as a half-graben controlled by the Guaymas

Transform Fault; such a drastic transition is not constrained, but likely occurred during Pleistocene time and must be localized <30 km north of the axial troughs. The faults within the central Gulf transpose the Miocene N-S oriented grabens of Basin and Range style preserved onshore in the conjugate rifted margins.

IV.2. Introduction

The Gulf of California hosts a zone of oblique extension that records the transition from spreading of new oceanic crust in the south to the rifting of continental crust in the north. Extension in north western México initiated during late Oligocene-mid Miocene time forming the continental-scale Basin and Range Province; later, in mid-Miocene time, the deformation was restricted to a broad region that surrounds the Gulf of California known as the Gulf Extensional Province ([Fig. 15](#)) ([Karig and Jensky, 1972](#); [Moore, 1973](#); [Stock and Hodges, 1989](#)). During late Miocene-early Pliocene time, the deformation localized in the western side of the Gulf Extensional Province, defining the Gulf of California rift and promoting a generalized marine incursion that formed the Gulf of California ([Lonsdale, 1989](#); [Stock and Hodges, 1989](#); [Holt et al., 2000](#); [Oskin and Stock, 2003a](#)).

Accommodation of oblique deformation varies along the Gulf of California Rift. In the southern and central portions of the active rift, strain is released through transform faults and basin-bounding normal faults ([Lonsdale, 1989](#)); whereas in the active northern rift, it is accommodated by dense arrays of oblique-slip faults ([Henye and Bischoff, 1973](#); [Persaud et al., 2003](#)). Evolution of oblique rifting involves the migration of deformation towards the west-northwest; it is suggested that the active spreading centers were preceded by now-abandoned rift zones preserved in the eastern Gulf ([Henye and Bischoff, 1973](#); [Lonsdale,](#)

1989; Fenby and Gastil, 1991; Stock, 2000). However, neither the current configuration of strain accommodation, nor the westward shifting of deformation are well constrained, and lack tectono-stratigraphic control.

Total extension in the Gulf Extensional Province is not well quantified, and estimates range between 350 and 600 km (Stock and Hodges, 1989; Lyle and Ness, 1991; Gans,

Figure 15. Main tectonic features of the central Gulf of California (after Fenby and Gastil, 1991) showing analyzed and compiled profiles from Albertin (1989); the bathymetric data are plotted as background. The shaded area over the Guaymas Basin shows the interpreted extent of transitional crust (Albertin, 1989). The five sites drilled by the Deep Sea Drilling Project Leg 64 are also shown (Curry et al., 1982a, 1982b). Note that the Ballenas Transform Fault strikes 6-7° more northerly than the Guaymas Transform Fault. The N-S oriented Bahía de los Ángeles (BAG) and Bahía de las Ánimas (BAnG) grabens in Baja California and the Empalme Graben in Sonora were formed during mid-Miocene time (Delgado-Argote et al., 2000; Mora-Álvarez and McDowell, 2000; Roldán-Quintana, et al., 2004), while the grabens in Loreto (LoB), Concepción (CoB) and Santa Rosalía (SrB) basins, in the Baja California coastal plain, evolved during late Miocene-early Pliocene time (Dorsey and Umhoefer, 2000; Ledesma-Vásquez and Johnson, 2001). The dashed box indicates area detailed in Figure 22. The inset sketches the main tectonic features around the Gulf of California, including the Gulf Extensional Province, the Gulf of California rift; and the area with new oceanic floor. The Gulf of California rift forms the transtensional boundary of the North America (NA) and Pacific (PA) plates. Other abbreviations: TF, transform fault; FZ, fracture zone; PI, Pedro Nolasco Island; TI, Tortuga Island; MAT, Middle America Trench.

Figura 15. Rasgos tectónicos principales en la parte central del Golfo de California (tomado de Fenby y Gastil, 1991), se muestran los perfiles analizados y compilados provenientes de Albertin (1989); la batimetría se presenta como información de fondo. El área sombreada sobre la Cuenca de Guaymas muestra la extensión interpretada de corteza transicional (Albertin, 1989). Se muestran también los cinco sitios perforados por el Deep Sea Drilling Project Leg 64 (Curry et al., 1982a, 1982b). Note que la Falla Transforme de Ballenas está orientada 6-7° más al norte que la Falla Transforme de Guaymas. Los graben de Bahía de los Ángeles (BAG) y Bahía de las Ánimas (BAnG), orientados N-S en Baja California y el Graben de Empalme, en Sonora, se formaron durante el Mioceno medio (Delgado-Argote et al., 2000; Mora-Álvarez y McDowell, 2000; Roldán-Quintana, et al., 2004), mientras que los graben que forman las cuencas de Loreto (LoB), Concepción (CoB) y Santa Rosalía (SrB), en la planicie costera de Baja California, evolucionaron durante el Mioceno Tardío al Plioceno temprano (Dorsey y Umhoefer, 2000; Ledesma-Vásquez y Johnson, 2001). El recuadro marcado con línea punteada indica el área detallada en la Figura 22. El mapa insertado esquematiza los rasgos tectónicos principales alrededor del Golfo de California, incluyendo la Provincia Extensional del Golfo, el Rift del Golfo de California y el área con piso oceánico nuevo. El Rift del Golfo de California forma el límite transtensivo entre las placas Norteamericana (NA) y Pacífica (PA). Otras abreviaciones: TF, falla transforme; FZ, zona de fractura; PI, Isla Pedro Nolasco; TI, Isla Tortuga; MAT, Trinchera Mesoamericana.

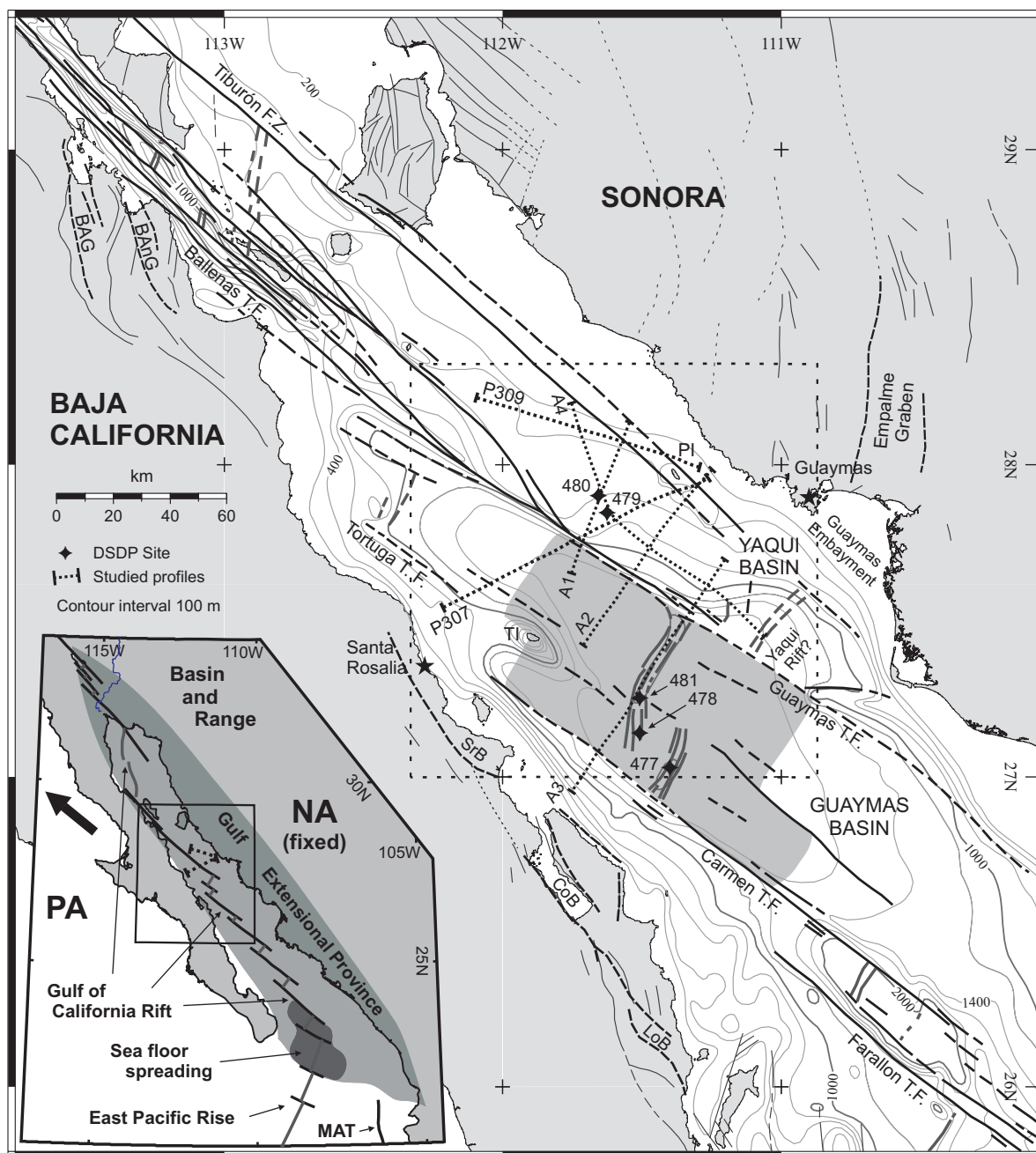


Figure 15.

1997). From this amount the Gulf of California rift has accommodated 270-300 km in the last ~6-6.5 Ma (Oskin et al., 2001; Oskin and Stock, 2003a). However, despite such large extension, only 220-230 km of new ocean floor has been created in the southernmost edge of the rift (Fig. 15) (Ness et al., 1991), whereas in the northern rift only ~30 km of transitional crust has been documented (Fuis and Kohler, 1984).

The Gulf of California is an attractive area to understand the kinematics of oblique rifting. Obliquity in the Gulf of California (defined as the acute angle formed by the rift direction and the extension direction) varies between 20-25° (Withjack and Jamison, 1986). Analog experiments of oblique rifting show strong disparities of strain accommodation as a function of obliquity, with fundamental changes at obliquity of 20-30° (Withjack and Jamison, 1986; Bonini et al., 1997). This makes the Gulf of California rift an interesting site to learn about particularities of continental rupture at critical obliquity angles.

The western Gulf hosts several well-studied active basins (Phillips, 1964; Lonsdale, 1985; Lonsdale, 1989; Persaud et al., 2003); while the eastern Gulf contains numerous older, poorly documented basins. Study of these basins appears critical to understanding the rifting history, since they are probably related to the early opening of the Gulf. The processing and interpretation of new, high-quality multichannel seismic reflection data, along with the compilation of published interpretations of seismic reflection profiles (Albertin, 1989), give us the opportunity to study the tectono-sedimentary evolution of the Yaqui and Guaymas Basins, two adjacent transtensional basins that document the shifting of deformation from the Sonoran shelf to the central and western Gulf of California. We document that localized rifting began with the accommodation of transtensional strain in the Sonoran margin; subsequently the deformation migrated to the west and formed the

modern configuration of transform faults linking youthful spreading centers (Fig. 15).

IV.3. Regional geological framework

The Gulf of California holds an active system of en echelon basins connected by right-step transform faults (Fig. 15) (Lonsdale, 1989; Fenby and Gastil, 1991). Structure of the active rift shows conspicuous changes along strike. In the southern and central Gulf, the active basins have water depths deeper than 2000 m, and contain sedimentary piles of <1 km thickness. The basins are bounded by transform faults, and the basement consists of transitional and oceanic crust. Basins of the southern and central Gulf form true nascent spreading centers (Curry et al., 1982a; Lonsdale, 1989). In the northern Gulf, the active basins have water depths shallower than 900 m, and contain sedimentary piles of >4 km thickness (Aragón-Arreola and Martín-Barajas, 2003). These basins have diffuse boundaries, and are located within a broad zone of deformation between the Cerro Prieto and the Ballenas transform faults (Fig. 15) (Henyey and Bischoff, 1973; Persaud et al., 2003). The basement appears to consist of continental or transitional crust (Phillips, 1964; González-Fernández et al., 2005). These basins resemble pull-apart structures instead of true spreading centers (Henyey and Bischoff, 1973). Furthermore the transform faults of the northern Gulf are oriented 6-7° more northerly than those in the southern and central Gulf (Fig. 15). This change has been related to the differences of crust juxtaposed by transform faulting: this is, oceanic-like, transitional and continental crust to the south, compared to continental and transitional crust to the north (Phillips, 1964; Lonsdale, 1989). The structure of the Gulf also shows conspicuous changes across strike. The crust thins towards Baja California and is thicker toward Sonora (Phillips, 1964; Fuis and Kohler,

1984; Couch et al., 1991). The eastern Gulf hosts abandoned faults and basins interpreted as aborted spreading centers, while the central and western Gulf holds the basins and transform faults that form the active rift system (Lonsdale, 1989, Fenby and Gastil, 1991; Stock, 2000). Also discrete volcanism, shallow intrusions and mid-ocean ridge volcanism has been documented only along the western and central Gulf (Curry et al., 1982a; Einsele et al., 1980; Lonsdale, 1989; Sawlan, 1991). These structural and magmatic differences across the Gulf indicate an asymmetric rifting process.

The central Gulf of California straddles the major structural transition along the rift. The bathymetry along the eastern Gulf is a gently westward deepening platform (Fig. 15) formed on subsided continental crust (Lonsdale, 1989). In this area eight seismic profiles studied by Albertin (1989) showed the presence of faulted acoustic basement covered by ~2.5 s of sediments; however this study did not discuss the interpreted structural features because it was focused on the Guaymas Basin. In the eastern Gulf, the Deep Sea Drilling Project (DSDP) drilled sites 479 and 480 (Fig. 15), recovering hemipelagic sediments. DSDP hole 479 bottomed at 440 m below the sea bed, in a late Pliocene sequence (1.8-2.4 Ma) (Curry et al., 1982b), which is here imaged in the upper 0.3 s of the seismic profiles. The Guaymas Basin is one of the best studied in the Gulf and contains evidence of oceanic lithosphere beneath the depocenter (Curry et al., 1982a; Saunders et al., 1982). This basin is bounded by prominent scarps formed by the Guaymas Transform Fault to the east and the Carmen and Tortuga transform faults to the west, while the southern and northern boundaries are formed by the bathymetric slopes of Sonora and Baja California, respectively (Fig. 15). The depocenter of the Guaymas Basin is controlled by two overlapping fault troughs that constitute the axis of a nascent spreading center (Curry et

al., 1982a; Einsele et al., 1980; Lonsdale, 1985). The basement here is interpreted to consist of recently accreted crust (Lonsdale, 1985; Albertin, 1989). DSDP sites 477, 478, and 481 reinforced this interpretation with the recovery of tholeiitic and dolerite sills intruding hemipelagic and turbiditic facies (Curry et al., 1982a; Einsele et al., 1980).

The free air gravity field in the central Gulf shows two domains bounded by the Guaymas Transform Fault (Fig. 16) (CONMAR, 1987). The northeastern domain is centered in the Guaymas Embayment and comprises a NW-oriented gravity low extending ~125x40 km. Its eastern and southern limits are formed by the gravity gradients related to the Sonoran coast; the western limit is formed by the abrupt gradient related to the Guaymas Transform Fault, whereas the northern limit is formed by a broad gravity high. Within this domain lie the Pedro Nolasco Gravity High and an adjacent gravity low oriented parallel to the Ballenas and Tiburón transform faults.

The southwestern domain coincides with the Guaymas Basin and consists of a NW-trending gravity low extending ~250x45 km. The eastern and western limits are the strong gravity gradients related to the Guaymas and Carmen transform faults, respectively; the northern limit is the San Miguel Gravity High, while the southern limit is not well defined. Within this domain lie the North Guaymas Low and the Tortuga Gravity High, oriented parallel to the Guaymas Transform Fault (Fig. 16).

Off-axis volcanism occurs in the northwest side of the Guaymas Basin (Figs. 15, 16). Tortuga Island is the emerged cone of a tholeiitic shield volcano younger than 1.7 Ma (Batiza, 1978). This island sits on the WNW-oriented Tortuga Volcanic Ridge (Fabriol et al., 1999), which produces the Tortuga Gravity High (CONMAR, 1987).

The rifted margins of the central Gulf preserve remnants of a Miocenic volcanic arc and

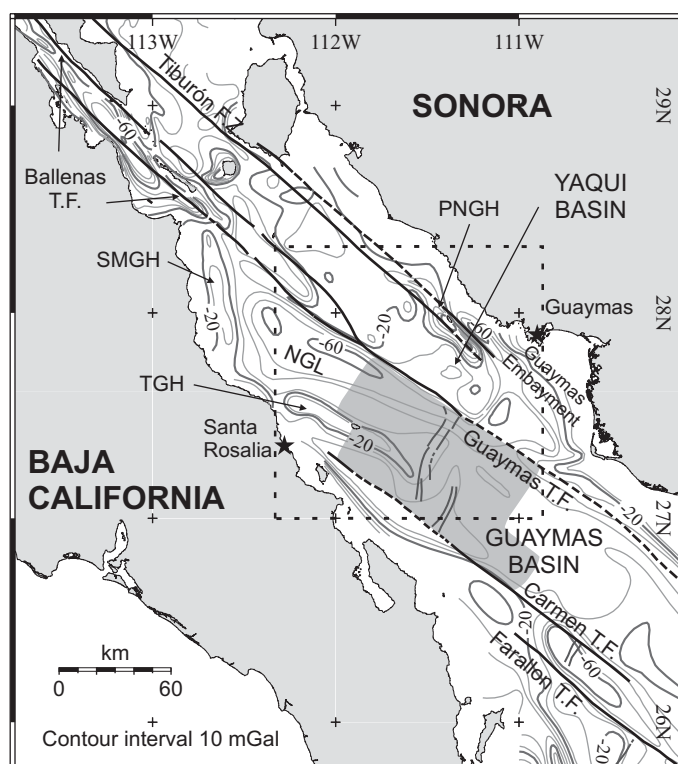


Figure 16. Free air gravity anomaly of the central Gulf of California (CONMAR, 1987), showing the simplified main tectonic features (after Fenby and Gastil, 1991). The shaded area over the Guaymas Basin represents the interpreted extent of transitional crust (Albertin, 1989). The Guaymas Transform Fault splits the central Gulf of California in two domains. The northeastern domain extends over the Yaqui Basin and contains the Pedro Nolasco Gravity High (PNGH) and an adjacent gravity low, lying parallel to the Ballenas and Tiburón transform faults. The southwestern domain coincides with the Guaymas Basin and contains the Tortuga Gravity High (TGH), oriented parallel to the Guaymas Transform Fault. The dashed box indicates the area detailed in **Figure 22**. Other abbreviation: TF, transform fault; FZ, fracture zone; SMGH, San Miguel Gravity High; NGL, North Guaymas Low.

Figura 16. Anomalía gravimétrica de aire libre en la parte central del Golfo de California (CONMAR, 1987) mostrando los rasgos tectónicos simplificados (modificado de Fenby y Gastil, 1991). El área sombrada sobre la Cuenca de Guaymas representa la extensión interpretada de corteza transicional (Albertin, 1989). La Falla Transforme de Guaymas divide la parte central del Golfo de California en dos dominios. El dominio noresteeste se extiende sobre la Cuenca Yaqui y contiene el Alto Gravimétrico Pedro Nolasco (PNGH) y un bajo gravimétrico adyacente, que yacen paralelos a las fallas transforme Ballenas y Tiburón. El dominio suroeste coincide con la Cuenca de Guaymas y contiene el Alto Gravimétrico Tortuga (TGH), paralelo a la Falla Transforme de Guaymas. El recuadro marcado con línea punteada indica el área detallada en la **Figura 22**. Otras abreviaciones: TF, falla transforme; FZ, zona de fractura; SMGH, Alto Gravimétrico de San Miguel; NGC, Bajo gravimétrico Guaymas norte.

exhumed sedimentary basins related to the early Gulf of California (Fig. 15). Rocks of the Miocene Comondú volcanic arc rest on Cretaceous granitoids and crop out in both margins of the central Gulf. These rocks were faulted between ~16-12 Ma, forming N-S oriented grabens of Basin and Range style, including the Bahía de los Ángeles and Bahía de las Ánimas grabens in Baja California and the Empalme graben in Sonora (Hausback, 1984; Gans, 1997; Delgado-Argote et al., 2000; Mora-Álvarez and McDowell, 2000; Roldán-Quintana, et al., 2004). A later stage of faults striking NW-SE produced half-graben type basins, such as the Loreto, Concepción and Santa Rosalía (Boleo) basins, preserved onshore Baja California. Marine sedimentation in these basins started between 5-7 Ma (Dorsey and Umhoefer, 2000; Holt et al., 2000), and lasted until early Pliocene time. Evolution of these basins was controlled by the development of oblique-slip and dip-slip listric faults (Wilson, 1955; Dorsey and Umhoefer, 2000; Ochoa-Landín et al., 2000; Ledesma-Vásquez and Johnson, 2001).

IV.4. Observations and interpretation

The major faults in the central Gulf of California outline the Yaqui and Guaymas basins (Figs. 15, 16). The following structural description is based on both available data sets, but the seismostratigraphic interpretation uses only the CORTES-P96 data (Figs. 17 to 20) since the Albertin (1989) profiles are available only in hardcopies that do not resolve small details. The joint interpretation of CORTES-P96 and Albertin (1989) data is shown in Fig. 21.

IV.4.1. Structure of the Yaqui Basin

The Yaqui Basin, offshore Sonora, is a half-graben built by faulted basement (Figs. 17 to

19). The eastern basin boundary consists of the Yaqui Fault (YF), a buried structure with a throw of up to ~ 2.5 s (~ 3.7 km), dipping $50\text{--}55^\circ$ west; this fault is well suggested by the free-air gravity data. The acoustic basement and the deeper sediments of the basin are cut by several faults antithetic to the YF, with vertical throws up to ~ 0.23 s (~ 0.45 km). The YF and the opposing faults define a ~ 10 km-wide graben structure in the deeper basin (Figs. 17 and 19). The acoustic basement of the northern Yaqui Basin lies at ~ 2.0 s, and has low-amplitude relief disrupted by one fault with <0.5 s of vertical offset (Fig. 18). The joint interpretation of Albertin (1989) and our data (Fig. 21) shows that the basement deepens southeastwards from ~ 2.0 to ~ 3.7 s, and suggests that the basement forms an elongated bowl-shaped sag. The Yaqui Basin is displaced by the Guaymas Transform Fault; thus the western end of the sedimentary deposits is not imaged by our data (Fig. 17). The Pedro Nolasco High, in the eastern Gulf (PNH in Figs. 15, 16), consists of uplifted basement cropping out on Pedro Nolasco Island (Fig. 15). This structural high consists of a ~ 15 km-wide horst limited to the east by an east-dipping fault with a throw of ~ 1 s, and to the west by the YF. This high is bisected by a west-dipping fault zone containing four fault branches, which produce a westward step-down configuration of the basement (Figs. 17,

Figure 17. Profile P307 across the Yaqui and northern Guaymas basins in the central Gulf of California showing the free-air gravity anomaly profile (upper), the migrated section (center), and the interpreted structural and seismostratigraphic features (lower). Location of sequence labels indicates the locus of sequence maximum thickness. Site 479 of the Deep Sea Drilling Project is projected onto the profile.

Figura 17. Perfil P307 a través de las cuencas Yaqui y norte de Guaymas en la parte central del Golfo de California, mostrando la anomalía gravimétrica de aire libre (arriba), la sección migrada (centro) y la interpretación estructural y sismoestratigráfica (abajo). La ubicación de las letras que identifican las secuencias indica la localización del espesor máximo de la secuencia. El sitio 479 del Deep Sea Drilling Project está proyectado al perfil.

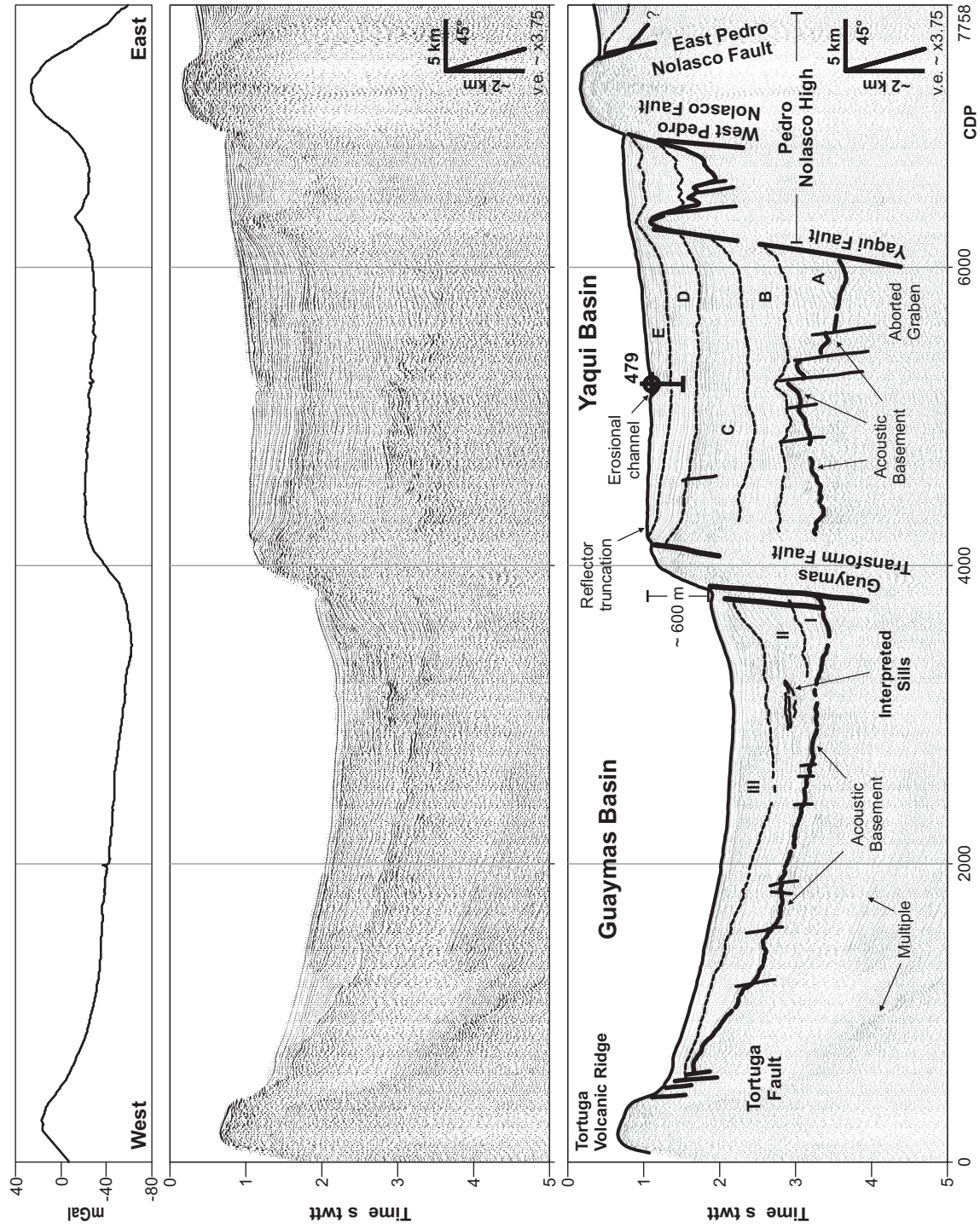


Figure 17.

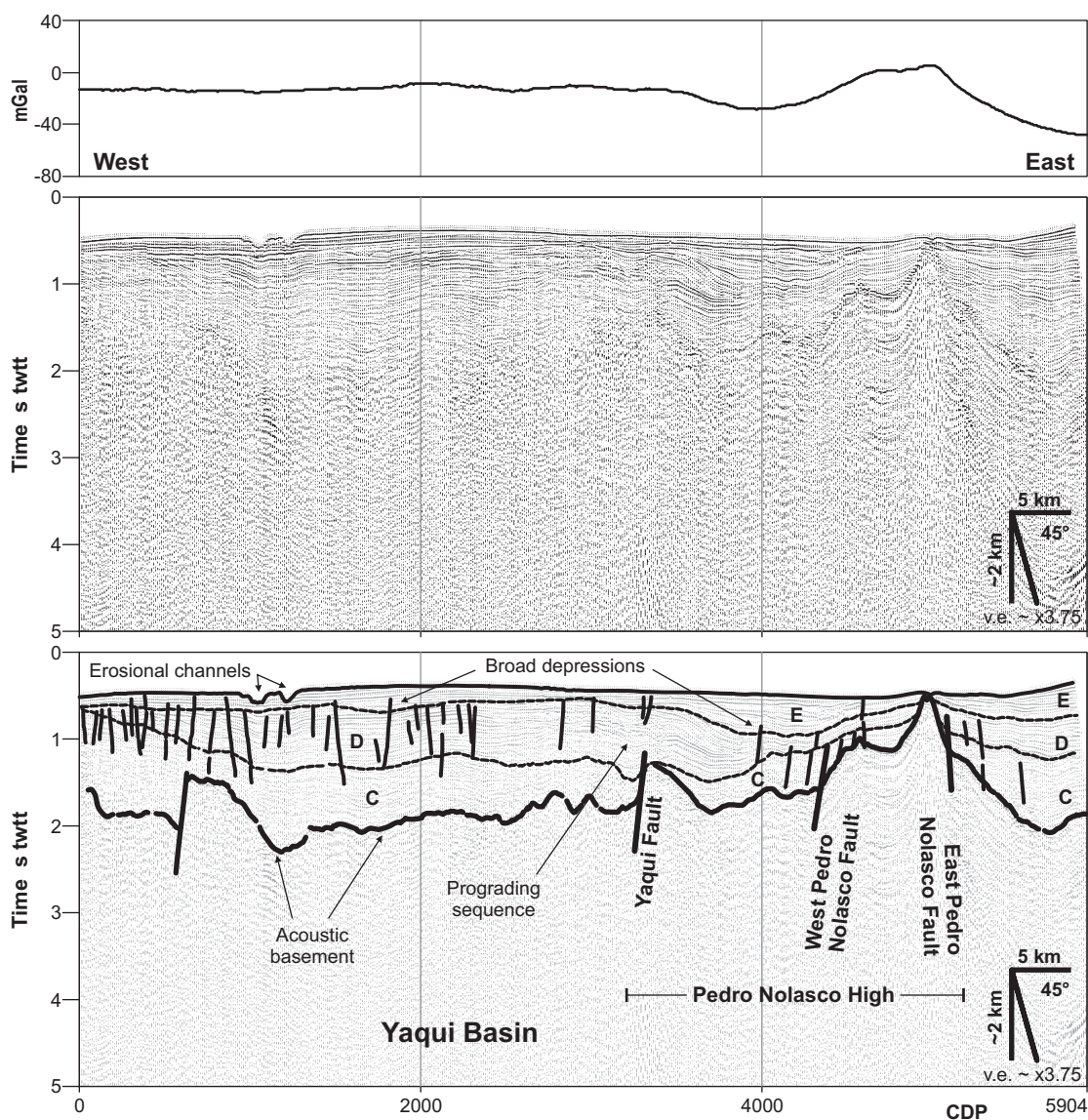


Figure 18. Profile P309 across the northern Yaqui Basins offshore Sonora in the central Gulf of California showing the free-air gravity anomaly profile (upper), the migrated section (center), and the interpreted structural and seismostratigraphic features (lower).

Figura 18. Perfil P309 a través del norte de la Cuenca Yaqui, frente a la costa de Sonora, en la parte central Golfo de California. Se muestran la anomalía gravimétrica de aire libre (arriba), la sección migrada (centro) y la interpretación estructural y sismoestratigráfica (abajo).

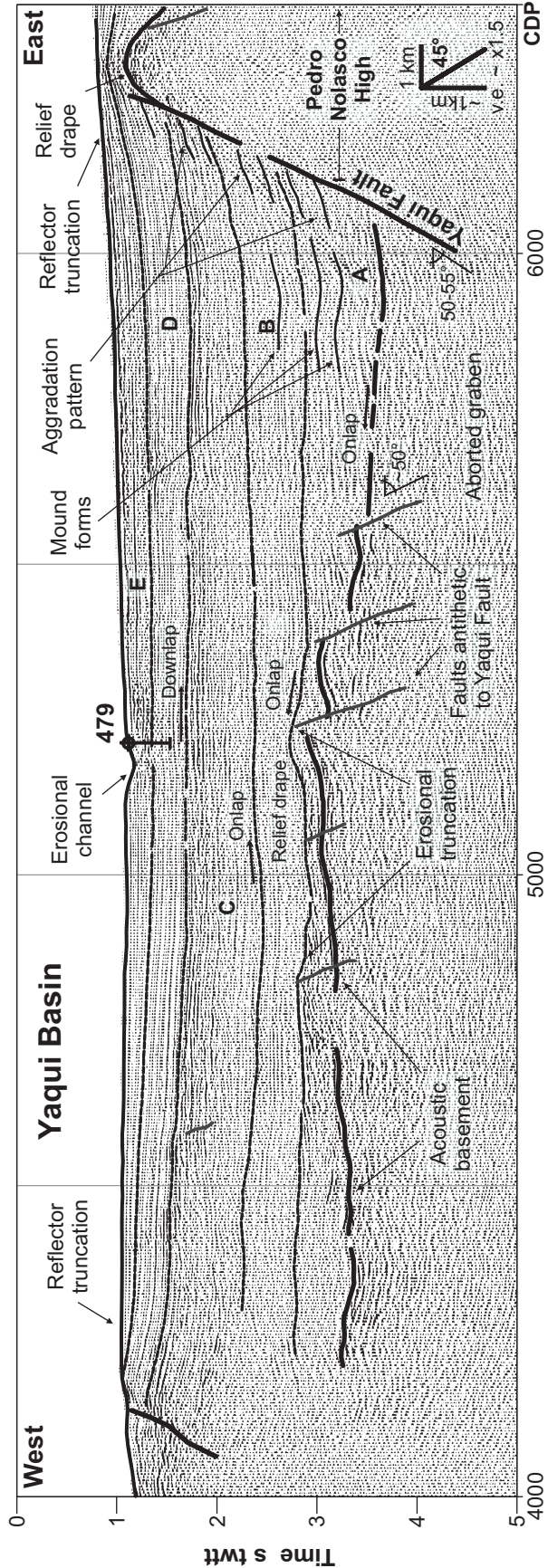


Figure 19. Detail of Profile P307 (migrated section) across the eastern margin of the Yaqui Basins highlighting interpreted structural and seismostratigraphic features. Location of sequence labels indicates the locus of the maximum sequence thickness. Site 479 of the Deep Sea Drilling Project is projected onto the profile.

Figura 19. Detalle del perfil P307 (sección migrada) a través del margen este de la Cuenca Yaqui, se resaltan los rasgos estructurales y seismostratigráficos interpretados. La ubicación de las letras que identifican las secuencias indica la localización del espesor máximo de la secuencia. El sitio 479 del Deep Sea Drilling Project está proyectado al perfil.

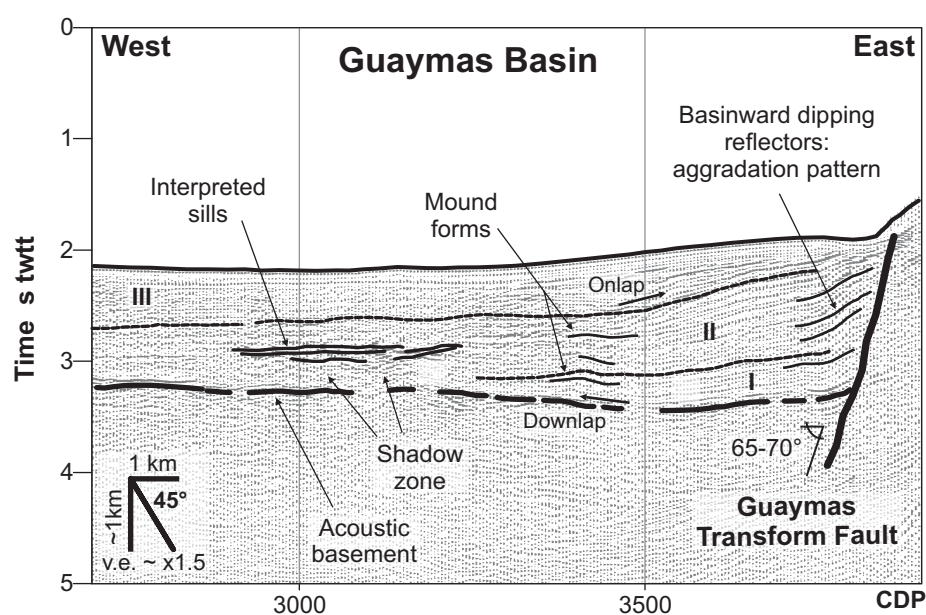


Figure 20. Detail of Profile P307 (migrated section) across the northern Guaymas Basins. Note the westward migration of the maximum sequence thickness (indicated by location of sequence labels). The highlighted high-amplitude reflectors are interpreted as a zone of sills intruding a shallow stratigraphic interval within Sequence II.

Figura 20. Detalle del perfil P307 (migrated section) a través del norte de la Cuenca de Guaymas. Note que el espesor máximo de las secuencias (indicado por la ubicación de las letras que identifican las secuencias) ha migrado hacia el oeste. Los reflectores de alta amplitud que se resaltan son interpretados como intrusivos tabulares que se alojan en los intervalos someros de la Secuencia II.

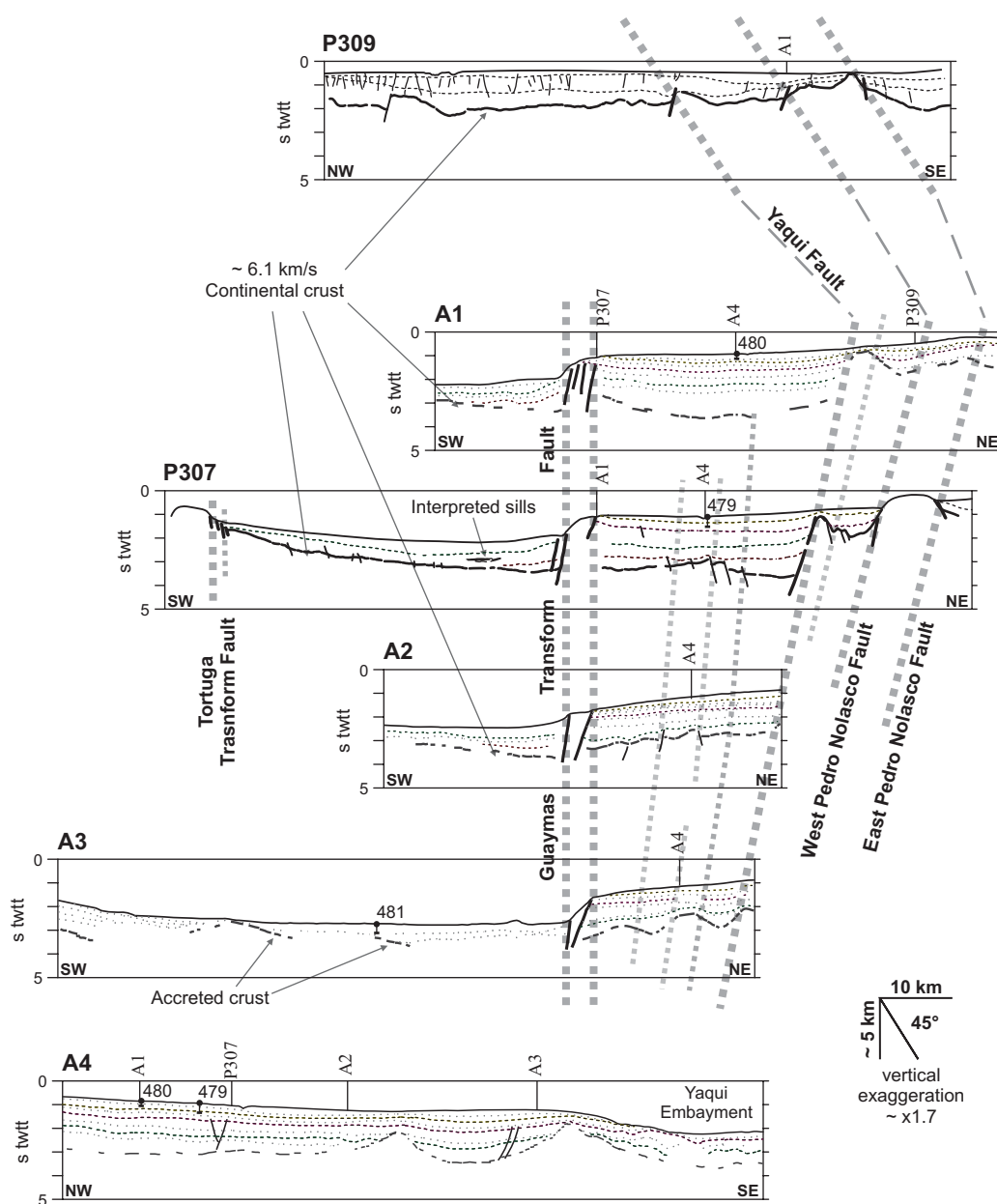


Figure 21. Seismostratigraphic interpretation of analyzed and compiled multichannel seismic reflection profiles. Profiles A1 through A4 were taken from Albertin (1989). The dashed lines show the structural correlation; line weight and dash length indicate the relative importance of each fault. This correlation was used to compile the structural map of Figure D8. Sites 479, 480 and 481 of the Deep Sea Drilling Project are projected into the corresponding profiles. Note that Profile P309 is oblique to the main structural fabric, while profile A4 lies nearly parallel to the main fault orientation.

Figura 21. Interpretación sismoestratigráfica de los perfiles analizados y compilados. Los perfiles A1 a A4 fueron tomados de Albertin (1989). Las líneas discontinuas muestran la correlación estructural; el ancho de las líneas y el largo de las discontinuidades en la línea indican la importancia relativa de cada falla. Esta correlación fue usada para compilar el mapa estructural de la Figura D8. Los sitios 479, 480 y 481 del Deep Sea Drilling Project se proyectaron en los perfiles cercanos. Note que el Perfil P309 es oblicuo a la fábrica estructural principal, mientras que el perfil A4 es casi paralelo a la orientación de las fallas principales.

18, 21). The faults limiting and disrupting the Pedro Nolasco High are oriented N44-48°W. This horst is imaged by the ~50 mGal anomaly of the Pedro Nolasco Gravity High (Fig. 16). Fenby and Gastil (1991) suggested that the Tiburón Fault system extends southwards and bounds the Pedro Nolasco Gravity High; however our profiles are located ~100 km of the southernmost exposures of the Tiburón Fault in western Isla Tiburón, making it difficult to positively correlate structures (Figs. 15, 16).

IV.4.2. Structure of the Guaymas Basin

The northern Guaymas Basin, offshore Baja California, outlines a nice half-graben structure. Its main boundary is the Guaymas Transform Fault, formed by several fault splays dipping west ~65-70° and striking N55-58°W. This large fault has a strong bathymetric scarp and a ~40 mGal step in the free-air gravity field (Figs. 17, 20). The western limit of the northern Guaymas Basin is formed by the Tortuga Transform Fault, which consists of three east-dipping fault splays. This fault also constitutes the eastern boundary of the ~5 km-wide Tortuga Volcanic Ridge, a basement high associated with the >40 mGal anomaly of the Tortuga Gravity High (Figs. 15, 16, 17). The acoustic basement of the Guaymas Basin forms a smooth reflector dipping ~3° to the east that deepens from 1.5 to 3.4 s (Figs. 17, 20). Further structural description of the central Guaymas Basin has been presented elsewhere (see Lonsdale, 1989).

IV.4.3. Seismic stratigraphy in the Yaqui Basin

We recognized five seismic sequences with a combined maximum thickness of up to ~2.70 s (~3.9 km, see Table 1) within the Yaqui Basin (Figs. 17 to 20). In this area Albertin (1989) interpreted up to seven sequence boundaries (profiles A1, A2 and A3, Fig. 21); we correlate three of them with the B-C, C-D and D-E sequence boundaries.

Sequence A is built by discontinuous and hummocky reflectors that onlap the basement. This sequence builds an accretion pattern against the YF, consisting of basinward-dipping reflectors. A set of mound forms is defined where the sequence has maximum thickness, located ~4 km west of the YF. Sequence A is cut by the faults antithetic to YF, and the reflectors in the hanging wall of these structures are eroded and truncated (Figs. 17, 19).

Sequence B is formed by sub-parallel and discontinuous reflectors that unconformably overlie and erosionally truncate Sequence A. The Sequence A-B boundary is an angular unconformity that varies across the basin; near the YF, Sequence B downlaps Sequence A, while to the west Sequence B onlaps Sequence A. Sequence B drapes the relief produced by the faults antithetic to YF, which results in the formation of broad mounds. A set of

Table 1. Maximum sequence thickness measured in seconds of two-way travel time, estimated interval velocities and computed maximum sequence thickness in meters of each interpreted seismostratigraphic sequence in the Yaqui and Guaymas basins, of the central Gulf of California. The interval velocities were estimated by semblance velocity analysis.

Tabla 1. Espesor máximo de secuencia medido en segundos de tiempo doble de viaje, velocidades de intervalo y espesor máximo de secuencia calculado en metros para cada una de las secuencias sismoestratigráficas interpretadas en las cuencas Yaqui y Guaymas, de la parte central del Golfo de California. Las velocidades de intervalo fueron estimadas con el análisis de velocidades por semblanza.

Sequence	Thickness [s twtt]	Velocity [m/s]	Thickness [m]
E	0.309	1600	247
D	0.447	1900	425
C	0.553	2600	719
B	0.555	3000	833
A	0.824	4000	1,648
Yaqui Basin	2.688		3,871
III	0.419	1600	335
II	0.694	1900	659
I	0.352	2600	458
Guaymas Basin	1.465		1,452

mound forms continues upwards the mounds defined in Sequence A. The maximum thickness of the sequence is found ~5 km west of the YF (Figs. 17, 19).

The hummocky-shaped Sequence C is built by parallel and continuous reflectors. The sequence B-C boundary is a laterally-varying unconformity; towards the east and west, Sequence C onlaps Sequence B, while the boundary is concordant where the sequence is thickest, located ~15 km west of YF. Sequence C aggregates and partially covers the YF (Figs. 17, 19), building a wedge of basinward-dipping reflectors. This sequence drapes by onlap the western side of the Pedro Nolasco High (Figs. 17, 18).

Sequence D consists of sigmoidal reflectors prograding southeastwards and unconformably overlies Sequence C and the Pedro Nolasco High. The C-D sequence boundary varies laterally; towards the north Sequence D pinches out and onlaps Sequence C; in the central-north basin, Sequence D downlaps Sequence C, while next to the Pedro Nolasco High, Sequence D onlaps Sequence C and drapes a large portion of the Pedro Nolasco High (Fig. 18). Perpendicular to the gulf axis, Sequence D onlaps Sequence C towards the east and west, and is concordant in the central basin (Figs. 17, 19). The northern end of Sequence D is cut by several small-throw faults that barely affect the upper and lower sequences (Fig. 18). The upper Sequence D correlates with the deeper sediments recovered in the DSDP sites 479 and 480 (Fig. 19).

Sequence E is built by parallel and continuous reflectors that unconformably drape and fill by onlap the broad depressions formed on top of Sequence D. The reflectors cover most of the basement protrusions of the Pedro Nolasco High, and are incised by active erosional channels. Sequence E is truncated by the sea bottom near the footwall of the Guaymas Transform Fault (Fig. 17). Deposits of this sequence correlate with the sediments of the

shallow section of the DSDP holes 479 and 480 (Fig. 19).

IV.4.4. Seismic stratigraphy in the Guaymas Basin

We recognized three seismic sequences in the Guaymas Basin with a combined thickness of up to ~1.46 s (~1.45 km, Table 1), while Albertin (1989) interpreted four sequence boundaries (profiles A1 and A2, Fig. 21); we correlate two of them with the I-II and II-III sequence boundaries.

The wedge-shaped Sequence I extends laterally ~12 km, and consists of parallel and discontinuous reflectors. Sequence I onlaps the basement and terminates against the Guaymas Transform Fault in a wedge of basinward-dipping reflectors. A set of mound forms is identified next to the sequence maximum thickness, located ~4 km west of the main boundary fault (Figs. 17, 20).

The wedge-shaped Sequence II is built by parallel and continuous reflectors. This sequence unconformably downlaps Sequence I, and onlaps the basement of the western basin. Sequence II terminates against the Guaymas Transform Fault in a wedge of basinward-dipping reflectors. Next to the sequence maximum thickness, located ~10 km west of the main boundary fault, and ~0.6 s (~0.55 km) beneath the sea bottom is observed a group of concordant, high-amplitude reflectors (Figs. 17, 20).

The hummocky-shaped Sequence III is built by parallel and continuous reflectors. This sequence partially fills by onlap the Guaymas Basin and unconformably covers Sequence II. The II-III sequence boundary varies across the basin; to the east and west Sequence III onlaps Sequence II, while the boundary is concordant near the sequence maximum thickness located ~18 km west of the Guaymas Transform Fault (Figs. 17, 20).

IV.5. Discussion

IV.5.1. Basement structure

The analyzed seismic profiles suggest that basement of the northern Yaqui and Guaymas basins likely consists of thinned continental crust. Beneath the Sonoran margin the well-defined basement is disrupted by faults, whereas basement in the northern Guaymas Basin forms a smooth and distinctive surface that gently dips to the east (Fig. 21). Between the western P307 profile and Santa Rosalía, offshore Baja California, the P-wave velocity of the basement of the sedimentary sequence was estimated as 6.1 km/s using seismic refraction data (Fabriol et al., 1999). This suggests that the northern Yaqui Basin and the northernmost Guaymas Basin are floored with continental crust, contrasting with the magmatically-accreted crust found in the central Guaymas Basin (Curry et al., 1982a; Lonsdale, 1985 and 1989; Albertin, 1989).

IV.5.2. Geometry of fault arrays

The faults mapped offshore Sonora reveal a block-faulted basement structure (Figs. 21, 22). Near the Sonoran coast the Pedro Nolasco High is bounded by structures that lie in the southeastern projection of the Tiburón Fault (Fenby and Gastil, 1991); however there is a ~100 km gap between the exposures of this fault in Isla Tiburón and the structures reported here (Fig. 15). Besides, the bounding faults of the Pedro Nolasco High dip in opposite directions and have noticeable along-strike variations of throw (Figs. 21, 22). Meanwhile, the Tiburón Fault branch cropping out in Isla Tiburón is vertical and has a strike-slip component (Oskin, 2002). Northwestward, in the Upper Tiburón Basin, the Tiburón Fault dips northeastwards and shows lateral variations of throw (Aragón-Arreola and Martín-Barajas, 2003). This suggests that the Tiburón Fault may be a system that consists of

several fault segments, instead of long and continuous structures. Thus, we refer to the faults bounding the San Pedro Nolasco High as the East and West Pedro Nolasco faults, and we suggest that they probably constitute the southernmost segments of the Tiburón Fault system.

The faults antithetic to the YF and the YF itself bound a graben in the deep Yaqui Basin, which extends >55 km; our data do not define the southern closure of this structure (Figs.

Figure 22. Structural map of the central Gulf of California compiled after the interpretation of multichannel seismic reflection profiles shown in **Figure 21**. The free-air gravity anomaly is presented as background (after CONMAR, 1987). Shaded area over the Guaymas Basin indicates the interpreted extent of transitional crust (Albertin, 1989); the sites drilled by the Deep Sea Drilling Project are also shown (Curry et al., 1982a, 1982b). The mapped faults are drafted with solid-bold lines, while the shaded zone tie to each fault represents the relative throw and dip direction. The tectonic features off the profile coverage were taken from Fenby and Gastil (1991). The central Gulf can be separated in two tectono-sedimentary domains. In the eastern domain, the East and West Pedro Nolasco faults, that probably form the southernmost segment of the Tiburón Fault System, co-evolved with the large-throw Yaqui Fault, which controlled the half-graben Yaqui Basin. In the western domain the active Guaymas Transform Fault controls evolution of the Guaymas Basin; in an early stage this basin evolved as a half-graben, but now hosts the Guaymas Spreading Center. The shift from continental to oceanic crust in the Guaymas Basin must be localized south of profile A2 and north of profile A3. Abbreviations: TF, transform fault; PN, Pedro Nolasco Island; TO, Tortuga Island; TGH, Tortuga Gravity High; TVR, Tortuga Volcanic Ridge.

Figure 22. Mapa estructural de la parte central del Golfo de California, compilado a partir de la interpretación de perfiles de sísmica de reflexión multicanal mostrados en la **Figura 21**. la anomalía gravimétrica de aire libre se presenta como información de fondo (CONMAR, 1987). El área sombreada sobre la Cuenca de Guaymas muestra la extensión interpretada de corteza transicional (Albertin, 1989), se muestran también los sitios perforados por el Deep Sea Drilling Project Leg 64 (Curry et al., 1982a, 1982b). Las fallas cartografiadas se dibujan con líneas continuas y gruesas, mientras las áreas sombreadas adjuntas a cada falla representan la caída relativa y la dirección del echado. Los rasgos tectónicos fuera de la cobertura de los perfiles analizados se tomaron de Fenby y Gastil (1991). La parte central del Golfo puede separarse en dos dominios tectono-sedimentarios. En el dominio este, las fallas Pedro Nolasco este y oeste, que probablemente forman los segmentos más al sur de la Falla Tiburón, coevolucionaron con la Falla Yaqui, de gran caída vertical, que controla el medio graben de la Cuenca Yaqui. En el dominio oeste, la Falla Transforme de Guaymas controla la evolución de la Falla Guaymas, en una etapa inicial, esta cuenca evolucionó como un medio graben, pero actualmente alberga el Centro de Dispersión de Guaymas. La transición de corteza continental a corteza oceánica en la Cuenca de Guaymas debe localizarse al sur del perfil A2 y al norte del perfil A3. Abreviaturas: TF, falla transforme; PN, Isla Pedro Nolasco Island; TO, Isla Tortuga; TGH, Alto Gravimétrico Tortuga; TVR, Cadena Volcánica Tortuga.

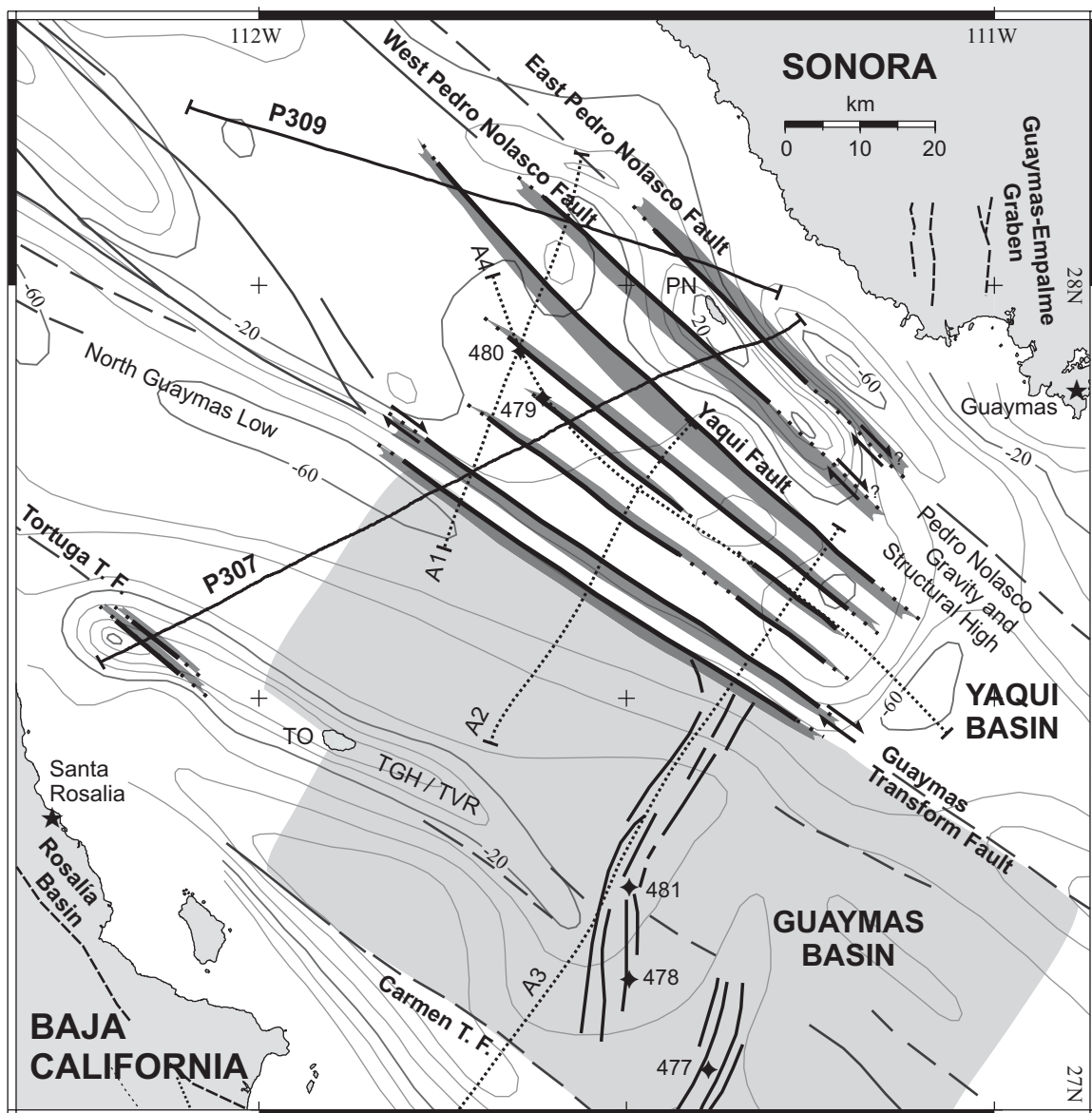


Figure 22.

21, 22). The faults antithetic to YF displace the basement and Sequence A, forming a system of along-strike segmented faults of smallest throw. The relief generated by this system is draped by Sequence B, indicating that fault activity is constrained to the early basin stage. This indicates that the extensional strain in the Yaqui Basin was initially split in several structures, but later was fully accommodated by the YF.

The inactive faults offshore Sonora strike N44-48°W, contrasting with the N55-58°W orientation of the active Guaymas and Tortuga transform faults in the western Gulf. The faults of the eastern Gulf only affect continental crust; while the transform faults in the western Gulf juxtapose continental and partially-accreted crust (Curry et al., 1982a; Lonsdale, 1985 and 1989; Albertin, 1989). The across-rift contrast in fault orientation and type of crust affected by faulting are similar to the changes observed along the rift, where the Ballenas Transform Fault, which displaces continental crust, is oriented 7-8° more northerly than the Guaymas Transform Fault, which juxtaposes continental and partially-accreted crust. These similarities support the suggestion that changes in crust type may induce changes in orientation of cross-cutting fault arrays within the rift (Lonsdale, 1989).

The NW-SE striking faults in the eastern Gulf are oblique to the N-S trending structures bounding the Miocene Bahía de los Ángeles and Bahía de las Ánimas grabens in Baja California and Empalme Graben in Sonora (Figs. 15, 22) (Delgado-Argote et al., 2000; Mora-Álvarez and McDowell, 2000; Roldán-Quintana, et al., 2004). We interpret that the northwest fabric offshore Sonora displaces the N-S striking faults of Basin and Range style. The Bahía de los Ángeles and Bahía de las Ánimas basins may restore near the Empalme Graben after ~250 km of oblique extension (Oskin et al., 2001).

The faults offshore Sonora outlined and controlled the evolution of the half-graben Yaqui

Basin. This fault array lies nearly parallel to the structures bounding the late Miocene-early Pliocene Loreto, Concepción and Santa Rosalía half-graben basins onshore Baja California (Figs. 15, 22); controlled by the development of oblique-slip and dip-slip listric faults (Wilson, 1955; Dorsey and Umhoefer, 2000; Ochoa-Landín et al., 2000; Ledesma-Vásquez and Johnson, 2001; Umhoefer et al., 2002).

IV.5.3. Strain accommodation in the central Gulf

Analog experiments indicate that behavior of strain accommodation in oblique rifting is a function of obliquity. At high obliquity the strain is usually partitioned and the main rift-bounding faults accrue most of the strike-slip deformation, whereas faults inside the extended zone accumulate mostly dip-slip motion. In contrast, at low obliquity the strain is mainly accommodated by oblique-slip faults (Withjack and Jamison, 1986; Bonini et al., 1997; Keep and McClay, 1997; Mart and Dauteuil, 2000).

The Gulf of California hosts a high obliquity rift system (Withjack and Jamison, 1986). In the Sonoran margin of the central Gulf the Pedro Nolasco High is limited by the East and West Pedro Nolasco faults, which probably constitute the southeastern segments of the Tiburón Fault System that once accommodated most of the strike-slip strain of the central Gulf of California (Lonsdale, 1989; Fenby and Gastil, 1991; Stock, 2000). Within the extended zone, the YF and the structures antithetic to YF accrued a variable amount of dip-slip motion (Figs. 21, 22). This suggests that the structural fabric of the eastern Gulf resulted from partitioning of transtensional extension. We invoke the analog experiments (Bonini et al., 1997; Keep and McClay, 1997) to suggest that the East and West Pedro Nolasco faults acted as the main rift-bounding faults and accommodated most of the strike-slip motion, while the variable-throw faults within the extended zone accrued most of the

orthogonal extension.

Our data show that the deep portion of the half-graben Yaqui Basin consists of an aborted graben defined by a conjugate system of faults. We suggest that the continued extension resulted in the localization of strain in the **YF** and the consequent abandonment of conjugate structures, which resulted in the evolution of the Yaqui Basin as a half-graben structure. We base our interpretation on the analogy with the Central African rifts, formed by along-strike segmented half grabens that evolved after early graben structures; it is proposed that when the graben-bounding faults intersected, one of them became inactive and the basins turned into half-graben structures (Scholz and Contreras, 1998).

The Guaymas Transform Fault now accommodates most of the strike-slip strain in the central Gulf (Lonsdale, 1985). The seismic data (Fig. 21) shows that this ~4 km-wide fault zone dips west ~65-70°, is continuous for >60 km and is built of several fault splays that reach a combined vertical offset of at least ~600 m (Figs. 20, 21, 22). We suggest that strain is partitioned within the Guaymas Transform Fault, such that some splays accrue dip-slip displacement, and the remaining accommodate strike-slip strain.

IV.5.4. Sedimentary basins

Our seismostratigraphic analysis indicates that evolution of the **YF** exerted control on deposition of the Yaqui Basin. The initiation-to-termination cycle of the main basin-bounding faults can explain several of the observed seismic signatures including the syn-tectonic deposition of wedge-shaped sequences, the sedimentary aggradation, the accumulation of hummocky sequences, and the relief drape (Prosser, 1993; Gawthorpe and Leeder, 2000).

Sequence A was deposited during the early stage of the Yaqui Basin. The aggradation

pattern suggests that sedimentary accretion was probably associated to the early growth of the YF. The irregular reflector configuration indicate that sedimentation energy was likely variable, while the mound forms, which are usually caused by contouritic currents, show that sedimentary transport was likely parallel to the YF (Prosser, 1993). The disruption of Sequence A by the faults antithetic to YF, and the erosion associated with these structures indicates that deposition of Sequence A predates the propagation of these faults (Fig. 19).

Deposition of Sequence B filled the graben formed by the faults antithetic to YF and the YF itself. The pinching and aggradation of this sequence suggest that growth of the basin-bounding YF controlled the sedimentary accretion. Besides, the sub-parallel configuration of reflectors shows that sedimentation energy was more uniform than the underlying sequence, while the mound forms suggest that sedimentary transport was likely parallel to the YF. Sequence B was deposited on an erosional surface and draped the relief generated by the faults antithetic to YF (Fig. 19), which indicates that activity of these faults is constrained to the depositional hiatus between sequences A and B.

The decrease and termination of tectonic subsidence due to the cessation of activity on the YF yield the accumulation of sequences C, D and E. The hummocky-shaped Sequence C marks the onset of draping of the Pedro Nolasco High, suggesting that during deposition of this sequence the YF activity and associated subsidence was waning (Figs. 18, 19). The sigmoidal reflectors of Sequence D progradated basinward and almost completely draped the Pedro Nolasco High (Fig. 18). Hence, we interpret that the YF, East and West Pedro Nolasco faults became inactive during deposition of Sequence D, resulting in the termination of tectonic subsidence in the Sonoran margin. The deposits of Sequence E

peneplaned the basin relief and draped the broad depressions probably related to compaction subsidence and erosion along tidal channels. The westward thinning and truncation of reflectors of Sequence E indicates uplift in the footwall of the Guaymas Transform Fault.

The seismic data show that the locus of maximum sequence thickness migrated to the west from Sequence A to C and then shifted back to the east during deposition of Sequence D (Fig. 19). The maximum sequence thickness is a proxy of basin depocenter and suggests migration in the location of maximum subsidence, which was probably related to slowing and cessation of tectonic activity in the YF.

The upper Sequence D and Sequence E correlate to the sequences found in DSDP sites 479 and 480 (Fig. 19), which were deposited at moderate rates during late Pliocene time (1.8-2.4 Ma) (Curry et al., 1982b). This stratigraphic range can be correlated to the upper Sequence D and Sequence E, and helps to constrain the age of extinction of the YF, East and West Pedro Nolasco faults. Assuming continuous subsidence and a sedimentation rate of 1-2 km/Ma (c.f. Curry et al., 1982a), throughout ~2.40 s (~3.6 km) of sediments in sequences A, B, C to D (Table 1), the Yaqui Basin may have initiated between 3.6-6.0 Ma; however this assumption does not consider the interpreted depositional hiatus. Thus the stratigraphic range of the Yaqui Basin may vary from late Miocene-Pliocene to late Pliocene. In addition, the extinction of faults in the Sonoran margin may have occurred during late Pliocene time, slightly prior to 2.4 Ma.

The Yaqui Basin shows similarities to the Loreto, Concepción and Santa Rosalía basins in Baja California (Fig. 15). These basins are half-grabens bounded by faults oriented parallel to the structures mapped offshore Sonora (Fig. 22) and were filled by late Miocene-

Pliocene marine sediments deposited syn-tectonically with slip on their main bounding faults (Umhoefer et al., 1994; Ledesma-Vásquez and Johnson, 2001; Holt et al., 2000; Ochoa-Landín et al., 2000). These similarities indicate that deformation of the Sonoran margin may be linked to deformation in the Baja California coastal plain. Our data allows the mapping of faults produced during the Pliocene oblique extension, but precludes the identification of preexisting structures, like these produced during the Miocene extension. The seismic data show that sediments of the northern Guaymas Basin filled a half-graben basin controlled by the Guaymas Transform Fault (Fig. 20). The seismic expressions of sequences within the Guaymas Basin are somehow similar to these described for sequences A, B and C of Yaqui Basin, and include the formation of aggradation patterns against faults, shifting of the locus of maximum sequence thickness away the basin-bounding fault, the deposition of wedge-shaped sequences followed by a hummocky-shaped sequence, and the formation of mound forms near the locus of maximum thickness (c.f. Figs. 19, 20). We argue that evolution of the Guaymas and Yaqui basins is somehow similar. Accumulation of the wedge-shaped sequences I and II of the Guaymas Basin appears to be related to the initiation and climax of subsidence of the Guaymas Transform Fault. The aggradation patterns indicate that sedimentation of these sequences was controlled by the vertical motion of the Guaymas Transform Fault. The mound forms suggest the presence of contouritic sedimentation. The accumulation of the hummocky-shaped Sequence III and the westward shift of locus of maximum sequence thickness from sequence I to III suggest the decrease of tectonic subsidence of the Guaymas Transform Fault.

The profiles A1, P307, and A2, surveyed 30 to 50 km north of the central Guaymas

Troughs (Figs. 15, 21) show the presence of the subsidence-associated sedimentary wedge. Instead profile A3 evidences that the axial Guaymas Troughs are filled by a thin and irregular sedimentary cover (Figs. 21, 22) formed by hemipelagic and turbiditic sediments (Curry et al., 1982a; Einsele et al., 1980). An approximation to the onset of sedimentation in the northern Guaymas Basin can be obtained by assuming that the ~1.46 s (~1.45 km) of sediments imaged in profile P307 (Fig. 20) had a constant sedimentation rate similar to the deposits found in DSDP sites 477, 478 and 481 (>1 km/Ma, see Curry et al., 1982a). Under this crude assumption deposition in the northern Guaymas Basin probably started ~1.5 Ma ago, which is consistent with the cessation of sedimentation in the Yaqui Basin estimated at ~1.8 Ma in the DSDP sites 479 and 480 (Curry et al., 1982b).

IV.5.5. Magmatism

The lack of magmatic-related features in the eastern Gulf suggests that the Yaqui Basin was not accompanied by magmatic intrusions and volcanism. This implies that the continental crust beneath this basin thinned without associated magmatism. Instead we interpret a zone of sills constrained to a shallow interval in the Guaymas Basin (Fig. 20). Albertin (1989) showed that the basement of the central Guaymas Trough consists of discontinuous, moderate relief, high-amplitude reflectors interpreted as shallow intrusions (profile A3, Fig. 21); thus he suggested the formation of ~130 km of newly accreted crust spread symmetrically away the central troughs (Figs. 15, 22; see also Lonsdale, 1985). The DSDP sites 477, 478, and 481 cut thick tholeiitic and dolerite sills intruding hemipelagic and turbiditic facies, which reinforced this interpretation (Curry et al., 1982a; Einsele et al., 1980). So we suggest that the interpreted sills within the half-graben deposits of Guaymas Basin (Fig. 20) represent off-axis magmatic accretion, where limited amounts of

magma intruded the sedimentary column.

IV.5.6. Kinematic implications

We propose that the oblique extension of the central Gulf of California involves two subsequent stages of deformation. During the older stage were formed the faults preserved in the eastern Gulf; while in the younger stage were defined the active faults offshore Baja California. The seismostratigraphic analysis indicates that extinction of the main faults offshore Sonora was coeval or closely followed by the initiation of the Guaymas Transform Fault. So we infer a kinematic link of these diachronic events, such that when the Sonoran margin was not able to accommodate deformation, the strain re-localized to the west. The late Miocene to early Pliocene transtensional deformation in Baja California yielded the formation of the Loreto, Concepción and Santa Rosalía basins ([Wilson, 1955](#); [Dorsey and Umhoefer, 2000](#); [Ochoa-Landín et al., 2000](#); [Ledesma-Vásquez and Johnson, 2001](#)). Similarities in age and deformation style of the eastern Gulf and the half-graben basins onshore Baja California suggests a kinematic link of these areas, however they would not restore together. Assuming a constant rate of transtensional strain of the 270-300 km accommodated by the Gulf of California rift in the last ~6-6.5 Ma ([Oskin et al., 2001](#)), the half-grabens in the Baja California coastal plain would have formed ~100 km southeastwards from their present location.

Orientation of fault arrays in the central Gulf had changed through time. The more obvious shift is recorded from the Miocene N-S striking faults onshore Sonora and Baja California to the mapped late Miocene-early Pliocene NW-SE oriented fault array offshore Sonora ([Figs. 15, 22](#)). This ~45° counterclockwise rotation in fault strike is close to the 35-40° change in extension direction documented from the pre-rift to the syn-rift structures of in

the Loreto and Santa Rosalía areas ([Angelier et al., 1981](#); [Umhoefer et al., 2002](#)). This drastic change in fault orientation locally confirms that localization of deformation within the Gulf of California rift was accompanied by a shift in extensional direction ([Stock and Hodges, 1989](#)).

We document a $\sim 10^\circ$ counterclockwise change in fault orientation from the older to the active faults in the central Gulf of California. It is notable that the mid-Miocene to Pliocene faults offshore Sonora and the basin-bounding faults onshore Baja California lie nearly parallel to the strike-slip faults of the northern Gulf of California; these faults disrupt only continental crust. In contrast, the active faults offshore Baja California juxtapose continental crust with oceanic-like and transitional crust ([Figs. 21, 22](#)). This suggests that besides a change in stress direction, the orientation shift of major faults can also be related to changes in the type of crust juxtaposed by faulting ([Lonsdale, 1989](#)).

The wedge-shaped sedimentary fill of the northern Guaymas Basin was controlled by subsidence related to the Guaymas Transform Fault ([Figs. 20, 21](#)). Subsidence may be associated to the contrasting type of crust transposed by this fault. Nevertheless, the conspicuous vertical component implies that at least one fault splay within the fault zone accrued dip-slip motion, while the remaining accommodated the well documented strike-slip component ([Lonsdale, 1985 and 1989](#)). The decrease of tectonic subsidence in the Guaymas Transform Fault may be related to the near achievement of isostatic equilibrium of the Guaymas Basin.

We proposed that partitioning of transtensional strain can explain the co-evolution of strike-slip and large-throw normal faults during the older stage of deformation in the central Gulf. We also invoke strain partition to explain the coeval dip-slip and strike-slip

motion within the Guaymas Transform Fault, meanwhile this structure controlled the evolution of the Guaymas Basin as a half-graben basin. Nowadays the Guaymas Transform Fault and the faults bounding the axial troughs of the Guaymas Basin accommodate most of the transtensional strain in this area (Lonsdale, 1989). So our suggestion implies that deformation in the central Gulf has been accommodated by strain partitioning since the onset of oblique rifting.

The Guaymas Basin forms now a nascent spreading center (Lonsdale, 1985 and 1989). However, prior to the formation of the active axial troughs, the Guaymas Basin evolved as a half graben controlled by the Guaymas Transform Fault (Fig. 21). The shift from continental to oceanic crust in the Guaymas Basin must be localized south of profiles P307, A1 and A2, but north of profile A3 (Figs. 15, 22). Assuming a half spreading rate of ~25 mm/a in the Guaymas Spreading Center, similar to the Pescadero Basin in the southern Gulf (Ness et al., 1991), the ~30 km of new oceanic and transitional crust south of profile A2 (Fig. 22) would have formed in ~1.2 Ma. However, our analysis does not provide further constraints to understand the kinematic history and the resulting structures of the drastic transition from a half-graben structure to a nascent spreading center.

IV.6. Conclusions

We compiled a structural map of the central Gulf of California based on the analysis of new and published seismic reflection data, and the inspection of free-air gravity data. This region can be separated in two tectono-sedimentary domains. In the northeastern domain, the long strike-slip East and West Pedro Nolasco faults, belonging to the segmented Tiburón Fault System, co-evolved with large-throw faults, as the YF, and produced the

half-graben Yaqui Basin, filled with ~2.5 s (~3.7 km) of sediments. The southwestern domain is bounded by the active Guaymas Transform Fault, which had controlled evolution of the Guaymas Basin. The northern Guaymas Basin evolved as a half-graben that holds ~1.46 s (~1.45 km) of sediments, while the central basin hosts the nascent Guaymas Spreading Center.

The seismostratigraphic analysis of the Yaqui and Guaymas half-graben basins indicates that their evolution was controlled by the development of the Yaqui and Guaymas Transform faults, respectively. The extrapolation of accumulation rates reported in the DSDP sites of the central Gulf to the complete sedimentary column of both basins suggests that the age of tectonic activity and sedimentation in the Yaqui Basin ranges from late Miocene-Pliocene to late Pliocene; while sedimentation in the Guaymas Basin may have initiated during late Pliocene-Early Pleistocene time.

The late Miocene-early Pliocene evolution of the eastern margin of the central Gulf post-date the formation of the mid-Miocene N-S oriented basins preserved onshore Sonora and Baja California. The faults mapped in the eastern Gulf likely transposed these Basin and Range style basins. Development of the Yaqui Basin, offshore Sonora, is coeval and probably kinematically linked with evolution of the transtensional Loreto, Concepción and Santa Rosalía basins, located onshore Baja California.

The faults studied in the central Gulf had accommodated transtensional strain associated with the opening of the Gulf of California. We propose that kinematics of oblique rifting involves the initial localization of strain offshore Sonora and along the coast of Baja California. When the YF, East and West Pedro Nolasco faults were not able to accommodate deformation, the strain re-localized to the west into the Guaymas Transform

Fault. Our results also suggest that strain has been partitioned since the initiation of oblique rifting, allowing the co-evolution of strike-slip and normal faults in the Sonoran margin and the coeval accrual of strike-slip and dip-slip strain within the Guaymas Transform Fault that controlled evolution of the early Guaymas Basin as a half-graben structure. Currently the Guaymas Transform Fault and the axial normal faults of the Guaymas Basin accommodate the transtensional strain in this area.

V. DISCUSSION

The reconfiguration of the Pacific-North America plate boundary from a convergent to a divergent margin involves the evolution of strain accommodation. The early rifting in this broad region (Figs. 1, 3, 6) started in Oligocene-Miocene time and gave rise to the Basin and Range Province that accommodated deformation in the core-complex and wide-rift modes of extension (Wernicke et al., 1988; Henry and Aranda-Gómez, 1992; Stewart, 1998). During late-middle Miocene time, at the latitude of northwestern México, extensional strain affected only the Gulf Extensional Province (Stock and Hodges, 1989; Gans, 1997; Axen and Fletcher, 1998), and was mainly accommodated in the wide-rift mode of extension (Buck, 1991). Finally, since the late Miocene, the rifting process localized into a narrow zone along the Gulf of California (Lonsdale, 1989; Stock and Hodges, 1989; Oskin et al., 2001) that appears to accrue deformation in the narrow mode of extension (cf. Buck, 1991). Thus, the Gulf of California rift is the last stage of a long-term and progressive process of continental rifting that has affected western North America; this process is likely evolving into generalized spreading of new ocean crust, which has already started in the mouth of the Gulf (Ness et al., 1991). The progressive localization of strain has resulted in different styles of rifting and a highly-asymmetrically extended region with respect to the initial area affected by extension; in this region the current rifting is localized toward the west, in the Gulf of California. The eastern side of the Gulf of California rift provides some insights about the early extensional stages that affected the broad region onshore Sonora.

V.1. The Gulf of California and the Basin and Range Province

The Gulf of California rift sits at the western edge of the Basin and Range Province and marks a departure in structural style from the latter province. The main structural fabric of the Basin and Range around the Gulf consists of ~NNW-SSE striking normal faults and subsidiary ~ENW-WSE oriented strike-slip faults (Stewart, 1998; Henry, 1989; Gans, 1997), and low-angle detachment faults (Nourse et al., 1994; Wong and Gans, 2003). This deformation occurred from late Oligocene to middle Miocene time and generally decreases in age toward the west (Gans, 1997; Gans et al., 2006). By contrast, the Gulf of California rift consists of large NW-SE striking faults linked by pull-apart basins (Lonsdale, 1989) that propagated since the late Miocene (Oskin et al., 2001; Oskin and Stock, 2003b). However, it is possible that the propagation of this rift system started since ~12.0 Ma, during the middle Miocene, soon after the cease of subduction along the Pacific margin of Baja California (Gans, 1997; Fletcher and Munguía, 2000).

The main structures of the Gulf of California rift displace structures of the Basin and Range Province, including the N-trending Bahía de los Ángeles and Bahía de las Ánimas grabens in Baja California and the Empalme Graben in Sonora (Fig. 22; Delgado-Argote et al., 2000; Roldán-Quintana et al., 2004; Aragón-Arreola et al., 2005). Thus, rifting in the Gulf of California represented a sharp change in the extensional style, in which the new structural fabric displaces the old Basin and Range structures. This change occurred in the 12.0-6.0 Ma time span (Stock and Hodges, 1989; Oskin et al., 2001), but a more exact timing of the change in structural style is still debatable (cf. Gans, 1997; Fletcher and Munguía, 2000; Fletcher et al., in press).

V.2. Structural geometry, strain partitioning and the accommodation of large amount of extension in the northern Gulf

In this thesis I have mapped the major structural elements in the central and northern Gulf segments of the Gulf of California rift system. The combined analysis of the orientation of major structures and the kinematic constraints of plate motion yield hints on how the strain has been accommodated in this oblique-extending system.

The main structural elements in a rift system include the rift direction or direction of rift axe, the motion vector of rifted plates and the orientation of major structures (cf. [Teyssier et al., 1995](#)). The axis of the Gulf of California rift lies parallel to the Gulf and strikes ~N35°W ([Fig. 1](#)). The relative motion of the Pacific-North America plates has been computed using plate kinematic models; for the northern Gulf, the relative motion vector of Baja California with respect to mainland México varies in orientation between N44-47°W and the velocity ranges between ~44.9-50.3 mm/a ([Fig. 23](#); after [DeMets et al., 1994](#); [González-García et al., 2003](#)). Furthermore, the net opening of conjugate margins across the Upper Tiburón-Upper Delfín basin segment has been quantified as 255±10 km along an orientation of N50°W ([Oskin et al., 2001](#)).

We have shown that the Gulf of California is composed by an active and an inactive rift margin that display similar structural characteristics ([Figs. 5](#); see Chapter II; [Aragón-Arreola and Martín-Barajas, 2007](#)). In the northern Gulf, the larger faults strike between N30-46°W, and include the inactive Tiburón, De Mar, and Amado faults, and the active Canal de Ballenas and Cerro Prieto faults; these major faults have a length of >100 km and display a kilometric vertical offset ([Figs. 3; 4, 6; 10; 13](#)). The main subsidiary structures

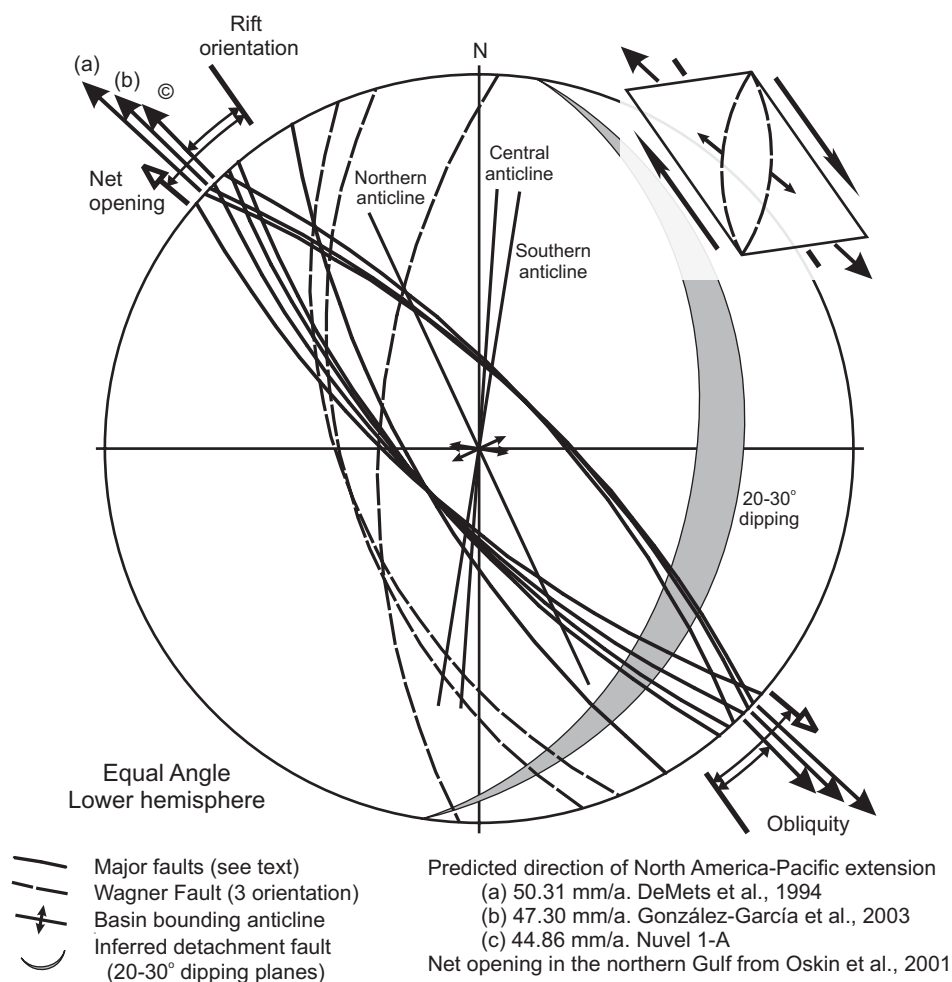


Figure 23. Main structural elements in the northern Gulf of California plotted in an equal angle stereographic projection. The rift obliquity in the northern Gulf varies between 9° and 12° , as can be estimated by the acute angle formed by the rift orientation and the predicted motion vectors of Baja California with respect to fixed North America. Assuming a simple shear model of deformation (upper right sketch), the major faults have accommodated most of the strike-slip motion of the North America-Pacific plate boundary, while the secondary structures mainly accrue the extensional deformation.

Figura 23. Principales elementos estructurales en el norte del Golfo de California graficados en una falsilla estereográfica de igual ángulo. La oblicuidad en el norte del Golfo varía entre 9° y 12° , como puede estimarse por el ángulo agudo formado entre la orientación del *rift* y los vectores de movimiento predichos entre Baja California y la Placa Norteamericana (fija). Suponiendo un modelo de deformación de cizalla simple (esquema superior derecho), las fallas principales han acomodado la mayor parte del movimiento lateral en el límite entre las placas Pacífico y Norteamérica, mientras que las estructuras secundarias han acomodado principalmente la deformación extensiva.

mapped in this region include the Wagner fault and its inferred southern extension oriented ~N-S, and the shallow fault arrays that control the active basin depocenters and are oriented NNW-SSE to NNE-SSW (Chapter II; [Persaud et al., 2003](#)). Although not mapped, another key structure is an inferred top-to-the east detachment fault, which appears to be oriented NNE-SSW, following the eastern flank of the traced doubly-hinge anticline ([Figs. 3; 6; 8; 9; 10F-10H](#)).

The structural layout obtained in analog models of oblique rifting display similarities with the structures described in the northern Gulf and yield hints on how the strain has been accommodated. These models show that strain in highly-oblique rifts is usually partitioned. The structural system obtained with these models is formed by larger faults that accrue mostly strike-slip motion; these faults lie nearly parallel to the rift direction and bound the resulting rift basins. The secondary faults accommodate mostly dip-slip motion, and their orientation lies clockwise oblique to the rift and plate motion directions, these structures also bound a portion of the rift basins and form relay ramps between the major strike-slip faults ([Withjack and Jamison, 1986](#); [Keep and McClay, 1997](#); [Bonini et al., 1997](#); [Schlische et al., 2002](#)).

The stereographic projection of the main structural elements in the northern Gulf suggests a kinematic relation of these two type of structures ([Fig. 23](#)). The rift obliquity in this region is markedly high and ranges between 9° and 12°. The orientation of the major faults lies between the rift and the plate motion directions; these faults display a large throw, but the seismic data do not constrain the net sense of fault slip. Another conspicuous feature is that the subsidiary faults, the doubly-hinged anticline and the inferred detachment fault are oriented between 30° and 50° clockwise oblique to the plate motion direction. These

geometric relations and their similarity with results obtained by analog modeling of oblique rifting, suggest that the whole structural system is consistent with a model of simple shear deformation ([Fig. 23, upper right sketch](#)), in which the major Amado, De Mar, Tiburón, Cerro Prieto and Canal de Ballenas faults have mostly accommodated strike-slip motion, while the Wagner fault, the dense fault arrays in the active basins and the inferred detachment fault have accommodated large amounts of the net extensional deformation. Thus, we propose that the structural fabric in the northern Gulf segment of the Gulf of California rift system has resulted from the accommodation of highly partitioned oblique strain.

It is well constrained that the Upper Tiburón-Upper Delfín basin segment of the northern Gulf accrues $\sim 255 \pm 10$ km of extension along an orientation of N50°W ([Oskin et al., 2001](#); [Oskin and Stock, 2003a](#)), however it is intriguing how this strain has been accommodated. [Nagy and Stock \(2000\)](#) explain that the northern Gulf contains the continental-ocean transition, which is characterized by diffuse deformation; they argue that oblique deformation is partitioned and is accrued throughout the known shallow structures and unknown submerged faults. [Persaud et al. \(2003\)](#) reject the idea of strain partitioning and favor that shear is distributed in a broad zone beneath a thick sediment cover. [González-Fernández et al. \(2005\)](#) find a lateral variability of crustal thickness across the Upper Tiburón-Upper Delfín basin segment, which includes the thick crustal block beneath the central Gulf; these authors propose that this block may represent a metamorphic core complex caused by detachment faulting. Nevertheless, the structures that may accrue a considerable amount of oblique strain had not been documented.

Our results do indicate that strain is partitioned. Candidates to accommodate large

magnitude extension and their related structures include the inferred top-to-the east detachment fault that flanks the southeastern edge of the mapped basement high, which may be the uplifted core of the lower plate; moreover, the doubly-hinged anticline that crown the basement high might represent a roll-over anticline (Figs. 3; 6; 8; 9; 10F-10H). Another candidate to accommodate extension is the listric Wagner fault, beneath the northernmost active marine basin in the northern Gulf. The tectonic transport in these newly presented structures, is likely oriented ~WNW-ESE, which agrees with the current direction of net extension of the Pacific-North America plate boundary in the northern Gulf (Fig. 23). Our results also favor the hypothesis of tectonic delamination of the crust (cf. González-Fernández et al., 2005) and document large low-angle faults that accommodate large magnitude extension. These low-angle structures appear to splay away the major NW-SE faults; a similar situation has already been documented onshore northern Baja California, where the Cañada David branch away the Cañón Rojo and Laguna Salada faults (Axen and Fletcher, 1998; Axen et al., 1999). The low-angle faults are probably hard-linking large splays of strike-slip faults within this transtensional deformation system; however, the description of hardly-linked faults has been applied for structural systems of one-order of magnitude smaller than the described in the northern Gulf of California (Peacock, 1991; Dawers and Anders, 1995; Gupta et al., 1998; Cowie et al., 2000; Cowie et al., 2000; McLeod et al., 2000; Manighetti et al., 2001. Morley, 2002). Thus, the kinematic and genetic relationships of detachment and strike-slip faulting in the Gulf of California needs to be investigated in future works.

V.3. Role of sedimentation in the accommodation of extension and the delay of spreading of new oceanic floor

The Gulf of California rift displays conspicuous along-strike variations in thickness of the sedimentary cover. Toward the north, the inactive Altar, Adair-Tepoca and Upper Tiburón basins, and the active Cerro Prieto, Wagner-Consag and Upper Delfín basins, contain sedimentary piles that reach ~4.0-6.0 km of thickness ([Núñez-Cornú et al., 1996](#); [Pacheco-Romero et al., 2006](#); [Aragón-Arreola and Martín-Barajas, 2007](#); [this study](#)); the main source of such large amount of sediments is the Colorado River, which entered into this system since Late Miocene time ([Winker and Kidwell, 1996](#); [Dorsey et al., 2006](#)). In the central Gulf, the inactive Yaqui basin and the active Guaymas basin contain sedimentary piles of ~4.0 and 1.5 km, respectively ([Aragón-Arreola et al., 2005](#)). Farther south, the inactive San Blas, Tamayo, Nayarit, and Tres Marías troughs contain <1.0 km of sediments, whereas the actively spreading Alarcón and Pescadero basins hold a thin sedimentary cover of <100 m ([Brown et al., 2006](#); [Sutherland et al., 2006](#)). Thus, the sedimentary cover in the northern rift basins is distinctively thick compared to its southern counterpart; moreover, the variations in sedimentary thickness is consistent in the eastern abandoned and in the western active rift margins.

The along-the-rift variability in the sedimentary cover concurs with strong variations in magmatism documented in the active rift margin. Toward the north, the known magmatic activity is concentrated in the Lower Delfín basin and consists of numerous volcanic knolls of andesitic and rhyolitic composition ([Persaud et al., 2003](#); [Martín-Barajas et al., 2002](#)). In the central Gulf, the Guaymas basin forms a nascent spreading center with ~60 km of new oceanic and transitional crust ([Lonsdale, 1985](#); [Lonsdale, 1989](#)); the flanks of this

spreading center are intruded by tholeiitic and dolerite sills, which are also interpreted using seismic reflection data (Curry et al., 1982a; Einsele et al., 1980; Aragón-Arreola et al., 2005). Farther south, the Alarcón and Pescadero basins hosts an appreciable width of true oceanic floor (Lonsdale, 1989; Ness et al., 1991). Thus, there are strong differences in the amount and style of magmatism along the rift; some authors had suggested that the sedimentary cover in the northern Gulf had assimilated a considerable volume of magmatic material, forming attenuated crust beneath this region (Fuis and Kohler, 1984; Persaud et al., 2003).

The extensional deformation during the rift process results in thinning of the continental crust that generates accommodation space, which is compensated by the accumulation of sediments in the uppermost levels (Contreras et al., 1997) and by the addition of magmatic material (Buck, 2005). The numerical models of rifting indicate that a thick sedimentary cover tends to weaken the lithosphere because it adds low density materials that are able to thermally insulate the lower crust; a weakened crust yields the reduction of the tectonic force needed for rifting, and the eventual decrease of flexural rigidity by crustal decoupling (Lavie and Steckler, 1997; Ruppel, 1995; Buck, 2005). Therefore, we suggest that the thick sedimentary lid in the northern half of the Gulf of California rift may be a key factor in the formation of the low-angle faults depicted across the basement high and active basins of the northern Gulf, which may accommodate large amount of extension (Figs. 3, 4, 8, 9, 10, 23).

The changes of major geologic variables such as sedimentation, magmatism and accommodation style along the Gulf of California rift bring back the question of why there is no spreading of new seafloor in the northern half of this rift system. We suggest that the

ability to accommodate large-magnitude extension in the northern Gulf due to the long-term thermal effects of a thick sedimentary cover is partially responsible for delaying the complete rupture of continental lithosphere and the consequent formation of true oceanic floor in the northern Gulf.

V.4. Asymmetry of rifting of western North America

The continental rupture of western North America is considered a continuous process over the last ~30-35 Ma. During this time, the accommodation style and strain locus have evolved, and large areas had become tectonically inactive. Currently, the rifting is localized in the western margin of the Gulf of California, which separates two inactive areas of considerably different extension. Toward the east, the inactive area includes from the foothills of the Sierra Madre Occidental to the abandoned basins in the eastern Gulf, while toward the west, the inactive region embraces a very narrow and discontinuous belt in the coastal plain of Baja California ([Fig. 24](#)). The formation of such large tectonically inactive region in the east is related to the consistent migration of deformation toward the west. This westward migration of strain locus has been documented onshore Sonora for areas extended during early-to-late Miocene time ([Gans, 1997](#); [Gans et al., 2006](#)). A similar behavior of strain migration is recognized from the eastern to the western margins of the Gulf of California rift (Chapter II and IV, [Aragón-Arreola et al., 2005](#); [Aragón-Arreola and Martín-Barajas, 2007](#)). However, the causes of such outstanding asymmetry of rifting are not clear.

The strength of continental lithosphere is a multivariate function that depends of crustal thickness, thermal state, strain rate, rheology and plate curvature (see [Bukov and Diamant,](#)

1995). Attending to the first two variables, strength of the lithosphere is proportional to the crustal thickness and inversely proportional to the geothermal gradient. In addition, the location of weak zones within the continental crust is also controlled by contrasts of geologic provinces and the presence of pre-existing structures. In the near field, the localization of rupture in an extending lithosphere is controlled by the location of zones of low yield stress (Ramsay and Lisle, 1983; Buck, 1991; Hopper and Buck, 1996).

The Gulf Extensional Province and thus, the Gulf of California rift, are located between the Peninsular Range of Baja California and the Sierra Madre Occidental (Figs. 1; 24). These

Figure 24. Composite schematic profile from the Pacific Ocean to the Sierra Madre Occidental across the Adair-Tepoca and Wagner-Consag basins segment of the northern Gulf of California showing the main tectonic features involved in the rupture of continental lithosphere of western North America. The lower part of the figure illustrates the temporal evolution of the major tectonic events. Triangles represent volcanic activity. See text for further explanations. References: *1: Stock and Hodges (1989); Bohannon and Parsons (1995); *2: Gastil et al. (1975); Núñez-Cornú et al. (1996); 3*: Lee et al. (1996); Martín-Barajas (2000); Axen and Fletcher (1998); *4: Persaud et al. (2003); Aragón-Arreola et al. (2003); Martín-Barajas et al. (2002); *5: Fuis and Kohler (1984); Couch et al. (1991); Núñez-Cornú et al. (1996); González-Fernández et al., (2005); *6: Aragón-Arreola et al. (2005); Aragón-Arreola and Martín-Barajas (2007); *7: Aragón-Arreola et al. (2003); Oskin et al. (2001); Oskin and Stock (2003b); *8: Phillips (1964); Henyey and Bischoff (1973); Couch et al. (1991); *9: Couch et al. (1991); Gans (1997); Mora-Álvarez and McDowell (2000); *10: Couch et al. (1991); Wernicke et al. (1988); Stewart (1998); *11: McDowell and Clabaugh (1979).

Figure 24. Perfil esquemático compuesto desde el Océano Pacífico hasta la Sierra Madre Occidental a través del segmento de las cuencas Adair-Tepoca y Wagner-Consag del norte del Golfo de California, mostrando los rasgos tectónicos mayores involucrados en la ruptura de litósfera continental del oeste de Norteamérica. La parte inferior de la figura ilustra la temporalidad de los eventos tectónicos mayores. Los triángulos representan la actividad volcánica. Favor de referirse al texto para más explicación. Referencias: *1: Stock y Hodges (1989); Bohannon ynd Parsons (1995); *2: Gastil et al. (1975); Núñez-Cornú et al. (1996); 3*: Lee et al. (1996); Martín-Barajas (2000); Axen y Fletcher (1998); *4: Persaud et al. (2003); Aragón-Arreola et al. (2003); Martín-Barajas et al. (2002); *5: Fuis y Kohler (1984); Couch et al. (1991); Núñez-Cornú et al. (1996); González-Fernández et al., (2005); *6: Aragón-Arreola et al. (2005); Aragón-Arreola y Martín-Barajas (2007); *7: Aragón-Arreola et al. (2003); Oskin et al. (2001); Oskin y Stock (2003b); *8: Phillips (1964); Henyey y Bischoff (1973); Couch et al. (1991); *9: Couch et al. (1991); Gans (1997); Mora-Álvarez y McDowell (2000); *10: Couch et al. (1991); Wernicke et al. (1988); Stewart (1998); *11: McDowell y Clabaugh (1979).

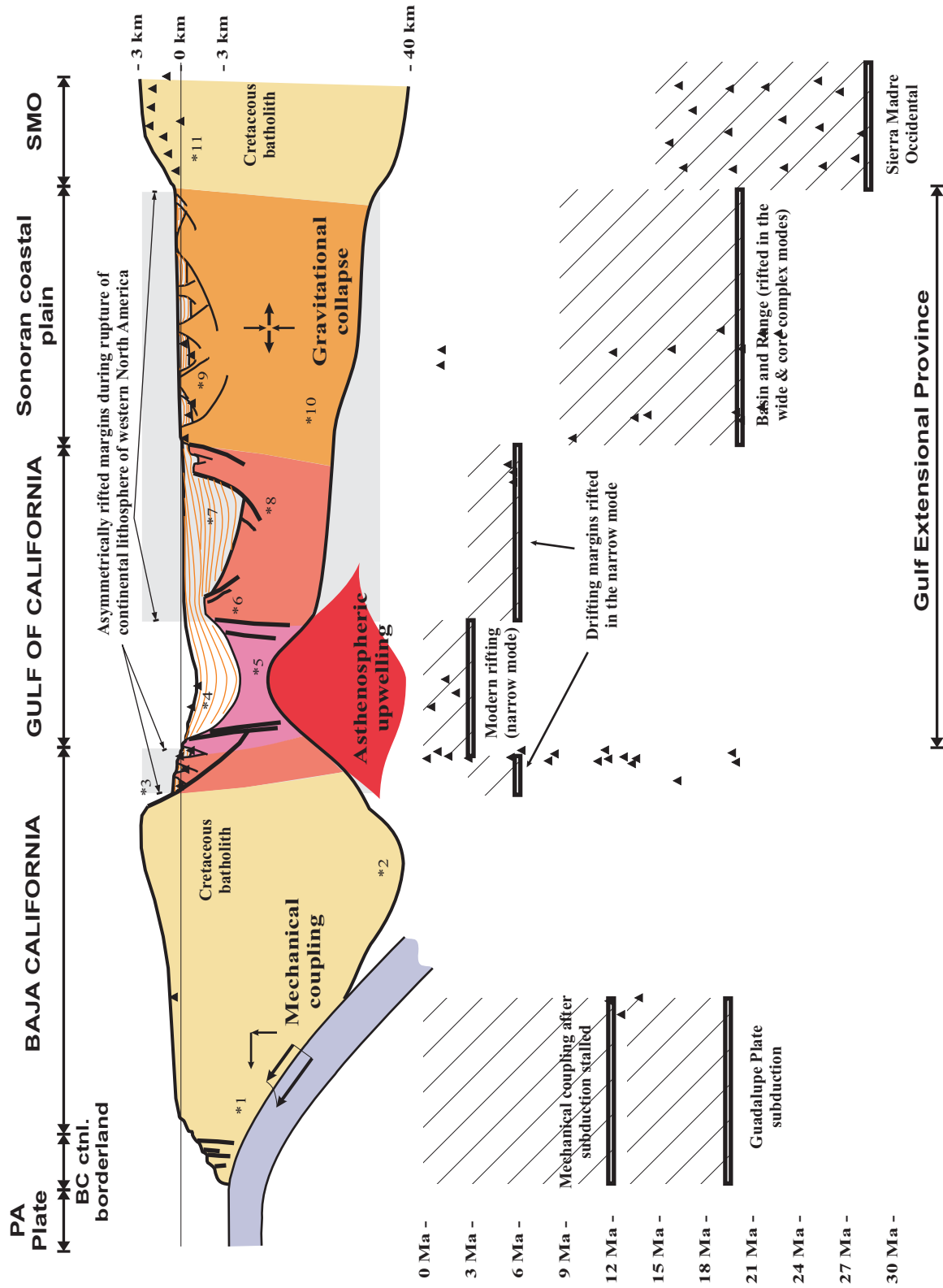


Figure 24. Aragón-Arreola

provinces reach up to 3000 m of elevation above the sea level and are rooted by batholiths of Cretaceous to Paleogene age (Gastil et al., 1975; McDowell and Clabaugh, 1979); the crustal thickness beneath these provinces reaches up to 40-45 km (Couch et al., 1991; Núñez-Cornú et al., 1996). By contrast, the Gulf Extensional Province is a zone of low topographic relief formed by elongated ranges that stand <300 m above nearly-flat regions elevated <100m above the sea level. The thickness of continental crust beneath this province is not well constrained (Fig. 24), but appears to vary from ~25 km onshore Sonora and Baja California (Wernicke et al., 1988; Couch et al., 1991; Núñez-Cornú et al., 1996); to ~18-20 km beneath the northeastern Gulf (Phillips, 1964; González-Fernández et al., 2005), and ~14-15 km beneath the active Salton Trough-Mexicali Valley and Lower Delfín basin (Fuis and Kohler, 1984; Couch et al., 1991; Núñez-Cornú et al., 1996; González-Fernández et al., 2005). Thus thickness of the continental crust is asymmetrically distributed across the Gulf Extensional Province, and tends to decrease toward the actively rifting zone; moreover, the continental crust in this province is bounded by regions of significantly thicker continental crust (Fig. 24).

The forces that drove rifting in the Gulf Extensional Province apparently evolved with time. It is suggested that gravitational collapse of very thick continental crust drove extension of the Basin and Range province, and therefore of the onshore region of the Gulf Extensional Province (Wernicke et al., 1988; Buck, 1991; Ruppel, 1995). By contrast, the further transtensional extension that resulted in the Gulf of California rift appears to be driven by the mechanical coupling of the Baja California continental sliver with the underlying Pacific Plate (Stock and Hodges, 1989; Bohannon and Parsons, 1995). However, the details of how mechanism of rifting changed from a gravitationally collapse

to passive rifting driven by the far-field stress has not yet addressed.

The western flank of the Gulf Extensional Province records a long, but intermittent volcanic activity since the early Miocene (Sawlan, 1991; Martín-Barajas, 2000). Volcanism yielded the formation of discrete volcanic fields preserved in coastal Baja California and in several Gulf islands; these fields include around the northern and central Gulf, the Cerro Prieto area, Puertecitos Volcanic Province, Lower Delfín basin, Isla Tiburón, Isla San Esteban, La Reforma-Aguajito Caldera, Isla Tortuga, Guaymas basin, and Loreto area (Batiza, 1978; Einsele et al., 1980; Curray et al., 1982a; Lonsdale, 1985; Lonsdale, 1989; Sawlan, 1991; Martín-Barajas et al., 1995; Gastil et al., 1999; Umhoefer et al., 2001; Persaud et al., 2003). This volcanic activity on such narrow geographic belt during the last ~20 Ma, suggests a sustained heat source near the Baja California flank of the Gulf Extensional Province.

I argue that the asymmetric rifting of western North America since the late-middle Miocene time can be related to the sustained high thermal flow near eastern Baja California since the early Miocene. The sustained presence of heat source in a fixed position may promote the decrease of crustal strength and yield-stress in the nearby region, which increases the ability to nucleate discrete faults. As extension continues, the discrete fault planes drift away the high heat source region, which increases their yield stress and their eventual healing. Nevertheless, the causes of asymmetric rifting of western North America are not well understood and deserve a detail geodynamic approach.

VI. CONCLUSIONS

The structural and seismostratigraphic interpretation of extensive seismic reflection data in the northern and central Gulf allowed mapping the regional structural fabric and the interpretation of the main tectono-sedimentary units. The results also allow the discussion of implications for rift kinematics and strain accommodation. The structure in the northern and central Gulf is characterized by two parallel basin systems; in the eastern system the early stratigraphic record is a marine sequence documented in the lower section of the Upper Tiburón Basin, which was probably deposited since the end of Middle Miocene time during the proto Gulf stage. The onset of focused rifting during late Miocene gave rise to the propagation of large strike-slip including the Amado, De Mar, Tiburón, San Pedro Nolasco and Yaqui faults, which controlled the coeval deposition of the Adair-Tepoca, Upper Tiburón and Yaqui basins. These fault-basin systems were probably active until middle to late Pliocene time, when deformation and subsidence migrated to the west into the active basin system. The configuration of the modern system in the northern and central Gulf is characterized by the staggered array of the Cerro Prieto, Canal de Ballenas, Guaymas and Carmen transform faults; these major structures control the evolution of the Wagner-Consag, Upper Delfín, Lower Delfín and Guaymas basins.

The westward migration of strain in the northern Gulf resulted in the formation of a basement high and a doubly-hinged anticline between the eastern and western basins; the eastern shoulder of this structural high is probably cut by an inferred top-to-the east detachment fault, such that the anticline between the active and inactive basins could represent a roll-over anticline. The correlation across the doubly-hinged anticline of the middle and upper sequences of the eastern inactive basins with the lower and middle

sequences of the western active basins support the migration of deformation, but also suggest that strain migration might be related to large detachment faulting that likely thinned the continental crust as the large strike-slip faults developed.

The pattern of inactive fault-basin systems in the east and active fault-basin systems in the active zone of rifting is present along the entire length of the Gulf, forming two distinct parallel rift margin; the abandoned rift margin to the east forms now an incipient drift margin, while active rifting is located in the western margin of the Gulf of California rift.

In conclusion, the structural fabric in the northern and central Gulf of California has resulted from the accommodation of highly partitioned oblique strain, in which the major Amado, De Mar, Tiburón, San Pedro Nolasco, Yaqui, Cerro Prieto, Canal de Ballenas, Guaymas and Carmen faults have mostly accommodated strike-slip motion. Whereas the large magnitude extension in the northern Gulf has been accommodated by several structures including the inferred top-to-the east detachment fault, the listric Wagner fault, and other dense arrays of shallow faults.

VII. CITED REFERENCES

- Albertin, M.L., 1989. Interpretations and analysis of Guaymas Basin multi-channel seismic reflection profiles: implications for tectonic history, University of Texas at Austin, M.A. Thesis, 127 pp.
- Angelier, J., Colletta, B., Chorowicz, J., Orlieb, L., and Rangin, C., 1981. Fault tectonics of the Baja California Peninsula and the opening of the Sea of Cortez, Mexico. *Journal of Structural Geology*, 3: 347-357.
- Aragón-Arreola, M., Martín-Barajas, A., and Stock, J. M., 2002. Estructura y evolución de las cuencas fósiles en el norte del Golfo de California a partir de sísmica de reflexión multicanal. III Reunión Nacional de Ciencias de la Tierra - Unión Geofísica Mexicana, Reunión Anual. *GEOS*, 22(3): 181.
- Aragón-Arreola M. and Martín-Barajas, A., 2003. Estructura de la corteza y cinemática de apertura continental en el Norte del Golfo de California. *GEOS* 23, 113.
- Aragón-Arreola, M., Morandi, M., Martín-Barajas, A., Delgado-Argote, L., and González-Fernández, A., 2005. Structure of the rift basins in the central Gulf of California: kinematic implications for oblique rifting. *Tectonophysics*, 409(1-4): 19-38, doi:10.1016/j.tecto.2005.08.002.
- Aragón-Arreola M. and Martín-Barajas, A., 2007. Westward migration of extension in the northern Gulf of California, México. *Geology*, 35(6).
- Axen, G., 1995. Extensional segmentation of the Main Gulf Escarpment, Mexico and United States. *Geology*, 23(6): 515-518.
- Axen, G.J., and Fletcher, J. M., 1998. Late Miocene-Pleistocene Extensional Faulting, northern Gulf of California, Mexico and Salton Trough, California. *International Geology Reviews*, 40: 217-244.
- Axen, G.J., Fletcher, J.M., Cowhill, E., Murphy, M., Kapp, P., MacMillan, I., Ramos-Velázquez, E., and Aranda-Gómez, J., 1999. Range-front fault scarp of the Sierra El Mayor, Baja California: formed above an active low-angle normal fault? *Geology*, 27(3): 247-250.
- Batiza, R., 1978. Geology, petrology, and geochemistry of Isla Tortuga, a recently formed tholeiitic island in the Gulf of California. *Geological Society of America Bulletin*, 89(9): 1309-1324.
- Bohannon, R.G., and Parson, T., 1995. Tectonic implication of post-30 Ma Pacific and North America relative plate motions. *Geological Society of America Bulletin*, 107(8): 937-959.
- Bonini, M., Souriot, T., Boccaletti, M., and Brun, J.P., 1997. Successive orthogonal and oblique extension episodes in a rift zone: laboratory experiments with application to the Ethiopian Rift. *Tectonics*, 16(2): 347-362.
- Brown, H., Umhoefer, P., and Holbrook, W. S., 2004. Upper Miocene to lower Pliocene sequence stratigraphy on SE Gulf of California margin defined by new seismic reflection data and the strata on the Tres Marias Islands suggest a simple rift to drift history. *GEOS*, 24(2): 367.
- Brown, H.E., Holbrook, S., Paramo, P., Lizarralde, D., Kent, G., Harding, A., Gonzalez, A., Fletcher, J., Umhoefer, P., and Axen, G., 2006. Crustal Structure of the Southern Gulf of California, the East Pacific Rise to the Jalisco Block. *Lithospheric*

- Rupture in the Gulf of California – Salton Trough Region, MARGINS-RCL Workshop: 14.
- Buck, W.R., 1991. Modes of continental lithospheric extension. *Journal of Geophysical Research*, 96(B12): 20161-20178.
- Buck, W.R., 2005. Consequences of asthenospheric variability on continental rifting. In: G.D. Karner, Taylor, B., Driscoll, N.W., and Kohlstedt, D.L. (Editor), *Rheology and deformation of the lithosphere at continental margins*. Columbia University Press, New York, pp. 1-30.
- Burov, E.V., and Diament, M., 1995. The effective elastic thickness (T_e) of continental lithosphere: What does it really mean? *Journal of Geophysical Research*, 100(B3): 3905-3927.
- CONMAR, 1987. Carta de anomalías de gravedad al aire libre, zona económica exclusiva y márgenes continentales del oeste de México. Carta DGON-G2 y G4. Secretaría de Marina, Dirección General de Oceanografía Naval, Carta DGON-G2 y G4.
- Contreras, J., Scholz, C.H., and King, G.C.P., 1997. A model of rift basin evolution constrained by first-order stratigraphic observations. *Journal of Geophysical Research*, 102(B4): 7673-7690.
- Contreras, J., and Scholz, C.H., 2001. Evolution of stratigraphic sequences in multisegmented continental rift basins: comparison of computer models with the basins of the East African rift system. *AAPG Bulletin*, 85(9): 1965-1981.
- Couch, R.W., Ness, G.E., Sánchez-Zamora, O., Calderón-Riveroll, G., Doguin, P., Plawman, T., Coperude, S., Huehn, B., Gumma, W., 1991. Gravity anomalies and crustal structure of the Gulf and Peninsular Province of the Californias. In: J.P. Dauphin, and Simoneit, B. R. (Editor), *The Gulf and Peninsular Provinces of the Californias*. American Association of Petroleum Geologists Memoir 47, pp. 25-45.
- Cowie, P.A., Gupta, S., and Dawers, N.H., 2000. Implication of fault array evolution for synrift depocentre development: insights from a numerical fault growth model. *Basin Research*, 12: 241-261.
- Curry, J.R., Moore, D.G., et al., 1982a. Guaymas Basin: sites 477, 478, and 481. Init. Repts. DSDP 64, 211-415.
- Curry, J.R., Moore, D.G., et al., 1982b. Guaymas Basin slope: sites 479, and 480. Init. Repts. DSDP 64, 417-446.
- Dañobeitia, J.J., Córdoba, D., Delgado-Argote, L.A., Michaud, F., Bartolome, R., Farrán, M., Carbonell, R., Núñez-Cornú, F., Canales, J.P., Diaz, J., Gallart, J., Rubio, E., Sallares, V., González, A., Romero, M., Castro, R., Fabriol, H., Frez, J., Frias, V.M., García-Abdeslem, J., Nava, A., Hello, Y., Louat, R., Monfret, T., Mezcuca, J., Oyamburu, Y., and Suárez, C., 1997. Expedition gathers new data on crust beneath Mexican west coast, Crustal Offshore Research Transect by Extensive Seismic Profiling (CORTES) P96 Working Group, (III). *Eos Trans.* 78, 565, 572.
- Dauteuil, O., Huchon, P., Quemeneur, F., and Souriot, T., 2001. Propagation of an oblique spreading centre: the western Gulf of Aden. *Tectonophysics*, 332: 423-442.
- Dawers, N.H., and Anders, M.H., 1995. Displacement-length scaling and fault linkage. *Journal of Structural Geology*, 17(5): 607-614.
- Dawers, N.H., and Underhill, J.R., 2000. The role of fault interaction and linkage in controlling synrift stratigraphic sequences: Late Jurassic, Stratfjord East Area,

- Northern North Sea. AAPG Bulletin, 84(1): 45-64.
- Delgado-Argote, L.A., López-Martínez, M., and Perrillat, M.C., 2000. Geologic reconnaissance and Miocene age of volcanism and associated fauna from sediments of Bahía de los Angeles, Baja California, central Gulf of California. In: H. Delgado-Granados, Aguirre-Díaz, G. and Stock, J. M. (Editor), Cenozoic Tectonics and Volcanism of Mexico. Geological Society of America Special Paper 334, pp. 111-121.
- DeMets, C., Gordon, R.G., Argus, D.F., and Stein, S., 1994. Effect of recent revisions to geomagnetic reversal time scale on estimates of current plate motions. *Geophysical Research Letters*, 21: 2191-2194.
- Dorsey, R.J., and Umhoefer, P.J., 2000. Tectonic and eustatic controls on sequence stratigraphy of the Pliocene Loreto basin, Baja California Sur, Mexico. *Geol. Soc. Am. Bull.* 112: 177-199.
- Dorsey, R.J., Fluette, A.L., Housen, B.A., McDougall, K.A., Janecke, S.U., Axen, G.J., and Shirvell, C., 2006. Chronology of Late Miocene to Early Pliocene sedimentation at Split Mt. Gorge, Western Salton Trough: Implications for development of the Pacific-North America plate boundary. *Lithospheric Rupture in the Gulf of California – Salton Trough Region, MARGINS-RCL Workshop*: 23.
- Dorsey, R.J., Fluette, A., McDougall, k., Housen, B.A., Janecke, S.U., Axen, G.J., and Shirvell, C.R., 2007. Chronology of Miocene–Pliocene deposits at Split Mountain Gorge, Southern California: A record of regional tectonics and Colorado River evolution. *Geology*, 35(1): 57-60.
- Einsele, G., Gieskes, J.M., Curray, J., Moore, D.M., Aguayo, E., Aubry, M.P., Fornari, D., Guerrero, J., Kastner, M., Kelts, K., Lyle, M., Motoba, Y., Molina-Cruz, A., Niemitz, J., Rueda, J., Saunders, A., Schrader, H., Simoneit, B., and Vacquier, V., 1980. Intrusion of basaltic sills into highly porous sediments, and resulting hydrothermal activit. *Nature*, 283: 441-445.
- Fabrial, H., Delgado-Argote L., Dañobeitia J.J., Córdoba D., González, A., García-Abdeslem, J., Bartolomé, R., Martín-Atienza, B. and Frías-Camacho, V., 1999. Backscattering and geophysical features of volcanic ridges offshore Santa Rosalia, Baja California Sur, Gulf of California, México. *J. Volcanol. Geotherm. Res.* 93, 75-92.
- Fenby, S.S., and Gastil, R.G., 1991. A seismo-tectonic map of the Gulf of California and surrounding areas. In: J.P. Dauphin, and Simoneit, B. R. (Editor), *The Gulf and Peninsular Provinces of the Californias*. American Association of Petroleum Geologists Memoir 47, pp. 79-83.
- Fletcher, J.M., and Munguía-Orozco, L., 2000. Active continental rifting in southern Baja California, Mexico: implications for plate motion partitioning and transition to seafloor spreading in the Gulf of California. *Tectonics*, 19(6): 1107-1123.
- Fletcher, J.M., Grove, M., Kimbrough, D., Lovera, O., and Gehrels, G.E., *in press*, Neogene tectonic evolution of the Magdalena Shelf and southern Gulf of California: insights from detrital zircon U-Pb ages from the Magdalena Fan and adjacent areas, *Geological Society of America Bulletin*.
- Fuis, G.S., and Kohler, W.M., 1984. Crustal structure and tectonics of the Imperial Valley Region, California. In: C.A. Rigsby (Editor), *The Imperial Basin tectonics*,

- sedimentation and thermal aspects. Pacific Section S.E.P.M., pp. 1-13.
- Gans, P.B., 1997. Large magnitude Oligo-Miocene extension in southern Sonora: Implications for the tectonic evolution of northwest Mexico. *Tectonics*, 16(3): 388-408.
- Gans, P.B., Blair, K., MacMillan, I., Wong, M., Till, C., Herman, S., and Roldan, J., 2006. Structural and Magmatic Evolution of the Sonoran Rifted Margin. *Lithospheric Rupture in the Gulf of California – Salton Trough Region*, MARGINS-RCL Workshop: 30.
- Gastil, R.G., Phillips, R.P. and Allison E.C., 1975. Reconnaissance geology of the state of Baja California. *Geological Society of America Memoir* 140: 170.
- Gastil, R.G., Neuhaus, J., Cassidy, M., Smith, J. T., Ingle, J. C. Jr., and Krummenacher, D., 1999. Geology and paleontology of southwestern Isla Tiburon, Sonora, Mexico. *Revista Mexicana de Ciencias Geológicas*, 16(1): 1-34.
- Gawthorpe, R.L., and Leeder, M. R., 2000. Tectono-sedimentary evolution of active extensional basins. *Basin Research*, 12: 195-218.
- González-Fernández, A., Dañobeitia, J. J., Delgado-Argote, L. A., Michaud, F., Córdoba, D., and Bartolomé, R., 2005. Mode of extension and rifting history of upper Tiburón and upper Delfín basins, northern Gulf of California. *Journal of Geophysical Research*, 110(B01313): doi:10.1029/2003JB002941.
- Gonzalez-Garcia, J.J., Prawirodirdjo, L., Bock, Y., and Agnew, D., 2003. Guadalupe Island, Mexico, as a new constraint for Pacific Plate motion. *Geophysical Research Letters*, 30(16): 1872, doi:10.1029/2003GL017732.
- Gupta, S., Cowie, P.A., Dawers, N.H., and Underhill, J.R., 1998. A mechanism to explain rift-basin subsidence and stratigraphic patterns through fault-array evolution. *Geology*, 26(7): 595-598.
- Gupta, S., and Cowie, P. A., 2000. Processes and controls in the stratigraphic development of extensional basins. *Basin Research*, 12: 185-194.
- Hausback, B.P., 1984. Cenozoic volcanic and tectonic evolution of Baja California Sur, Mexico. In: V.A. Frizzell (Editor), *Geology of the Baja California Peninsula*. Pacific Section Society of Economic Paleontologist and Mineralogist 39, pp. 219-236.
- Helenes, J., and Carreño, A. L., 1999. Neogene sedimentary evolution of Baja California in relation to regional tectonics. *Journal of South American Earth Sciences*, 12: 598-605.
- Helenes, J., Carreño, A.L. Esparza, M.A., and Carrillo, R.M., 2005. Neogene paleontology in the Gulf of California and the geologic evolution of Baja California, VII Reunión Internacional sobre Geología de la Península de la Baja California. *Sociedad Geológica Peninsular*, pp. 2.
- Henry, C.D., 1989. Late Cenozoic Basin and Range structure in western Mexico adjacent to the Gulf of California. *Geological Society of America Bulletin*, 101: 1147-1156.
- Henry, C.D., and Aranda-Gómez, J.J., 1992. The real southern Basin and Range Mid-to-late Cenozoic extension in Mexico. *Geology*, 20(8): 701-704.
- Henry, C.D., and Aranda-Gomez, J.J., 2000. Plate interactions control middle-late Miocene, proto-Gulf and Basin and Range extension in the southern Basin and Range. *Tectonophysics*, 318(1-4): 1-26, doi:10.1016/S0040-1951(99)00304-2.

- Heney, T.L., and Bischoff, J.L., 1973. Tectonic elements in the northern part of the Gulf of California. *Geological Society of America Bulletin*, 84(1): 315-330.
- Holt, J.W., Holt, E.W., and Stock, J.M., 2000. An age constraint on Gulf of California rifting from the Santa Rosalía basin, Baja California Sur, Mexico. *Geological Society of America Bulletin*, 112(4): 540-549.
- Hopper, J.R., and Buck, W.R., 1996. The effect of lower crustal flow on continental extension and passive margin formation. *Journal of Geophysical Research*, 101(B9): 20175-20194.
- <http://phys.ocean.dal.ca/~deping> SeisWide, a public domain software to manage multichannel seismic data developed by Deping Chian at Dalhousie University, Canada.
- <http://www.cwp.miles.edu/cwpcodes/> Seismic Unix, Public domain codes for managing and processing multichannel seismic data developed at Center for Wave Phenomena ~ Colorado School of Mines
- Hurtado, A.D., 2002. Modelo estructural de la Cuenca Wagner en el Golfo de California basado en sísmica de reflexión multicanal. M. Sc. Thesis, Universidad Nacional Autónoma de México, Instituto de Geofísica, México D.F., 84 pp.
- Karig, D.E., and Jansky, W., 1972. The proto-gulf of California. *Earth and planetary science letters*, 17: 169-174.
- Keep, M., and McClay, K.R., 1997. Analogue modelling of multiphase rift systems. *Tectonophysics*, 273: 239-270.
- Lavier, L.L., and Steckler, M., 1997. The effect of sedimentary cover on the flexural strength of continental lithosphere. *Nature*, 389: 476-479.
- Lavier, L.L., Buck, R., and Poliakov, A.N.B., 2000. Factors controlling normal faults offset in an ideal brittle layer. *Journal of Geophysical Research*, 105(B10): 23431-23442.
- Ledesma-Vásquez, J., and Johnson, M. E., 2001. Miocene-Pleistocene tectono-sedimentary evolution of Bahía Concepción region, Baja California Sur (México). *Sedimentary Geology*, 144(1-2): 83-96.
- Lee, J., Miller, M.M., Crippen, R., Hacker, B., and Ledesma-Vásquez, J., 1996. Middle Miocene extension in the Gulf Extensional Province, Baja California: Evidence from the southern Sierra Juárez. *Geological Society of America Bulletin*, 108(5): 505-525.
- Lonsdale, P., 1985. A transform continental margin rich in hydrocarbons, Gulf of California. *AAPG* 69, 1160-1180.
- Lonsdale, P., 1989. Geology and tectonic history of the Gulf of California,. In: D. Winterer, Hussong, M., and Decker, R. W. (Editor), *The Eastern Pacific Ocean and Hawaii*. Geological Society of America, *The Geology of North America N*, pp. 499-521.
- Lyle, M., and Ness, G.E., 1991. The opening of the Southern Gulf of California. In Dauphin, J.P., and Simoneit, B. R. (Eds.), *The Gulf and Peninsular Provinces of the Californias*, AAPG Mem. 47. pp. 403-423.
- Manighetti, I., King, C.P., Gandemer, Y., Scholz, C.H., and Doubre, C., 2001. Slip accumulation and lateral propagation of active normal faults in Afar. *Journal of Geophysical Research*, 106(B7): 13667-13696.

- Mart, Y., and Dauteuil, O., 2000. Analogue experiments of propagation of oblique rifts. *Tectonophysics*, 316: 121-132.
- Martín-Barajas, A., 2000. Volcanismo y extensión en la Provincia Extensional del Golfo de California. *Boletín de la Sociedad Geológica Mexicana*, LIII: 72-83.
- Martín-Barajas, A., Stock, J., Layer, P., Hausback, B., Renne, P., and López-Martínez, M., 1995. Arc-rift transition magmatism in the Puertecitos Volcanic Province northeastern Baja California, Mexico. *Geological Society of America Bulletin*, 107(4): 407-424.
- Martín-Barajas, A., Weber, B., y Aragón-Arreola, M., 2002. Petrología de la actividad volcánica reciente en las cuencas del Norte del Golfo de California. *GEOS*, 22(3): 239.
- Martín-Barajas, A., Helenes-Escamilla, J., Aragón-Arreola, M., and García-Abdeslem, J. (coords.), 2005. Evolución Tectonoestratigráfica de las Cuencas del Norte del Golfo de California. Proyecto: PEMEX Exploración y Producción - CICESE, Clave: 410303843.
- McDougall, K., Poore, R., and Matt, J., 1999. Age and paleoenvironment of the Imperial Formation near San Gorgonio Pass, Southern California. *Journal of Foraminiferal Research*, 29(1): 4-25.
- McDowell, F.W., and Clabaugh, S.E., 1979. Ignimbrites of the Sierra Madre Occidental and their relation to the tectonic history of western Mexico. In: C.E. Chapin, and Elston, W.E. (Editor), *Ash flow tuffs*. Geological Society of America Special Paper 180, pp. 113-124.
- McLeod, A.E., Dawers, N.H. and Underhill, J.R., 2000. The propagation and linkage of normal faults: insights from the Strathspey-Brent-Stratfjord fault array, northern North Sea. *Basin Research*, 12: 263-284.
- Moore, D.G., 1973. Plate-edge deformation and crustal growth, Gulf of California Structural Province. *Geol. Soc. Am. Bull.* 84, 1883-1906.
- Morley, C.K., 2002. Evolution of large normal faults: Evidence from seismic reflection data. *AAPG Bulletin*, 86(6): 961-978.
- Mora-Álvarez, G., and McDowell, F. W., 2000. Miocene volcanism during late subduction and early rifting in the Sierra Santa Ursula of western Sonora, Mexico. In: H. Delgado-Granados, Aguirre-Díaz, G. and Stock, J. M. (Editor), *Cenozoic Tectonics and Volcanism of Mexico*. Geological Society of America, Special Paper 334, pp. 123- 141.
- Nagy, E., and Stock, J.M., 2000. Structural controls on the continent-ocean transition in the northern Gulf of California. *Journal of Geophysical Research*, 105(B7): 16251-16269.
- Ness, G.E., Lyle, M.W., and Couch, R.W., 1991. Marine magnetic anomalies and oceanic crustal isochrons of the Gulf and Peninsular Province of the Californias. In Dauphin, J.P., and Simoneit, B. R. (Eds.), *The Gulf and Peninsular Provinces of the Californias*, AAPG Mem. 47. pp. 47-69.
- Nourse, J.A., Anderson, T.H., and Silver, L.T., 1994. Tertiary metamorphic core complexes in Sonora, northwestern Mexico. *Tectonics*, 13(5): 1161-1182.
- Núñez-Cornú, F., Frez, J., Montana, C., Munguía, L., Nava, A., González, J., Mendoza, L., Aragón, M., Sánchez-Mora, C., Morandi, M., Madrid, J., y el Grupo de Perfiles

- Sísmicos del CICESE, 1996. Un Modelo de la Estructura de la Corteza para el Sistema de Fallas de San Andrés en la Zona Fronteriza México-EEUU. *Geotermia Revista Mexicana de Geoenergía*, 12(1): 43-51.
- Ochoa-Landín, L., Ruiz, J. Calmus, T., Pérez-Segura, E., and Escandón, F., 2000. Sedimentology and stratigraphy of the Upper Miocene El Boleo Formation, Santa Rosalía, Baja California, México. *Revista Mexicana de Ciencias Geológicas*, 17(2): 83-96.
- Oskin, M., 2002. Tectonic Evolution of the Northern Gulf of California, Mexico, Deduced from Conjugate Rifted Margins of the Upper Delfín Basin. California Institute of Technology, Doctor of Philosophy Thesis (Part I), 321 pp.
- Oskin, M., Stock, J.M., and Martín Barajas, A., 2001. Rapid localization of Pacific-North America plate motion in the Gulf of California. *Geology*, 29(5): 459-462.
- Oskin, M., and Stock, J. M., 2003a. Pacific-North America plate motion and opening of the Upper Delfín basin, northern Gulf of California, Mexico. *Geological Society of America Bulletin*, 115(10): 1173-1190.
- Oskin, M., and Stock, J.M., 2003b. Marine incursion synchronous with plate-boundary localization in the Gulf of California. *Geology*, 31(1): 23-26.
- Pacheco-Romero, M., 2004. Estructura y evolución de la Cuenca de Altar, Sonora, a partir de la integración de datos geofísicos y geológicos. M.S. Thesis, Centro de Investigación Científica y Educación Superior de Ensenada, Ensenada B. C., 124 pp.
- Pacheco-Romero, M., Martín-Barajas, A., Elders, W., Espinosa-Cardena, J. M., Helenes, J. and Segura, A., 2006. Stratigraphy and structure of the Altar basin of NW Sonora: Implications for the history of the Colorado River delta and the Salton trough. *Revista Mexicana de Ciencias Geológicas*, 23(1): 1-22.
- Peacock, D. C. P. 1991. Displacement and segment linkage in strike-slip fault zones. *Journal of Structural Geology* 13(9): 1025-1035.
- Persaud, P., Stock, J.M., Steckler, M.S., Martín-Barajas, A., Diebold, J.B., González-Fernández, A., and Mountain, G.S., 2003. Active deformation and shallow structure of the Wagner, Consag, and Delfín Basins, northern Gulf of California, Mexico. *Journal of Geophysical Research*, 105(B7): 2355, doi: 10.1029/2002JB001937.
- Phillips, R.P., 1964. Seismic refraction studies in the Gulf of California. In: T. van Andel, and Shor, G.G. (Editor), *Marine geology of the Gulf of California*. American Association of Petroleum Geologist Memoir 3, pp. 90-121.
- Ponce, M., 1971. Sobre la presencia de estratos marinos del Mioceno en el Estado de Sonora, México. *Revista del Instituto Mexicano del Petróleo, Hojas técnicas*(Octubre): 77-78.
- Prosser, S., 1993. Rift-related linked depositional systems and their seismic expression, in Tectonic and seismic sequence stratigraphy. In Williams, G.D., and Dobb, A. (Eds.). pp., Geol. Soc., Spec. Pub. 71, 35-46.
- Ramsay, J.G., and Lisle, M. I., 1983. The techniques of modern structural geology. Volume 1: strain analysis, 1: strain analysis. Academic Press, 307 pp.
- Roldán-Quintana, J., Mora-Klepeis, G., Calmus, T., Valencia-Moreno, M., y Lozano-Santacruz, R., 2004. El graben de Empalme, Sonora, México: magmatismo y

- tectónica extensional asociados a la ruptura inicial del Golfo de California. *Rev. Mex. Cien. Geol.* 21: 320-334.
- Rosendahl, B.R., 1987. Architecture of continental rifts with special reference to East Africa. *Annual Review of Earth and Planetary Sciences*, 15: 247-276.
- Ruppel, C., 1995. Extensional process in continental lithosphere. *Journal of Geophysical Research*, 100(B12): 24187-24215.
- Sandiford, M., Frederiksen, S., and Braun, J., 2003. The long-term thermal consequences of rifting: implications for basin reactivation. *Basin Research*, 15: 23-43.
- Saunders, A.D., Fornari, D.J. and Morrison M.A., 1982. The composition and emplacement of basaltic magmas produced during the development of continental-margin basins: The Gulf of California, Mexico. *J. Geol. Soc. London*, 139: 335-346.
- Sawlan, M.G., 1991. Magmatic evolution of the Gulf of California Rift. In: J.P. Dauphin, and Simoneit, B. R. (Editor), *The Gulf and Peninsular Provinces of the Californias*. American Association of Petroleum Geologists Memoir 47, pp. 301-369.
- Schlische, R.W., Withjack, M.O. and Einsenstaddt, G., 2002. An experimental study of the secondary deformation produced by oblique-slip normal faulting. *American Association of Petroleum Geologist*, 86(5): 885-906.
- Scholz, C.H., and Contreras, J.C., 1998. Mechanics of continental rift architecture. *Geology* 26, 967-970.
- Sheriff, R.E., and Geldart, L.P., 1995. *Exploration seismology* 2nd Ed. Cambridge University Press, 592 pp.
- Spencer, J.E., and Normark, W.R., 1979. Tosco-Abreojos fault zone: a Neogene transform plate boundary within the Pacific margin of southern Baja California, Mexico. *Geology*, 7(11): 554-557.
- Stewart, J.H., 1998. Regional characteristics, tilt domains, and extensional history of the late Cenozoic Basin and Range province, Western North America. In: J.E. Faults, and Stewart, J.H. (Editor), *Accommodation Zones and Transfer Zones: The regional Segmentation of the Basin and Range Province*. Geological Society of America Special Paper 323, pp. 47-74.
- Stock, J.M., and Hodges, K.V., 1989. Pre-Pliocene extension around the Gulf of California and the transfer of Baja California to the Pacific plate. *Tectonics*, 8(1): 99-115.
- Stock, J.M., and Lee, J., 1994. Do microplates in subduction zones leave a geological record? *Tectonics*, 13(6): 1472-1487.
- Stock, J.M., 2000. Relation of the Puertecitos Volcanic Province, Baja California, México, to development of the plate boundary in the Gulf of California. In: H. Delgado-Granados, Aguirre-Díaz, G. and Stock, J.M. (Editor), *Cenozoic Tectonics and Volcanism of Mexico*. Geological Society of America, Special Paper 334, pp. 143-156.
- Sumner, J.R., 1972. Tectonic significance of gravity and aeromagnetic investigations at the head of the Gulf of California. *Geological Society of America Bulletin*, 83: 3103-3120.
- Sutherland, F.H., Harding, A., Kent, G.M., Lizarralde, D., Umhoefer, P., Holbrook, S., Fletcher, J. Gonzalez-Fernandez, A., and Axen G., 2006. Crustal Structure and Basin Analysis Across the Southern Gulf of California. *Lithospheric Rupture in the*

- Gulf of California – Salton Trough Region, MARGINS-RCL Workshop: 71.
- Teyssier, C., Tikoff, B., and Markley, M., 1995. Oblique plate motion and continental tectonics. *Geology*, 23(5): 447-450.
- Umhoefer, P.J., Dorsey, R. J. and Renne, P., 1994. Tectonics of the Pliocene Loreto Basin, Baja California Sur, Mexico, and evolution of the Gulf of California. *Geology*, 22(7): 649-652.
- Umhoefer, P.J., Dorsey, R.J., Willsay, S., Mayer, L., and Renne, P., 2001. Stratigraphy and geochronology of the Comondú Group near Loreto, Baja California Sur, México. *Sedimentary Geology*, 144: 125-147.
- Umhoefer, P.J., Mayer, L., and Dorsey, R.J., 2002. Evolution of the margin of the Gulf of California near Loreto, Baja California Peninsula, Mexico. *Geological Society of America Bulletin*, 114(7): 849-868.
- Wernicke, B., Axen, G.J., and Snow, J.K., 1988. Basin and range extensional tectonics at the latitude of Las Vegas. *Geological Society of America Bulletin*, 100: 1738-1757.
- Wilson, I.F., and Rocha-Moreno, V.S., 1955. Geology and mineral deposits of the Boleo copper district, Baja California, Mexico, Report: P 0273. U. S. Geological Survey Professional Paper, 134 pp.
- Winker, D.C., and Kidwell, M.S., 1996. Stratigraphy of a marine rift basin: Neogene of the western Salton Trough, California. In: L.P. Abbot, and Cooper, D.J (Editor), *Field Conference Guidebook American Association of Petroleum Geologist Annual convention. Pacific Section American Association of Petroleum Geologist and Society of Economic Paleontologist and Mineralogist, Bakersfield California*, pp. 236-295.
- Withjack, M.O., and Jamison, W.R., 1986. Deformation produced by oblique rifting. *Tectonophysics*, 126: 99-124.
- Wong, M.S., and Gans, P.B., 2003. Tectonic implications of early Miocene extensional unroofing of the Sierra Mazata´n metamorphic core complex, Sonora, Mexico. *Geology*, 31(11): 953–956.
- Yilmaz, Ö. 1987. *Seismic Data Processing*, 1. The Society of Exploration Geophysics, 526 pp.

**APPENDIX 1. MIGRATED AND INTERPRETED MULTICHANNEL
SEISMIC REFLECTION PROFILES OF THE NORTHERN GULF OF
CALIFORNIA.**

SEE ATTACHED CD

PROFILES USED FOR:

**STRUCTURAL EVOLUTION OF BASINS IN THE NORTHERN AND
CENTRAL GULF OF CALIFORNIA. IMPLICATIONS FOR RIFT
KINEMATICS AND STRAIN ACCOMMODATION**

presented by **Manuel de Jesús Aragón Arreola** as a partial
requirement to obtain the DOCTOR OF SCIENCE degree in
EARTH SCIENCES.

CENTRO DE INVESTIGACIÓN CIENTÍFICA Y DE EDUCACIÓN SUPERIOR DE ENSENADA

**APPENDIX 2. TYPE SCRIPTS FOR PROCESSING OF MULTICHANNEL
SEISMIC REFLECTION DATA USING THE PUBLIC DOMAIN CODES OF
SEISMIC UNIX.**

SEE ATTACHED CD

SCRIPTS USED FOR:

**STRUCTURAL EVOLUTION OF BASINS IN THE NORTHERN AND
CENTRAL GULF OF CALIFORNIA. IMPLICATIONS FOR RIFT
KINEMATICS AND STRAIN ACCOMMODATION**

presented by **Manuel de Jesús Aragón Arreola** as a partial
requirement to obtain the DOCTOR OF SCIENCE degree in
EARTH SCIENCES.

CENTRO DE INVESTIGACIÓN CIENTÍFICA Y DE EDUCACIÓN SUPERIOR DE ENSENADA